united nations
educational, scientific
and cultural
organization

international atomic
energy agency

the
abdus salam
international centre for theoretical physics

SMR.1227 - 5

SUMMER SCHOOL ON ASTROPARTICLE PHYSICS AND COSMOLOGY

12 - 30 June 2000

PARTICLE AND ASTROPHYSICS ASPECTS OF ULTRAHIGH ENERGY COSMIC RAYS

Lectures I, II, III and IV

G. SIGL
DARC
Observatoire de Paris-Meudon
Meudon
FRANCE

G. SIGL

Physics and Astrophysics of Ultrahigh Energy Cosmic Rays

see http://astro.uchicago.edu/home/web/sigl

also astro-ph/9811011 → Physics Reports 327 (2000) p. 109-247

Outline of Lectures

1.) Introduction to cosmic rays:
experimental techniques and facts
upcoming experiments
basic theoretical issues

2.) interactions: acceleration and propagation
connection to γ-ray and ν astrophysics
astrophysical sources

3.) ultra high energy cosmic rays as decay products of early Universe relics
a window into the primordial Universe?

4.) New interactions / new particles
Cosmic rays as probes of physics beyond the Standard Model

5.) Cosmic rays as probes of cosmic magnetic fields

supernova remnants | plerions galactic wind | AGN 2 top-down 2

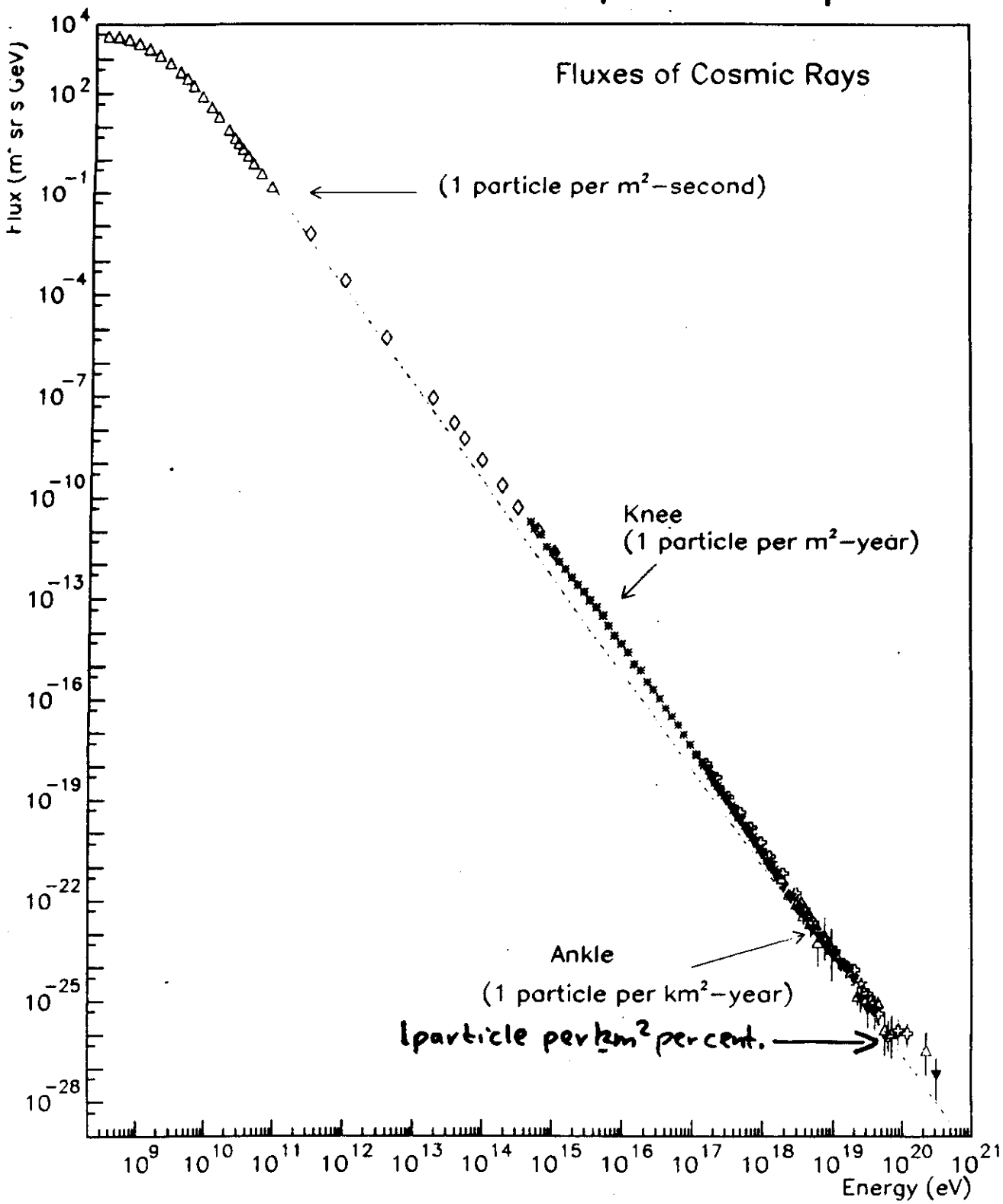

S. Swordy

All particle spectrum and proton component
(Mannheim, Protheroe, Rachen)

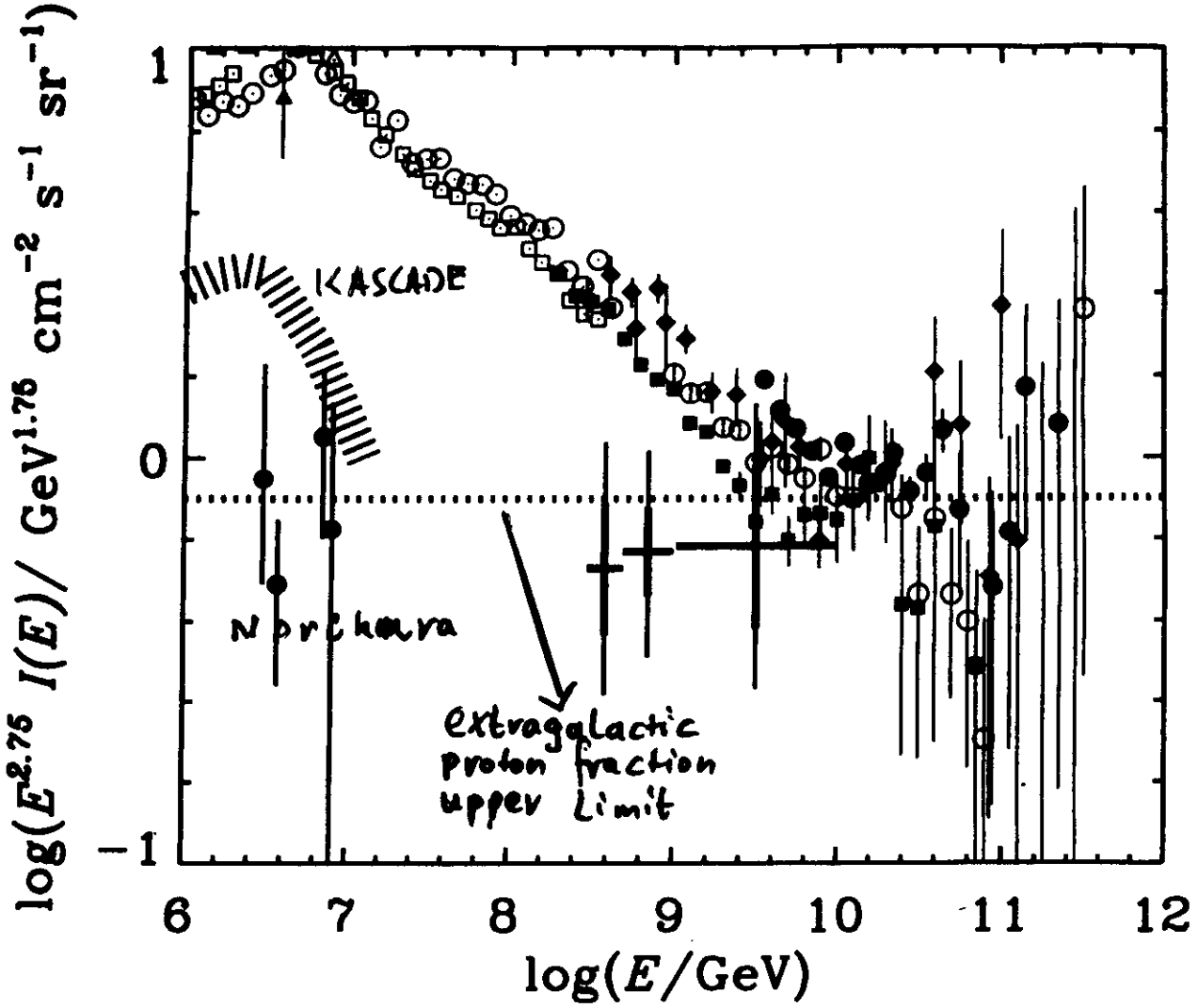

○ > 10^8 GeV: Fly's Eye monocular
● > 10^8 GeV: AGASA

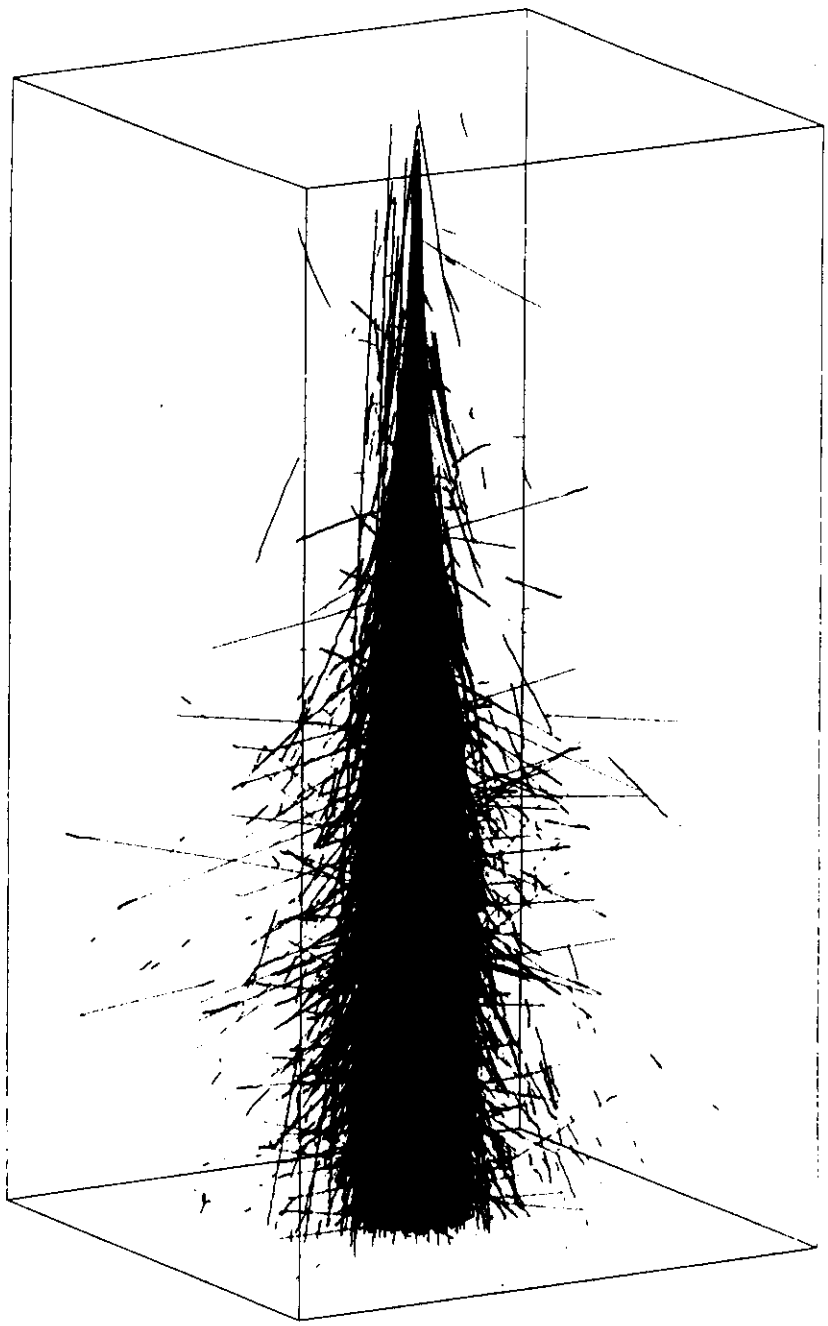

Simulation of a 10^{19} eV proton EAS using the MOCCA program. A sample of tracks at > 300 m from the shower axis are shown. Frame box: 6 × 6 × 12 km high. Color code: γ green, e red, μ blue. ***Drawn by Clem Pryke — University of Chicago***

Shower Development

$$N(X) \propto N_s^{X/\lambda}$$

X: column depth; N_s: # secondaries; λ: interaction length

$$E(X) = \frac{E_0}{N(X)}$$

$E(X)$: secondary mean energy

$$E_c = \frac{E_0}{N(X_{max})} \quad \Rightarrow \quad X_{max} = X_0 + X_1 \log E_0$$

E_c: below E_c secondaries do not multiply

99% $\gamma, e^\pm$ of $\simeq 1$–10 MeV 1% muons of $\simeq 1$ GeV

$$N_\mu \propto A \left(\frac{E_0}{A}\right)^{0.85} = A^{1-0.85} E_0^{0.85}$$

heavy nuclei produce more muons

$$(X_{max})_{Fe} < (X_{max})_p$$

heavy nuclei of same energy initiate shower development earlier (higher cross section)

Lateral profile:

$$\rho(r) \propto 12\, r^{-[\eta + f(r)]}$$

η depends on primary incident angle

f, h depend on detector type

Two Complementary Detection Methods above $\sim 10^{17}$ eV

• **Grounds Arrays of scintillation detectors** measure **lateral distributions** of secondary charged shower particles. The primary energy is proportional to the particle density at some given distance (600 m) from the shower core. Information on composition from muon content. The AGASA array near Tokyo, Japan is the largest operative array. ($\simeq 100$ km^2)

• **The "Fly's Eye" technique** measures **longitudinal shower profile from air-nitrogen fluorescence light** using mirrors and photomultiplier tubes. The primary energy E_p is proportional to the total fluorescence yield. The shower maximum is given by

$$X_{max}\,[\mathrm{g\,cm^{-3}}] = X_0 + X_1 \cdot \log E_p\,,$$

where X_0 depends on the nature of the primary. The HIGH RESOLUTION FLY'S EYE and the Japanese TELESCOPE ARRAY are under construction.

The INTERNATIONAL GIANT AIR SHOWER ARRAY proposed by the PIERRE AUGER PROJECT will be a combination of these techniques. Both the northern site (at Utah, USA) and the southern site (in Argentina) will cover $\simeq 3000\,\mathrm{km}^2$. Construction probably starts late 1998. Data taking with growing array can commence soon thereafter.

Experimental Results and Standard Interpretation in a Nutshell

- Spectrum: piecewise power law with breaks at "knee" ($\simeq 4 \cdot 10^{15}$ eV) and "ankle" ($\simeq 5 \cdot 10^{18}$ eV). No obvious "GZK cutoff"
- composition: growing heavier below "knee"
  ankle correlated with change to light composition?
- anisotropy: $\sim 10^{-3}$ below 10^{14} eV (significant)
  above 10^{14} eV in general insignificant except $\simeq 4\%$ around 10^{18} eV correlated with Galactic plane. possible clustering with Supergalactic plane AND on small (degree) scales above $\sim 4 \cdot 10^{19}$ eV?

$\Rightarrow$ galactic origin up to "knee": non-universality suggested by secondary $\bar{p}$-flux from SMC
Energetics suggests supernova remnants as source
however: too few secondary γ's from supernova remn.
knee, as magnetic deconfinement effect
extragalactic origin above "ankle"

1.) Introduction: Present Experimental Facts

Some numbers for the integral particle flux $\phi(E) = \int_E^\infty dE' j(E')$:

$$\phi(10^{14}\,\mathrm{eV}) \simeq \frac{1}{(100\,\mathrm{m})^2\,\mathrm{sec}}$$

$$\phi(10^{19}\,\mathrm{eV}) \simeq \frac{1}{\mathrm{km}^2\,\mathrm{yr}}$$

Highest energy $E \simeq 3 \times 10^{20}\,\mathrm{eV} \simeq 50\,\mathrm{J}$ observed by Fly's Eye (Utah).

Are cosmic rays up to the "knee" at $\simeq 3 \times 10^{15}\,\mathrm{eV}$ universal? The γ-ray flux from the SMC is about factor 3 lower than expected for universality.

Standard explanation of galactic (local) cosmic rays: 1st order Fermi acceleration at shocks in supernova remnants. Energetics: $u_{CR} \sim 1\,\mathrm{eV\,cm^{-3}} \sim u_{MWB}$ (coincidence?) satisfies

$$u_{CR} \sim \frac{L\,t_c}{V_{gal}}$$

where $t_c \sim 10^7\,\mathrm{yr}$ = confinement time (at $10^{15}\,\mathrm{eV}$), $V_{gal} \sim 10^{61}\,\mathrm{m^3}$. The resulting total galactic luminosity $L \sim 10^{48}\,\mathrm{erg/yr}$ is about 10% of kinetic energy release rate of galactic supernovae.

The Fly's Eye experiment observed a composition change to a light component correlated with the "ankle" structure in the spectrum around $\simeq 3 \times 10^{18}\,\mathrm{eV}$ (not confirmed by AGASA). Hint for extragalactic origin?

Dip, ankle : crossover ? $j(E) = j_{gal}(E) + j_e(E)$

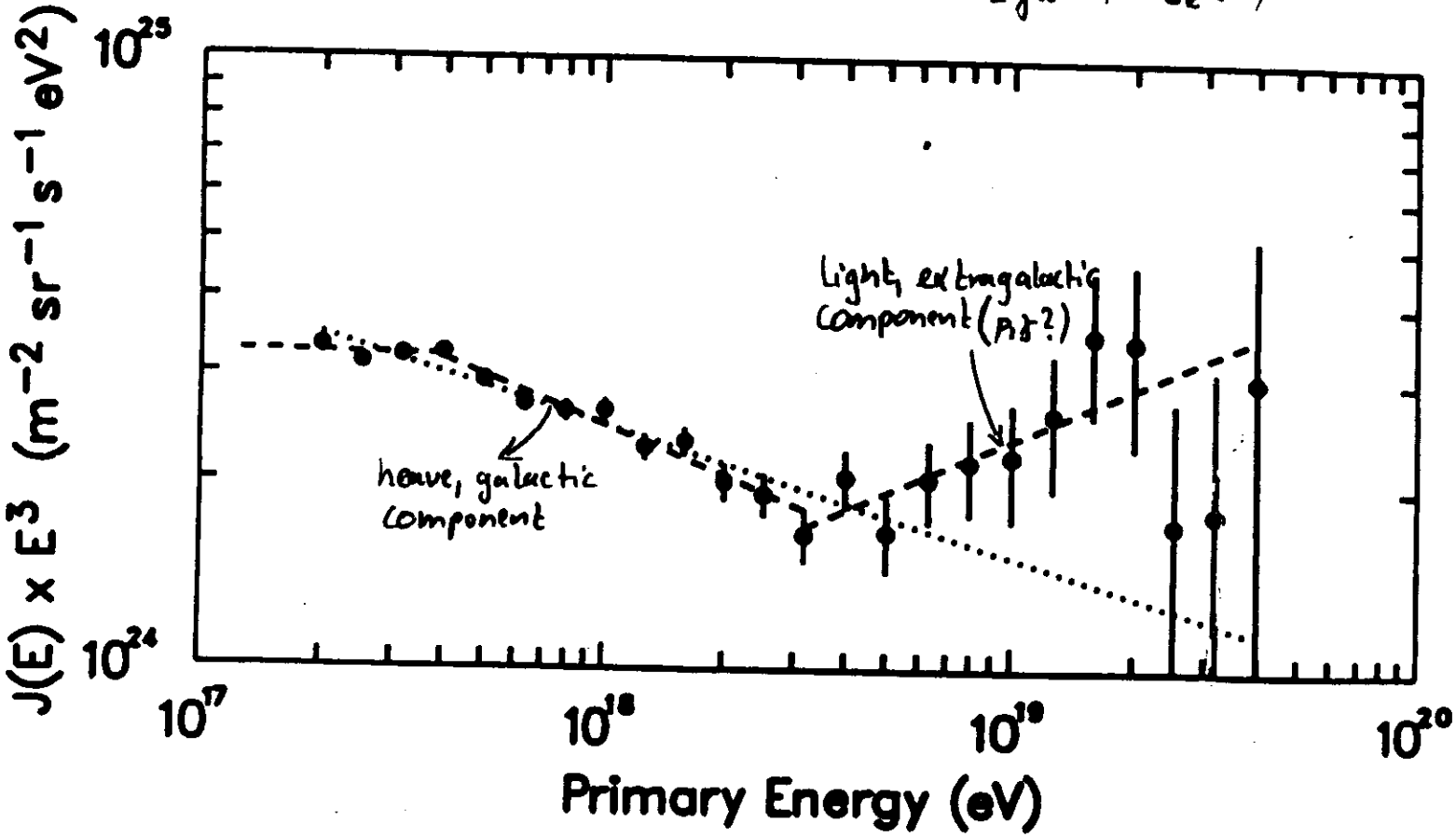

(D.J. Bird et.al.)

Figure 5: Fly's Eye stereo energy spectrum. Points: data. Dashed line: best fit in each region. Dotted line: best fit up to $10^{18.5}$eV.

best fit: $\log[j_{gal}(E)\,(eV^{-1}m^{-2}s^{-1}sr^{-1})] = 33.185 - 3.496 \cdot \log[E/eV]$

$\log[j_e(E)\,(eV^{-1}m^{-2}s^{-1}sr^{-1})] = 16.782 - 2.610 \cdot \log[E/eV]$

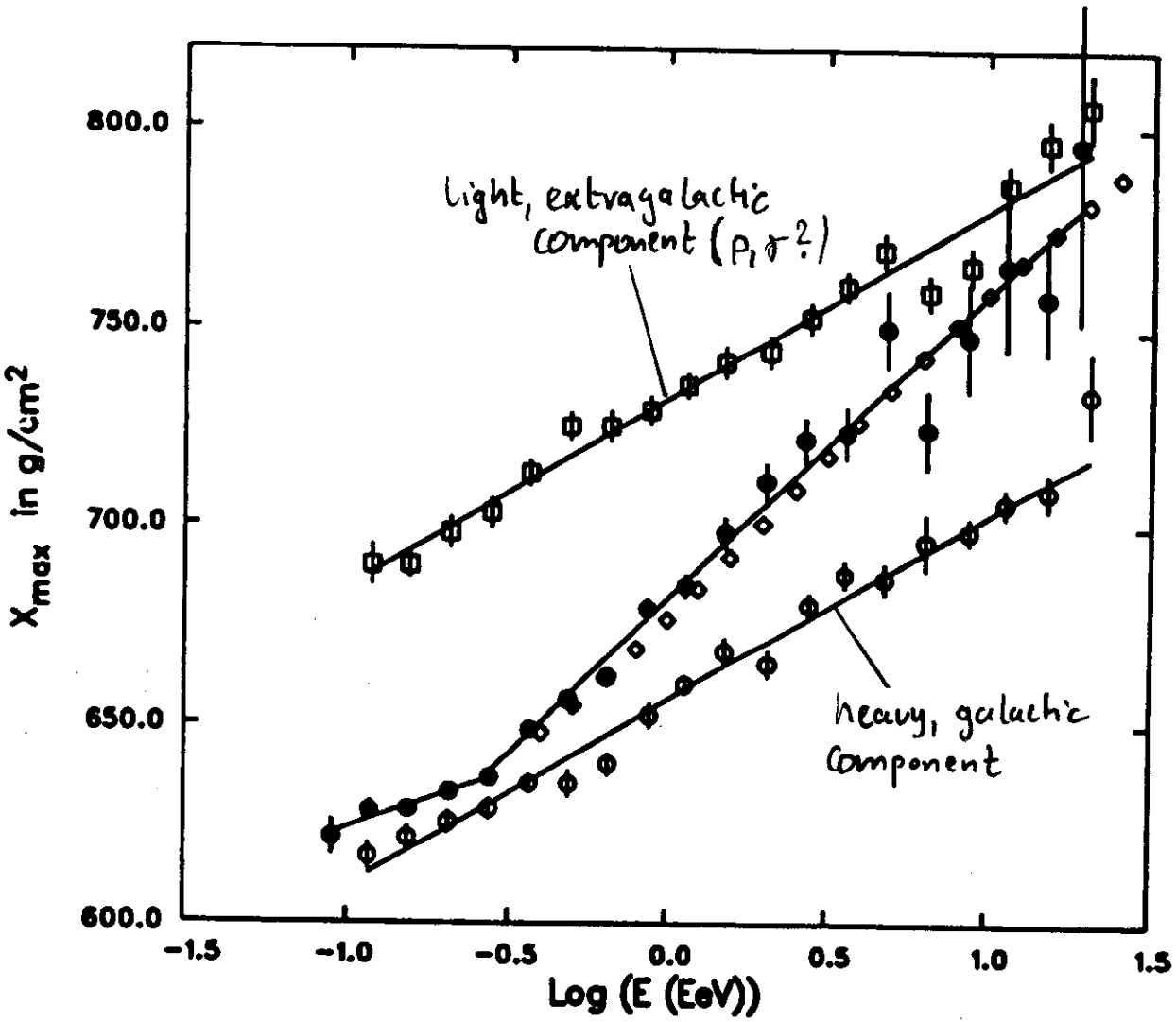

Composition change correlated with dip in the energy spectrum

Middle curve uses fluxes fit to energy spectrum

(D.J. Bird et.al.)

Figure 16: X_{max} elongation rate. Black dots: Fly's Eye data. Open squares : proton X_{max} distribution based on KNP model. Open circles: iron X_{max} distribution based on KNP model. Diamonds: expected mean X_{max} distribution based on a simple two component assumption of cosmic rays.

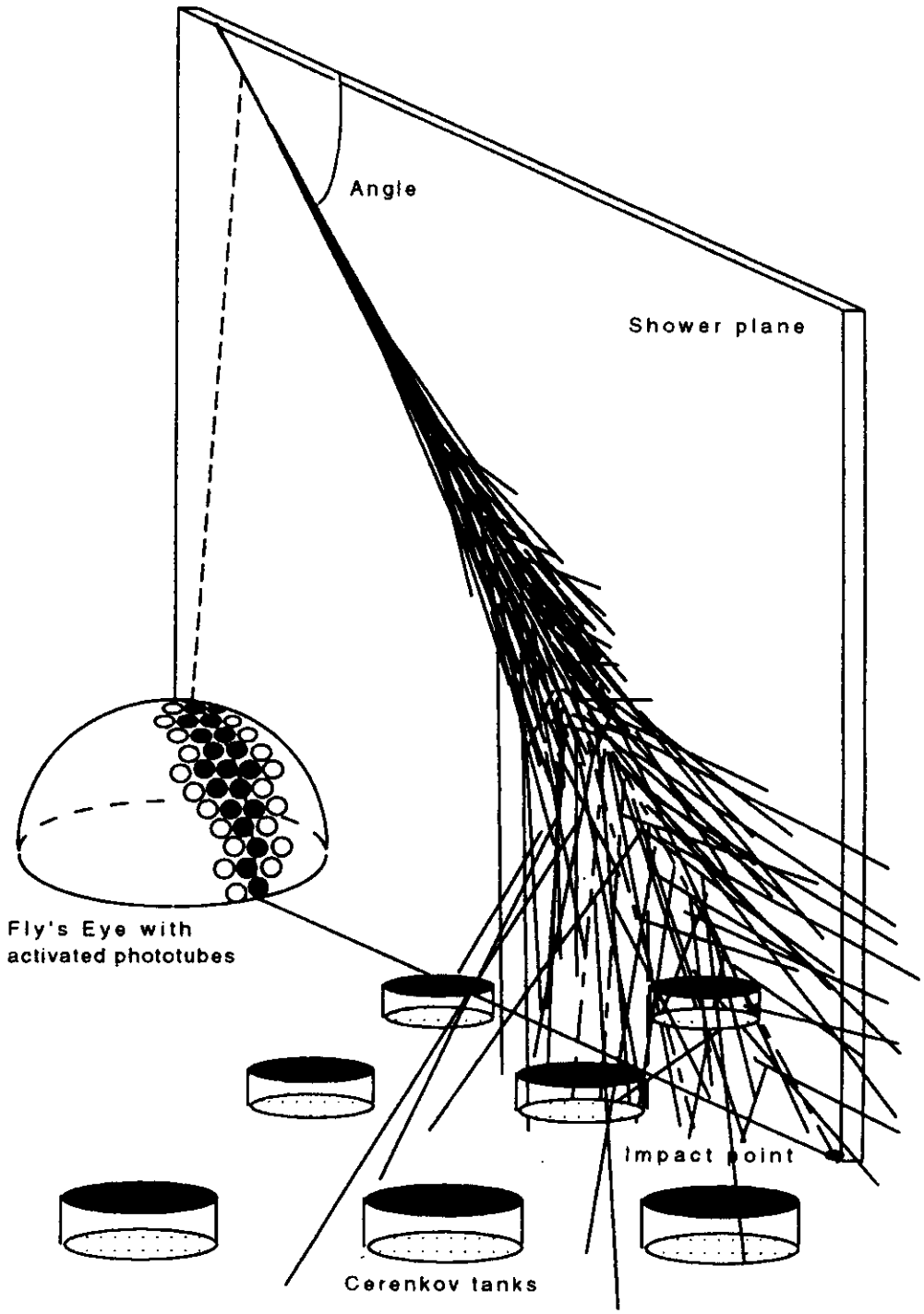

Schematic representation of the operation of a hybrid air shower detector.

Layout of the proposed Auger detector

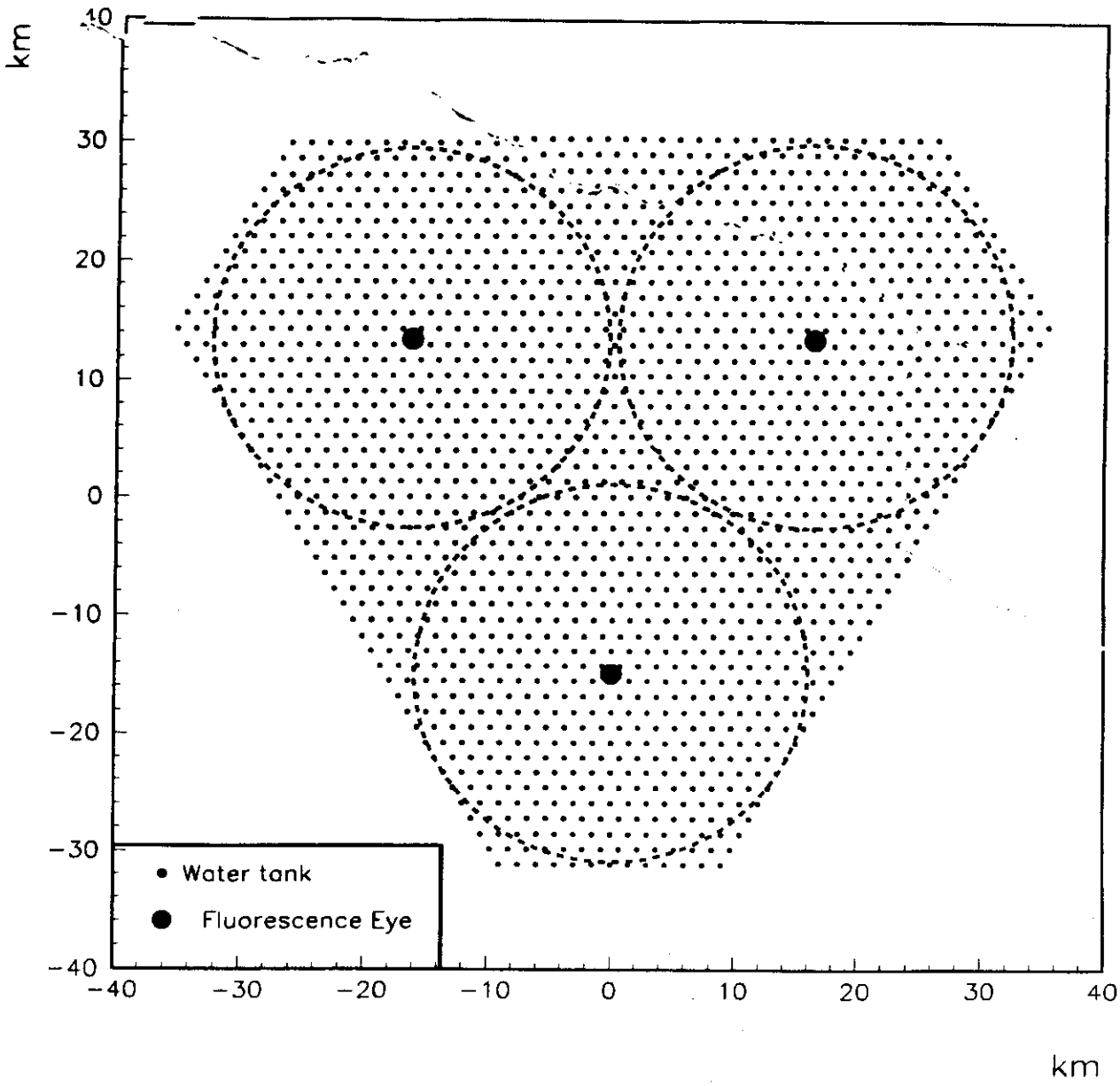

Future UHE CR Experiments

		start	Acceptance / AGASA	angular resolution	energy resolution	# events / cluster in 5 yr
ti Res	Fly's Eye	~ 1999	~7			~10
elescope	Array	~2000	~15			~20
ıger	ground	2001/2003	~150	$\lesssim 2°$	~20%	~200
	hybrid	2001/2003	~15	$\simeq 0.25°$	~10%	~20
IWL		$\gtrsim$ 2010	$\gtrsim 5 \cdot 10^3$?	$\lesssim 1°$	$\lesssim 30\%$	Few 10^3 ?

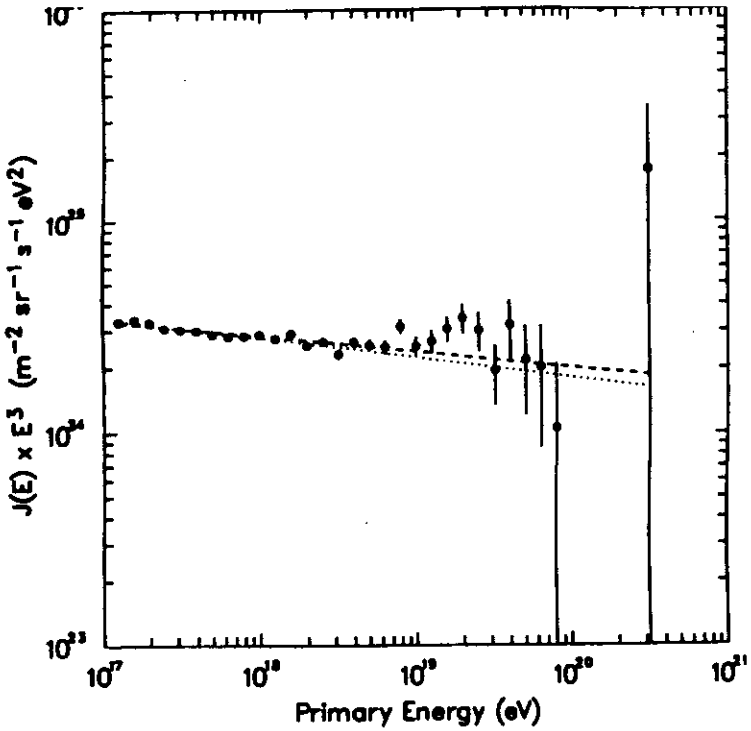

FIG. 11.—Fly's Eye monocular energy spectrum. *Points*: data. *Dashed line*: best fit of the total spectrum. *Dotted line*: best fit up to $10^{18.5}$ eV.

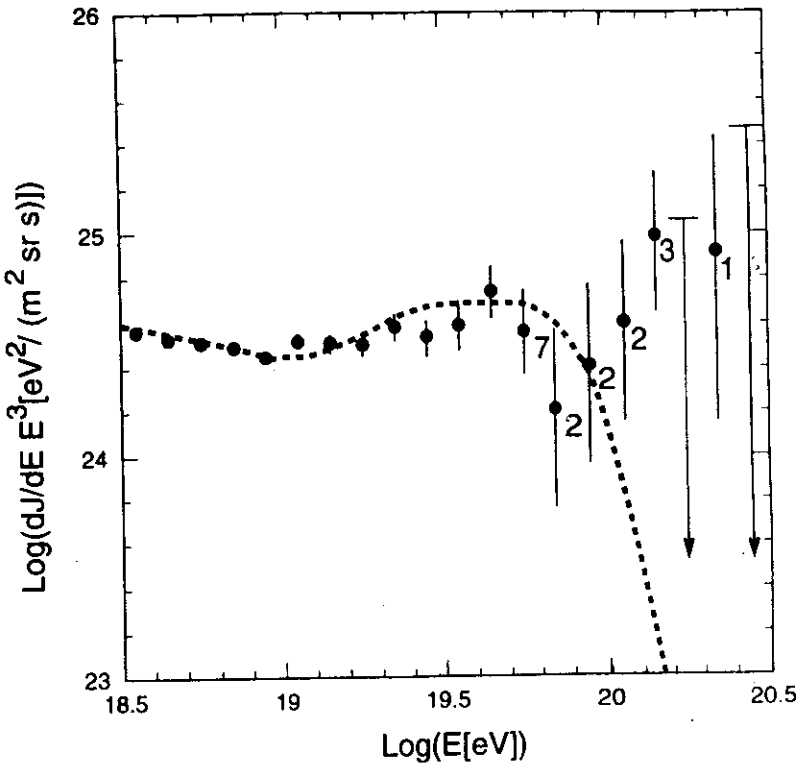

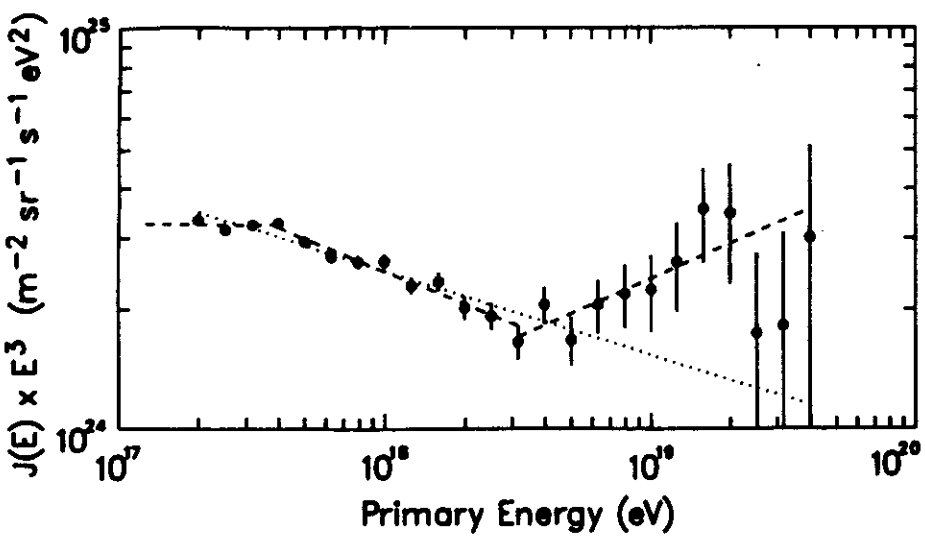

FIG. 5.—Fly's Eye stereo energy spectrum. *Points*: data. *Dashed line*: best fit in each region. *Dotted line*: best fit up to $10^{18.5}$ eV.

Neutrino detection - relevant

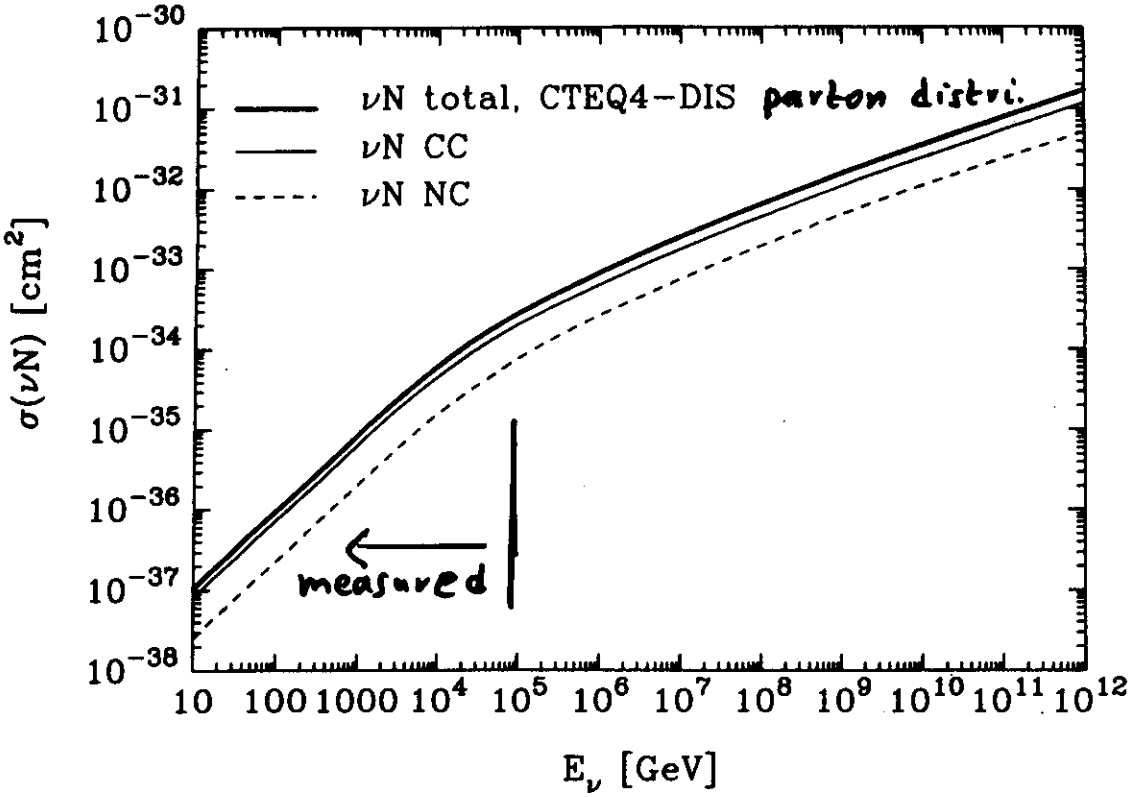

Neutrino propagation - relevant

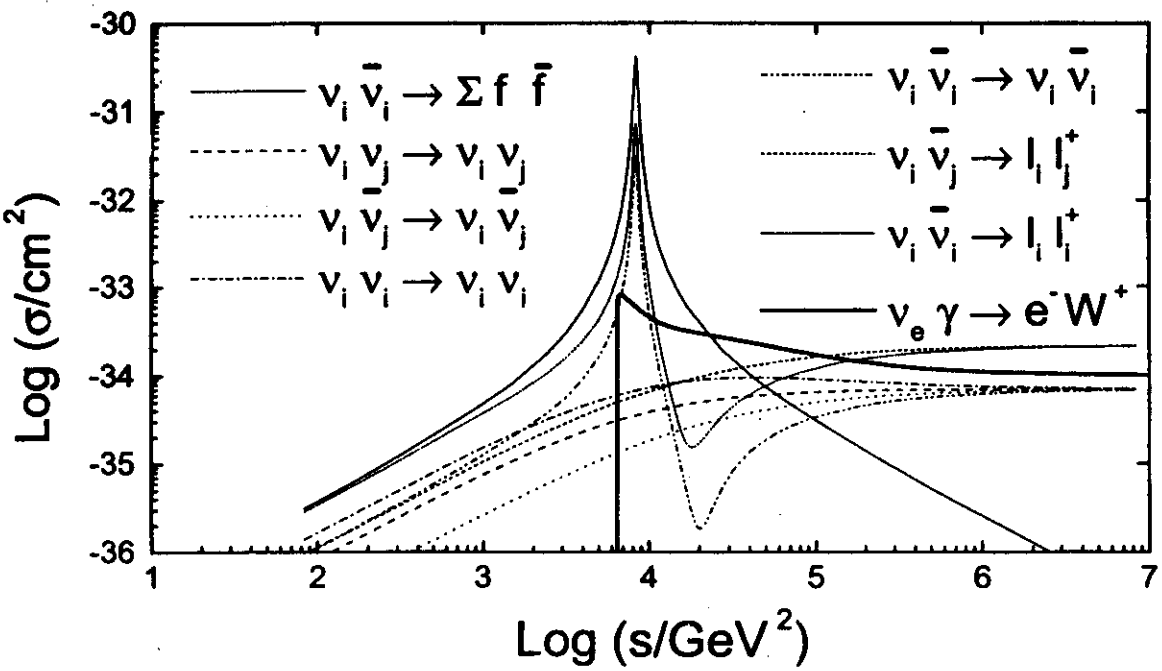

$$\langle s \rangle \simeq 10^3 \left(\frac{E_\nu}{10^{12}\,\mathrm{GeV}}\right)\left(\frac{m_\nu}{1\,\mathrm{eV}}\right)\ 6\,\mathrm{eV}^2$$

Ultrahigh Energy Neutrino Detection

basically uses charged-current reaction

$$\nu_\mu + N \rightarrow \mu^- + N$$

i) look for Cherenkov radiation from muon in the deep sea or in ice

- Antares, Baikal, Nestor
- Amanda

aim at km^3 scale ν observatories

ii) look for horizontal air showers

background free !

Rates:

fold flux with $O(2)$ uncertain cross sections

TD fluxes: With $r \equiv \delta_\nu / \delta_\gamma$ diffuse γ-ray background yields:

$$R(E) \lesssim 0.3\, r \left(\frac{A(E)}{1 km^3\, 2\pi\, sr}\right)\left(\frac{E}{10^{19} eV}\right)^{-0.6} yr^{-1}$$

$\longrightarrow$ a few per year with Auger !

$\Longrightarrow$ testable

Attenuation of cosmic rays

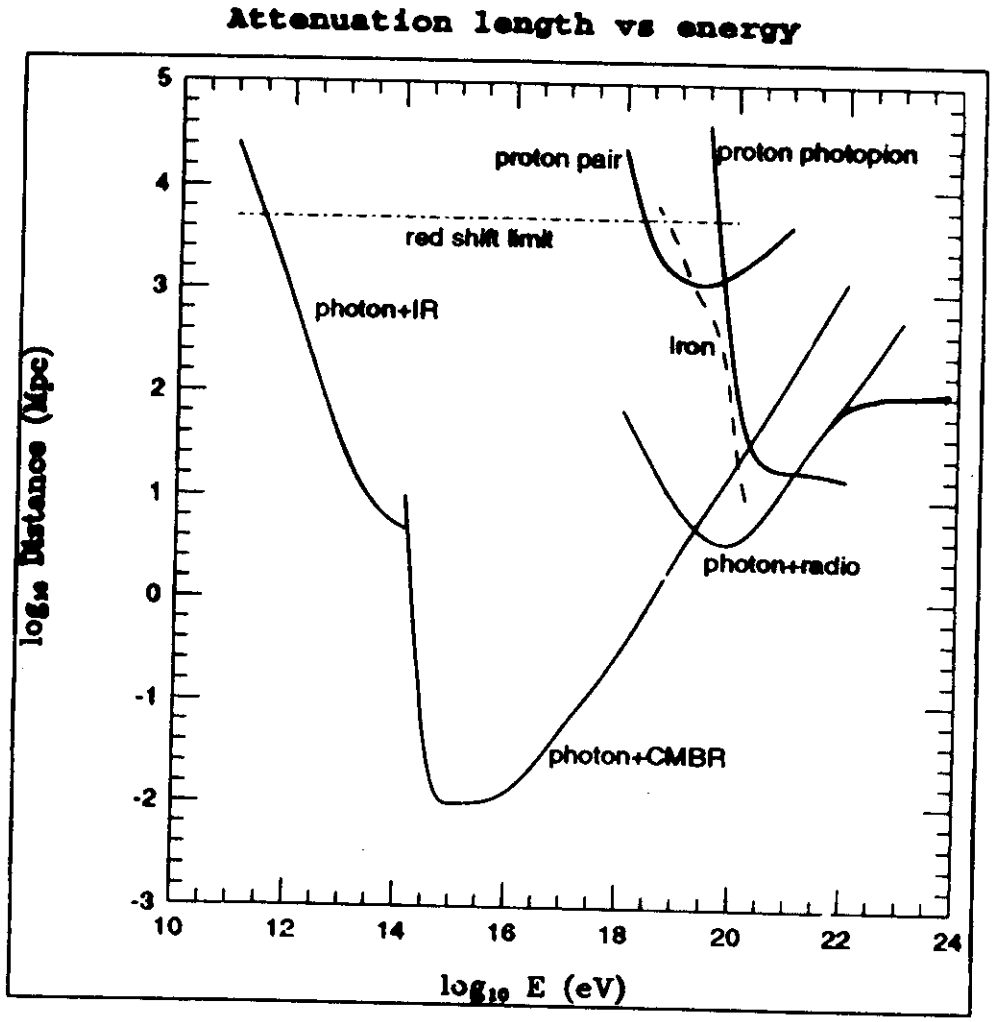

All particles except neutrinos undergo interactions with the CMBR :

This is the GZK cutoff

Greisen - Zatsepin - Kuzmin Effect

threshold:

$$E_{th} = \frac{2 m_N m_\pi + m_\pi^2}{4\varepsilon} \simeq 4 \cdot 10^{19}\,eV \quad \text{in CMB}$$

Limits range of nucleons above few $\cdot 10^{19}$ eV to a few tens of Mpc

=> Source must be in cosmological "backyard"

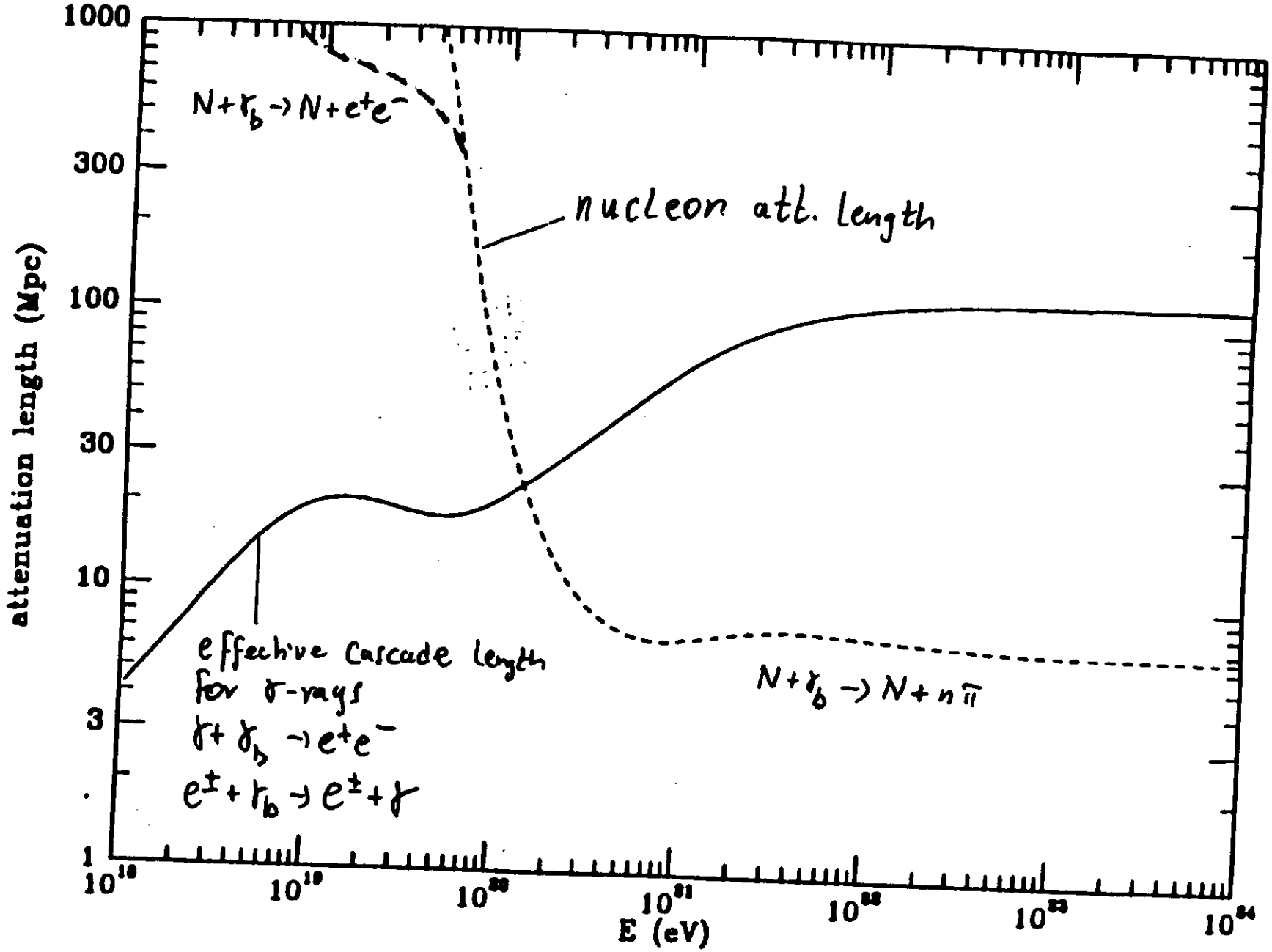

S. Lee, G.S., P. Coppi, in preparation

Origin of Cosmic Rays and Cosmic Magnetic Fields are strongly related Problems

i) CRs up to $\simeq 10^{18}$ eV confined in Galaxy

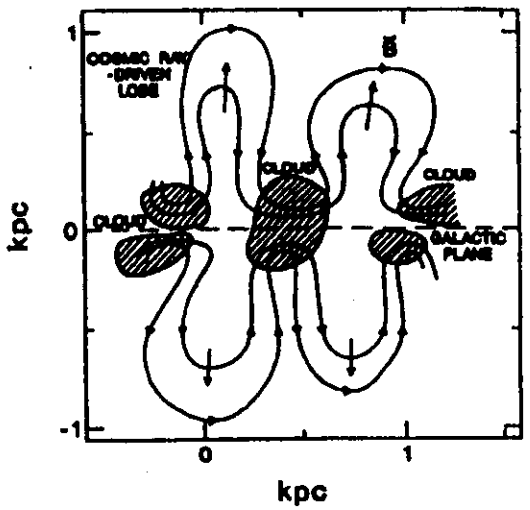

$u_{CR} \simeq u_{BG} \simeq u_{turb} \simeq u_{grav}$

dynamic (unstable) interplay

required luminosity

$L \simeq u_{CR} \cdot V_{gal} / t_{confine} \simeq 0.1 L_{SN}$

$\Rightarrow$ Galactic Origin ?

ii) CRs $\gtrsim 10^{19}$ eV deflect in extragalactic fields B_{xG}

- influences anisotropy
- weak correlation to Supergalactic Plane
- deflection $\lesssim 10^{\circ}$ above 10^{20} eV

$\Rightarrow$ particle astronomy, probe B_{xG}

iii) B_{xG} and B_G are related:

$$B_{xG} \simeq (10^{-6} - 10^{-3})\, B_G$$

if B_G produced by compression, B_{xG} primordial

$$B_{xG} \simeq 10^{-20}\ G$$

if dynamo produces B_G

iv) Magnetic Fields can be main Players in CR acceleration

Cosmic Magnetic Fields

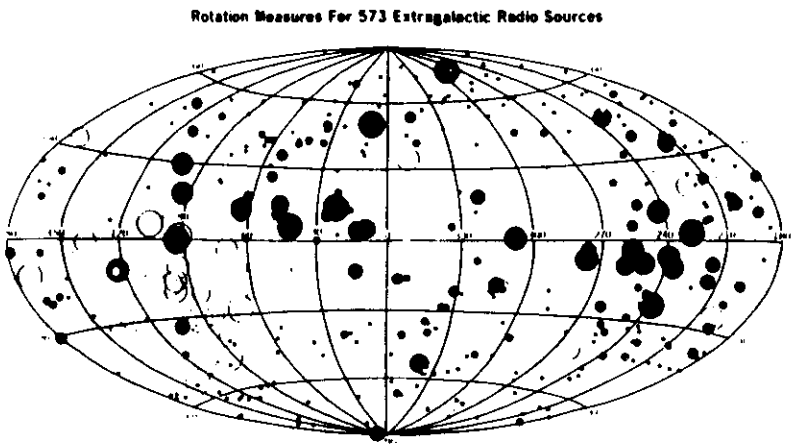

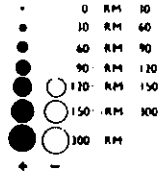

$$RM \propto \int n_e B_{\parallel} \, dl$$

$$B_{\text{Large scale}} \lesssim 10^{-9} \left(\frac{l_c}{1\,\text{Mpc}}\right)^{-1/2} \text{G}$$

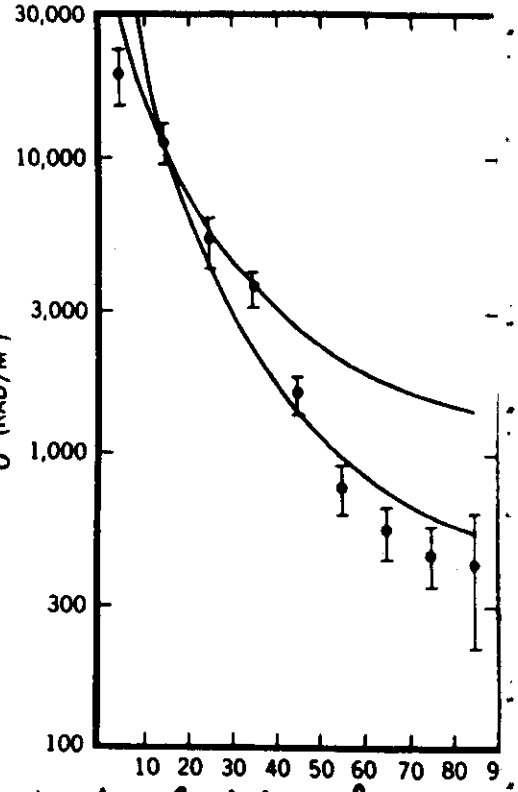

halo field of our Galaxy

NGC4631 VLA D-array 6cm + B-field

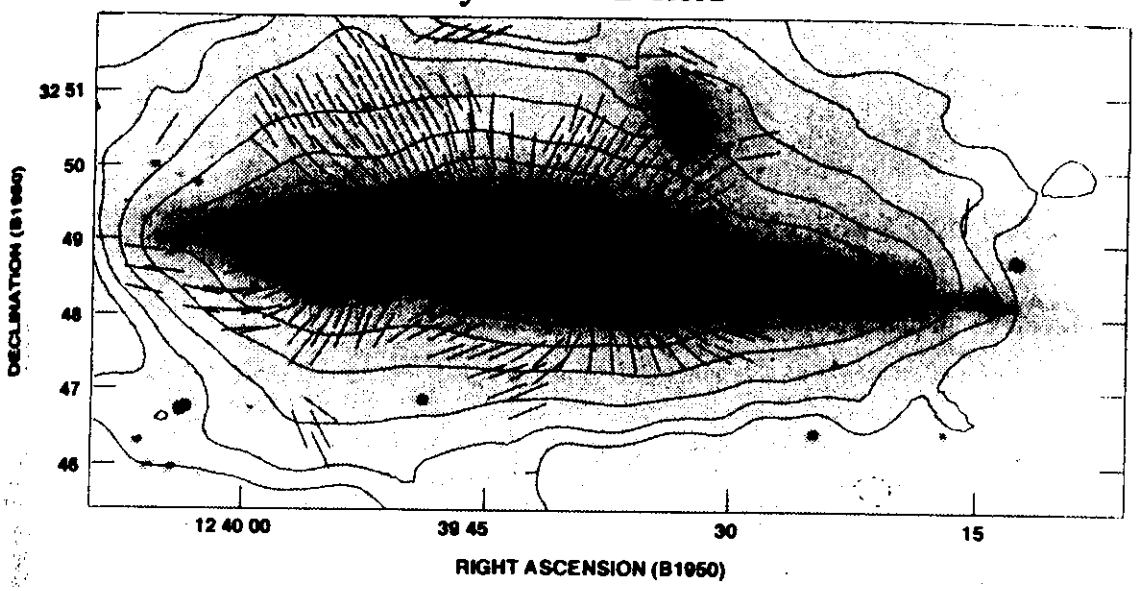

galactic fields

galaxy cluster fields

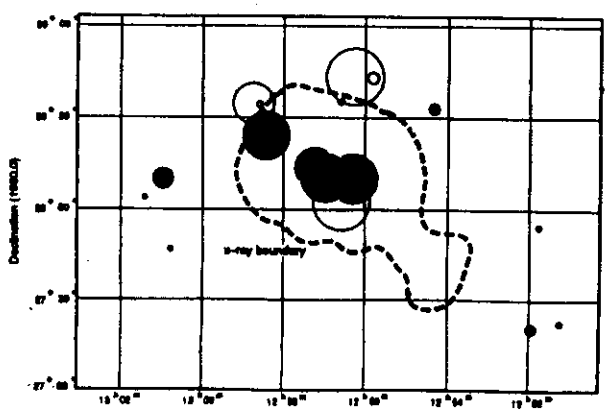

Why angular resolution needed?

Limits : sampling rate of electronics

physical fluctuations

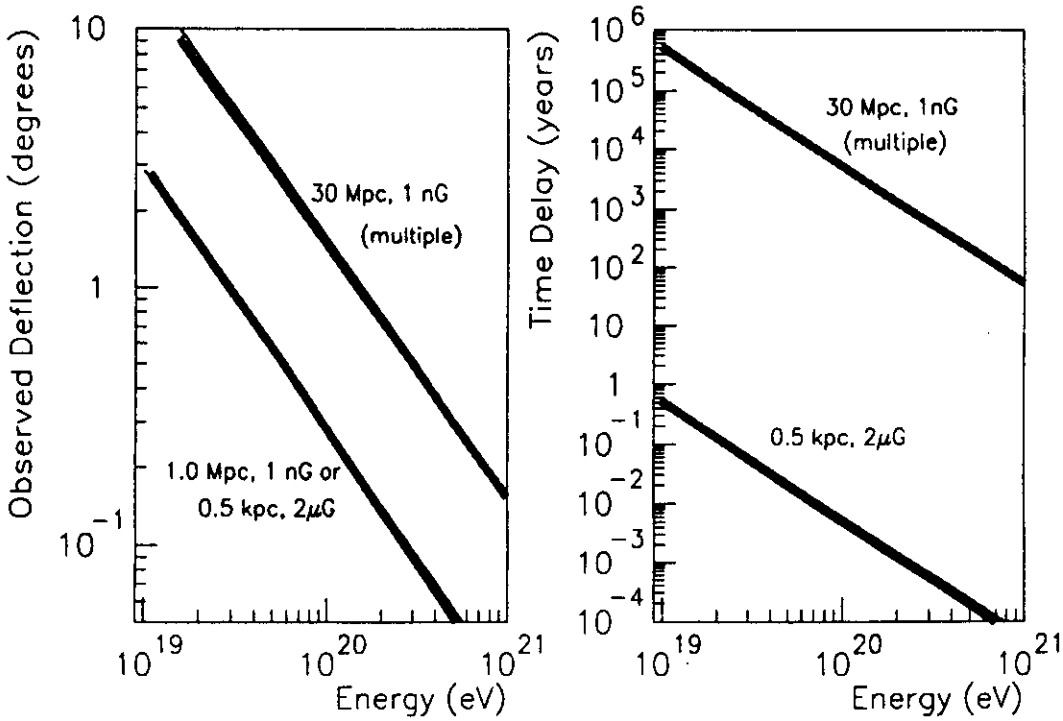

Pierre Auger $\Delta\theta$ **for a vertical shower:**

	10 EeV	100 EeV
Array alone	2°	<1°
Hybrid	0.25°	0.20°

Proton astronomy possible !

AGASA data

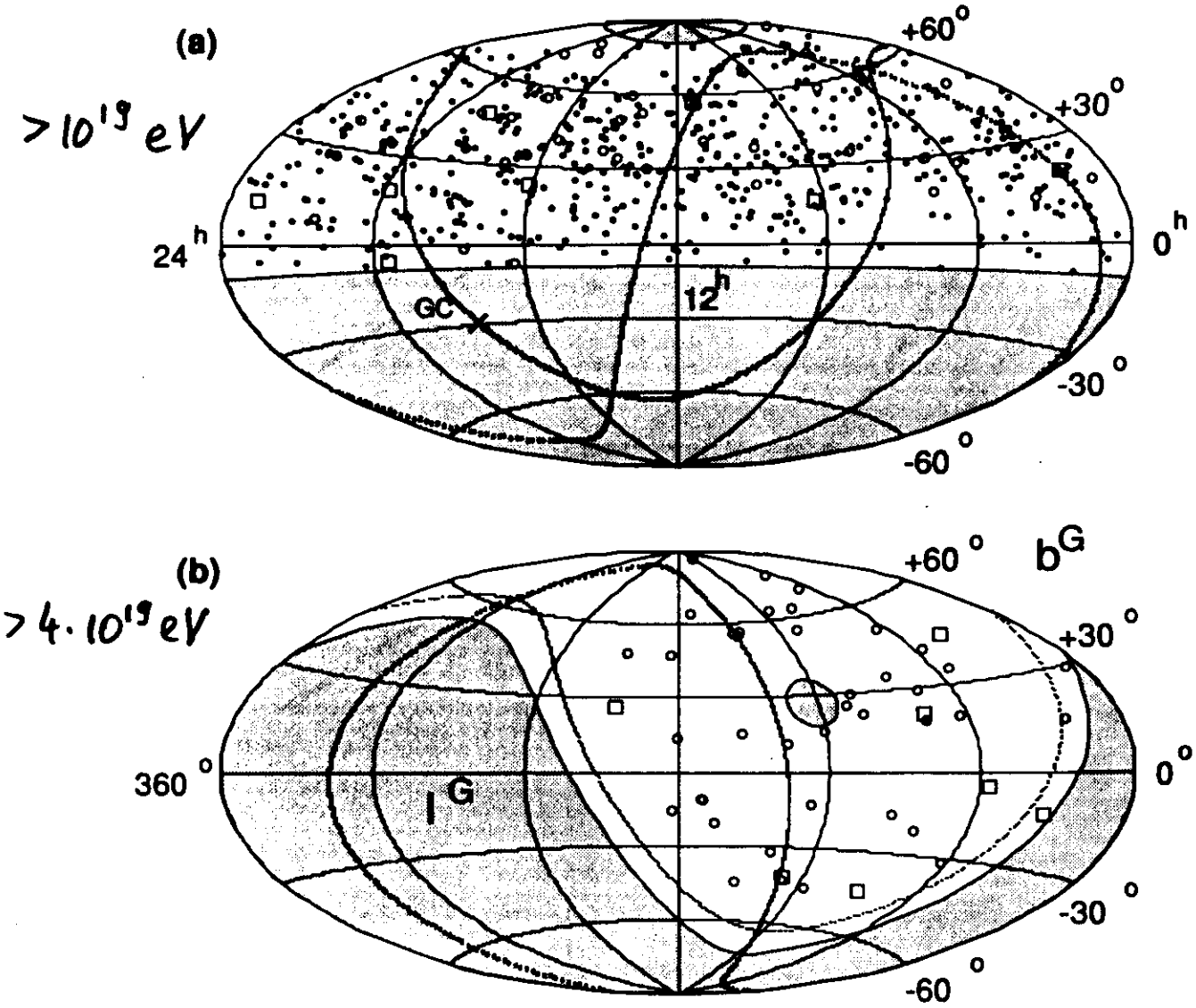

blue = Supergalactic Plane, red = Galactic Plane

consistent with isotropy, but 3 doublets and 1 triplet within 2.5° above 4×10^{19} eV

out of 47 total events

$\simeq$ 0.3% chance from isotropic distribution

AGASA data

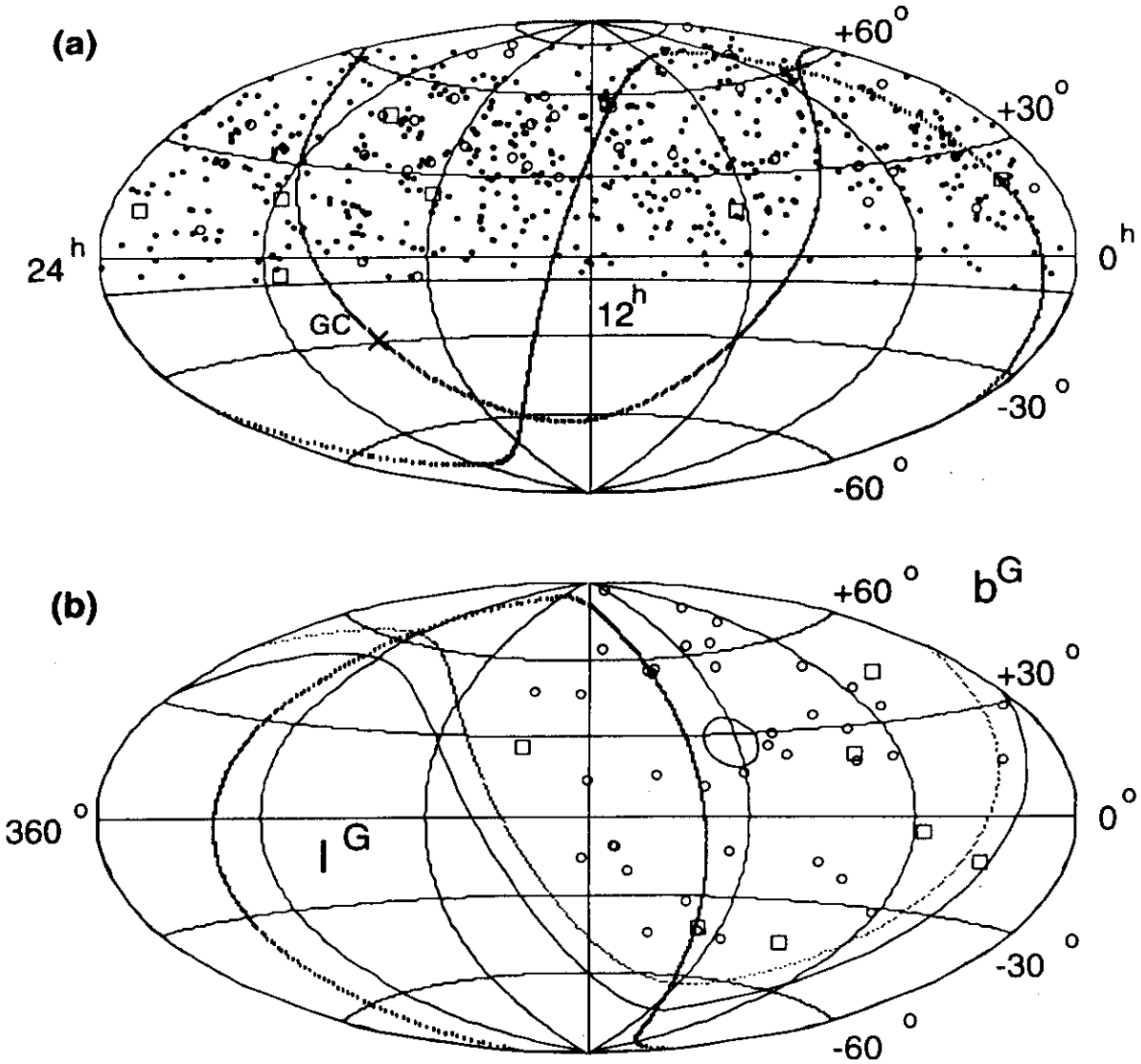

blue=Supergalactic Plane, red=Galactic Plane

581 events above 10^{19} eV, 47 above 4×10^{19} eV, 7 above 10^{20} eV

2.) Acceleration versus "Top-Down" Scenarios

Acceleration

The most widely accepted model of CR production is 1st order Fermi acceleration at magnetized astrophysical shocks.

upstream medium encounters shock with velocity u_1

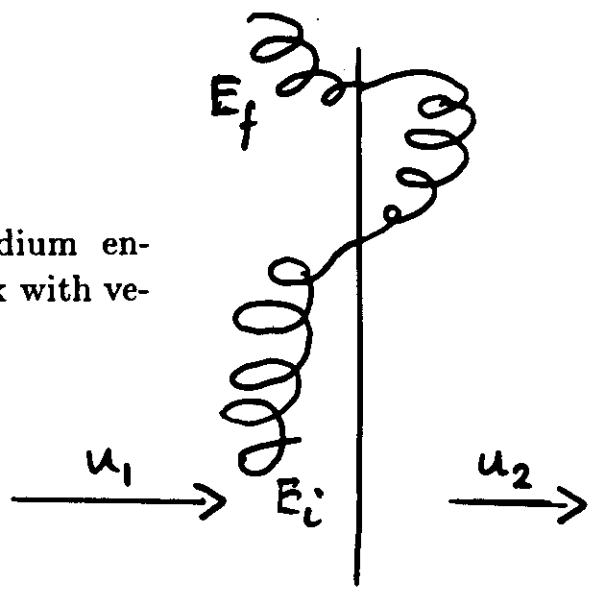

downstream medium streams away from shock with velocity u_2

Average fractional energy gain per shock crossing

$$\xi = \frac{\langle E_f - E_i \rangle}{E_i} = \frac{4}{3}\frac{u_1 - u_2}{c}$$

Together with the loss processes this leads to a power-law spectrum with index $q \geq 2$. Maximum energy comes from the condition that the gyro-radius of the charged particle is smaller than the spatial extent of the shock.

$$E_{\max} \leq 10^{18}\, Z \left(\frac{R_{\text{shock}}}{\text{kpc}}\right)\left(\frac{B}{\mu\text{G}}\right)$$

For optimistic models of AGN, e.g., $E_{\max} \leq 10^{21}$ eV.

"Hillas plot" for proton accelerators

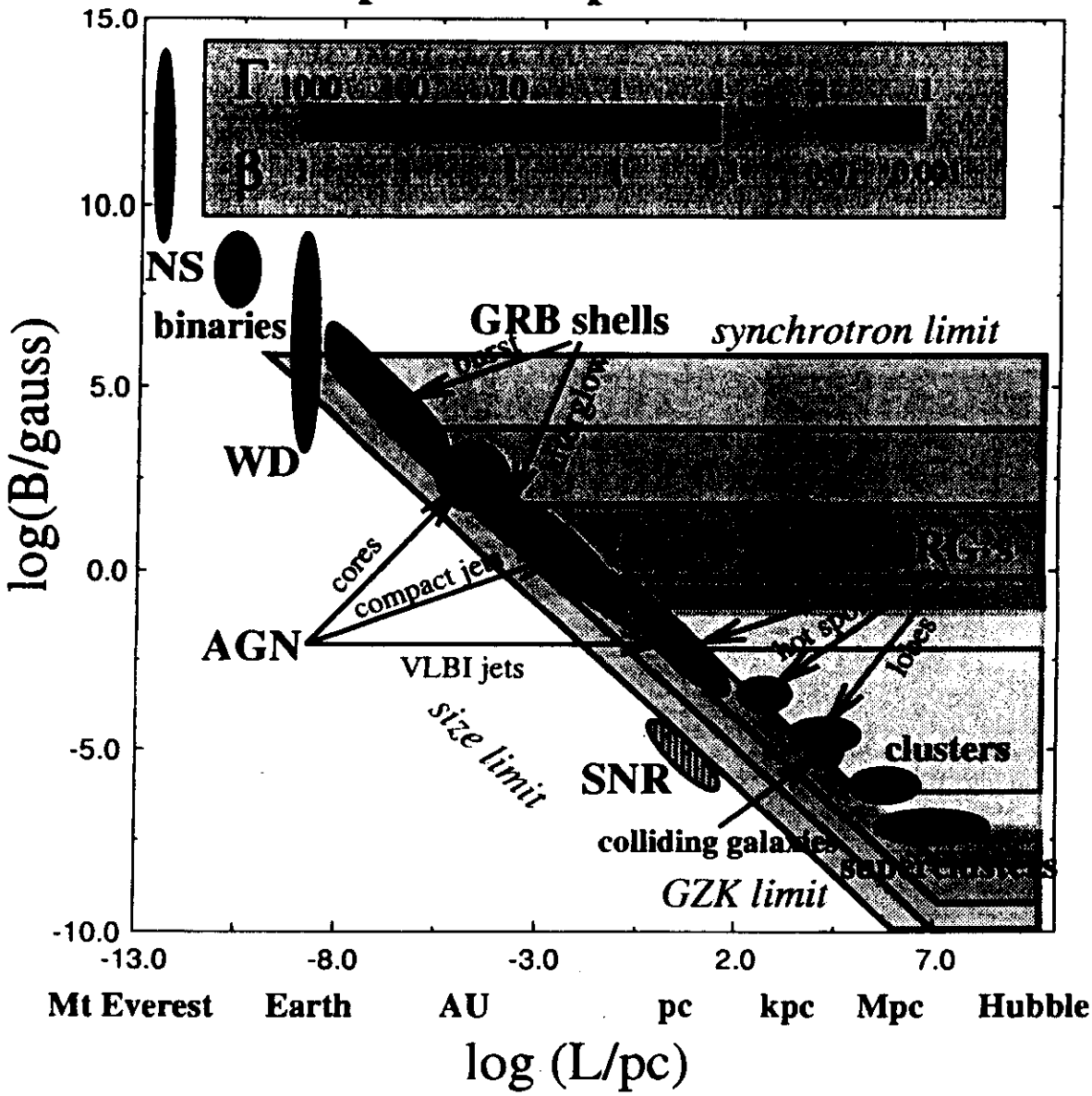

Total nonthermal luminosity of object class determines "brightness"

Core of Galaxy NGC 4261

Hubble Space Telescope

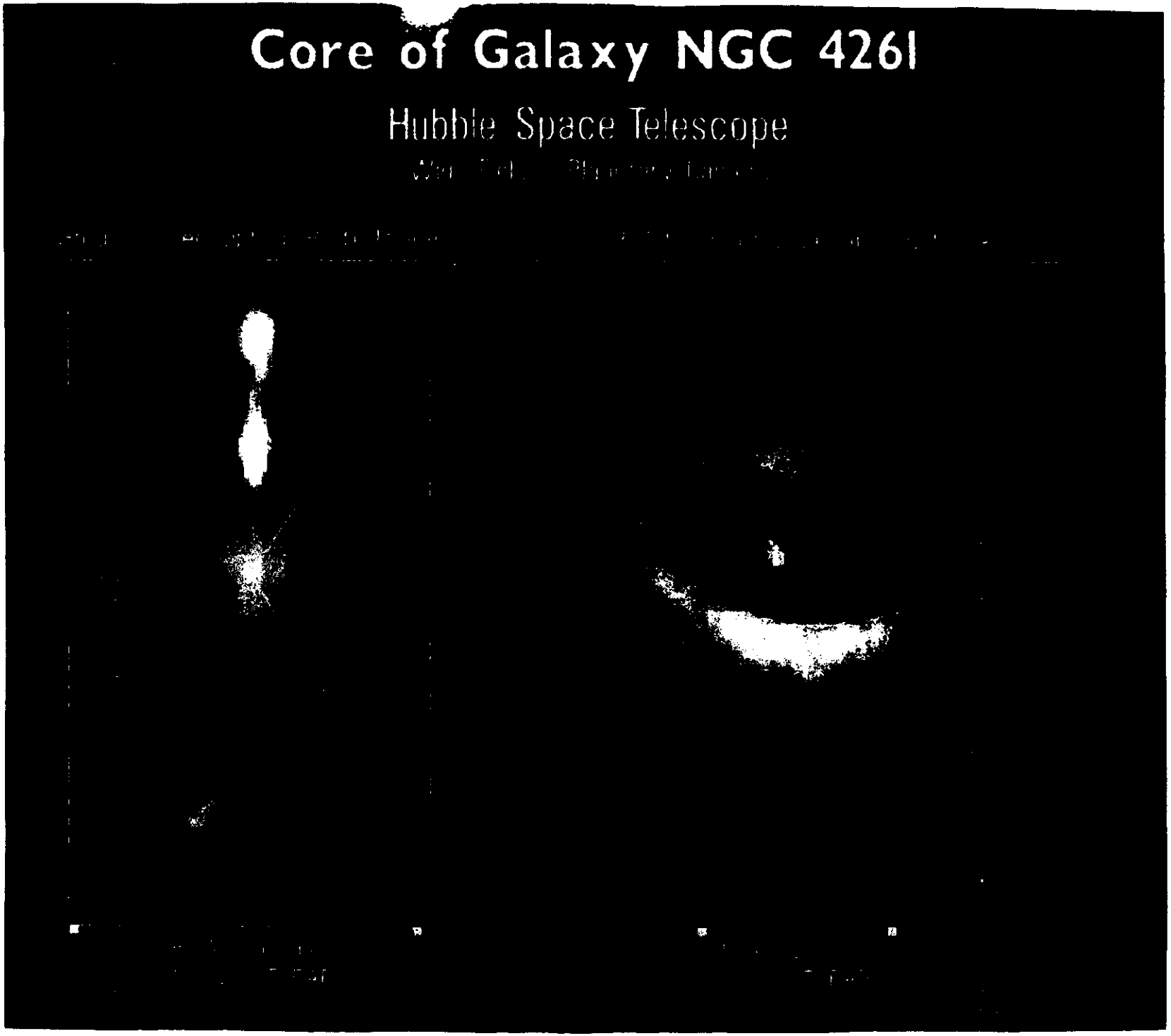

Proton maximum energy

- Acceleration timescale:

$$\boxed{t_{\rm acc} = \theta\, t_{\rm Larmor} \propto E_p/B}$$

  - 1st order Fermi: $\theta \sim y^2\, \beta_{\rm sh}^{-2} \geq 1$
  - 2nd order Fermi: $\theta \sim y^2\, \beta_{\rm A}^{-2} \gg 1$

  [$y = (B/\delta B)^2$, measures mean free path]

- **Relativistic shocks ($\beta_{\rm sh} \approx 1$) can accelerate particles on their Larmor timescale**

- Maximum proton energy: $\boxed{t_{\rm acc} = t_{\rm loss}}$

  - $t_{\rm loss}^{-1} = t_{\rm ad}^{-1} + t_{\rm syn}^{-1} + t_{p\gamma}^{-1}$
  - $t_{\rm ad} = R/v_{\rm exp}$, $t_{\rm syn} \propto E_p^{-1} B^{-2}$, $t_{p\gamma} \propto E_p^{\alpha} L^{-1}$

  [α = photon spectral index]

- **Larmor limit:** $E_p \leq eBR$

ELLIPTICAL GALAXY NGC 4261
Wide Field/Planetary Camera vs
National Radio Astronomy Observatory

STSCI PR-92-27A

Left:- Ground Based Composite Visual/Radio View: The giant elliptical galaxy NGC 4261 is one of the twelve brightest galaxies in the Virgo cluster, located 45 million light-years away. Photographed in visible light (white) the galaxy appears as a fuzzy disk of hundreds of billions of stars. A radio image (orange) shows a pair of opposed jets emanating from the nucleus and spanning a distance of 88,000 light-years.

Right:- HST Image of NGC 4261: A giant disk of cold gas and dust fuels a possible black hole at the core of the galaxy. Estimated to be 300 light-years across, the disk is tipped enough (about 60 degrees) to provide astronomers with a clear view of the bright hub, which presumably harbors the black hole. The dark, dusty disk represents a cold outer region which extends inwards to an ultra-hot accretion disk with a few hundred million miles from the suspected black hole. This disk feeds matter into the black hole, where gravity compresses and heats the material. Hot gas rushes from the vicinity of the black hole's creating the radio jets. The jets are aligned perpendicular to the disk, like an axel through a wheel. This provides strong circumstantial evidence for the existence of black hole "central engine" in NGC 4261.

"Hillas Plot" with losses

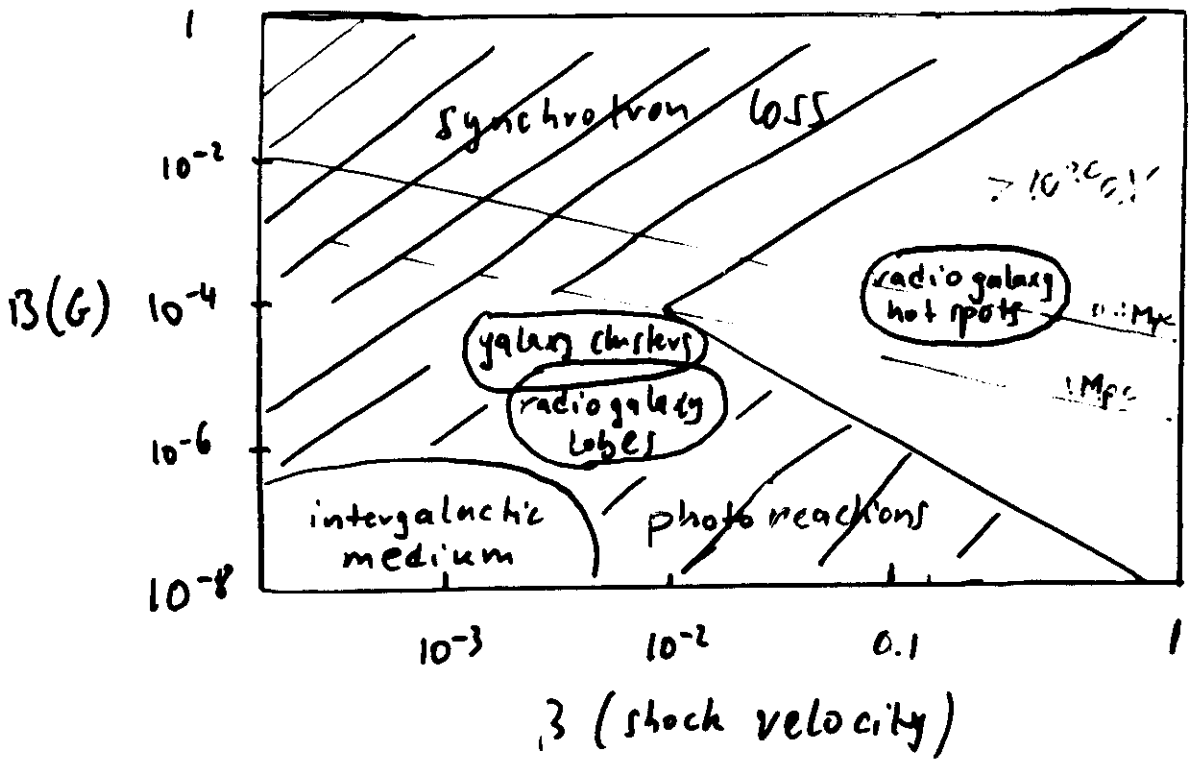

only radio galaxy hot spots survive as source candidates

Signature of UHE cosmic rays

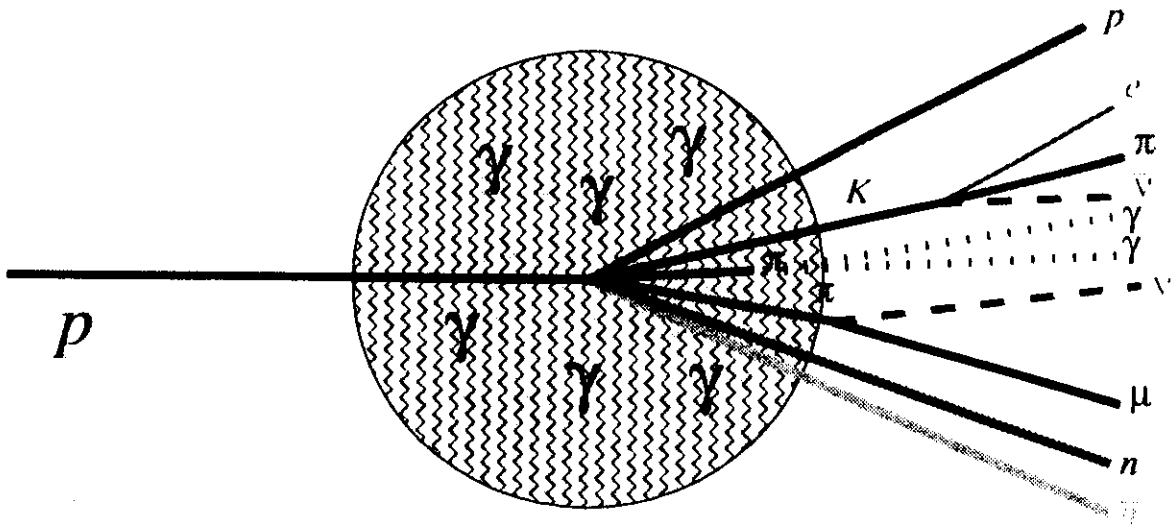

Photohadronic interactions produce

- Neutrons $\longrightarrow$ cosmic ray ejection
- Neutrinos
- Gamma-rays

} comparable power due to isospin symmetry

with comparable luminosities

Co-accelerated electrons provide target photons

Flux per decade (νF_ν), erg/cm² second
10⁻¹⁰
10⁻¹¹
10⁻¹²
10
15
20
25
log frequency (Hertz)
Markarian 421 – broad-band spectrum
Radio
Infrared
Optical / UV
X-rays
γ rays
VLA
HST
EUVE
ROSAT
EGRET
Cerenkov
log (E/eV)

SSC = Synchrotron-Self Compton
SS-PIC = Synchrotron-Self Proton Induced Cascades

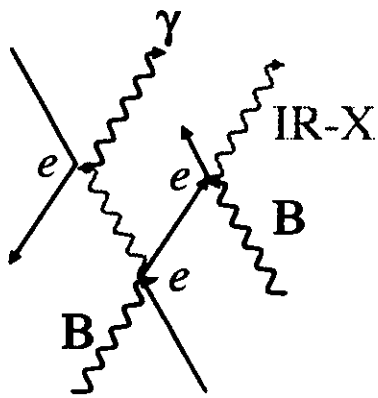

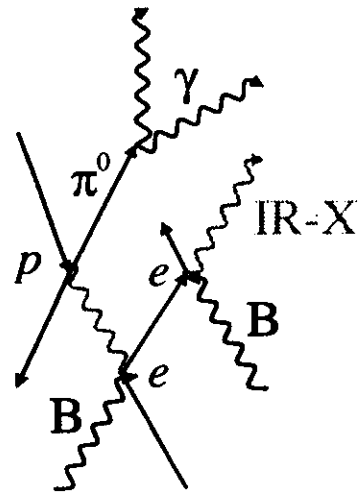

SSC

leptonic

synchrotron-self Compton

$$L_{\rm SSC} = L_{\rm t}\frac{u_{\rm ph}}{u_B}$$

SS-PIC

hadronic

synchrotron-self proton induced cascade

$$L_{\rm PIC} = L_p\frac{\sigma_{p\gamma}\kappa_\gamma u_{\rm ph}}{\epsilon_{\rm th}/2\gamma_p}$$

$$\gamma_p = eBR: \quad \frac{L_{\rm PIC}}{L_{\rm SSC}} \sim 0.1\frac{L_p}{L_{\rm t}}\left[\frac{B}{\rm G}\right]^3\left[\frac{R}{10^{16}\,\rm cm}\right]^2$$

Rough model independent estimates in jet models.

i) acceleration size $R \simeq \gamma t$
(boost; variability time scale)

ii) magnetic field strength $B^2 \simeq \beta(\text{electron})$
(equipartition)

iii) gyroradius determines E_{max}

$$E_{max} \simeq eBR$$

$$E_{max,\nu} \simeq 0.1\, E_{max}$$

($p\gamma \to \pi$ kinematics)

iv) $L_\nu \simeq \frac{3}{13} L_\gamma$
($p\gamma \to \pi$ kinematics)

assume $\frac{dN_p}{dE_p} \propto E^{-2-\varepsilon}$ $\frac{dN_\gamma}{dE_\gamma} \propto E^{-2-\alpha}$

$\Rightarrow$ $\frac{dN_\nu}{dE_\nu} \propto E_\nu^{-1-\varepsilon+\alpha}$ in optically thin jet

everything taken together:

$$\frac{dN_\nu}{dE_\nu} \simeq \frac{3}{13} \frac{L_\gamma}{E_{\nu max}} \frac{1-\varepsilon+\alpha}{E_\nu} \left(\frac{E_\nu}{E_{\nu max}}\right)^{-\varepsilon+\alpha}$$

v) fold in luminosity function of AGNs

$\Rightarrow$ diffuse spectrum

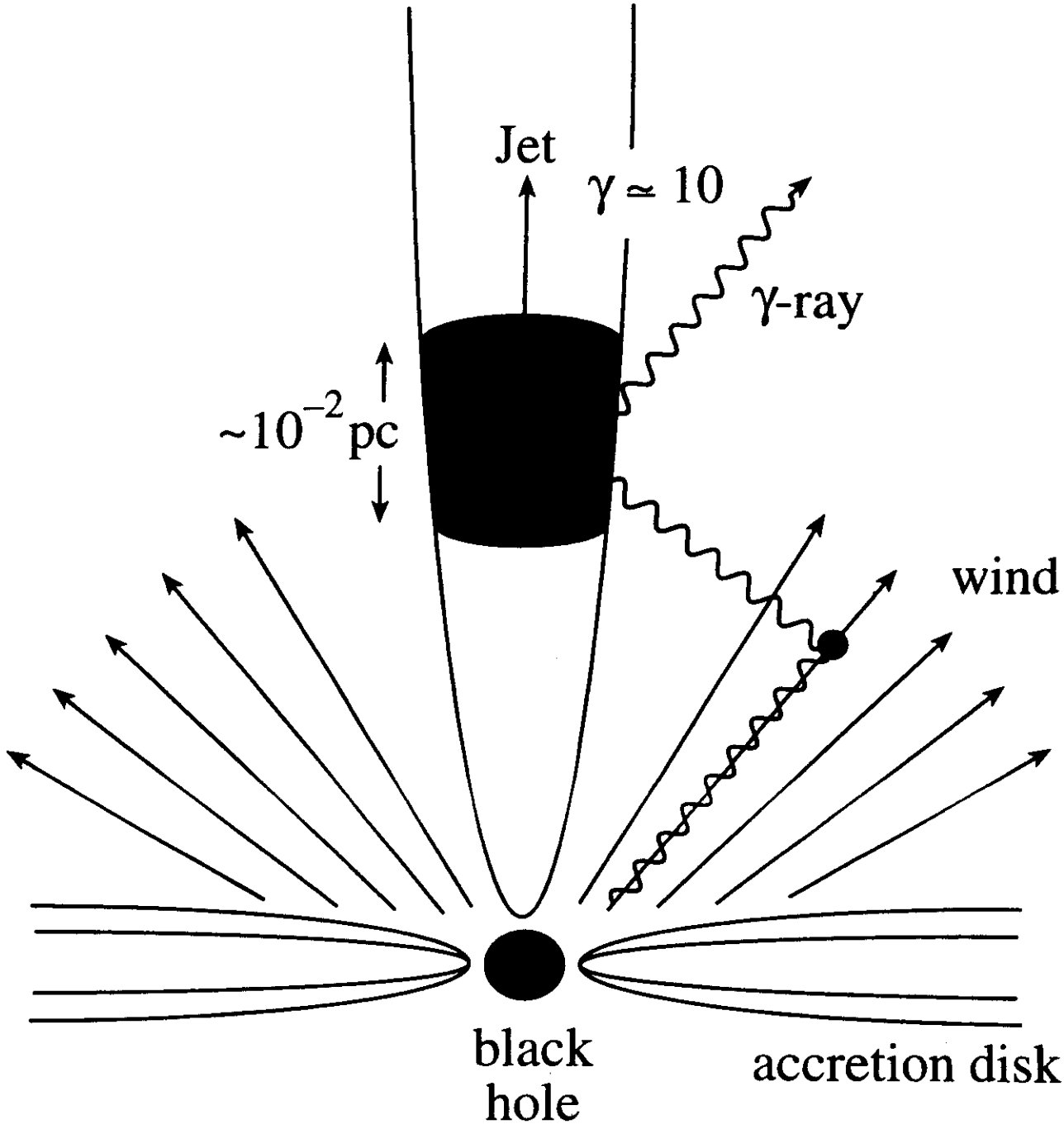

Most AGN ν emission models concern production in jets due to limited proton acceleration in optically thick AGN cores.

Rough approximation of jet models:

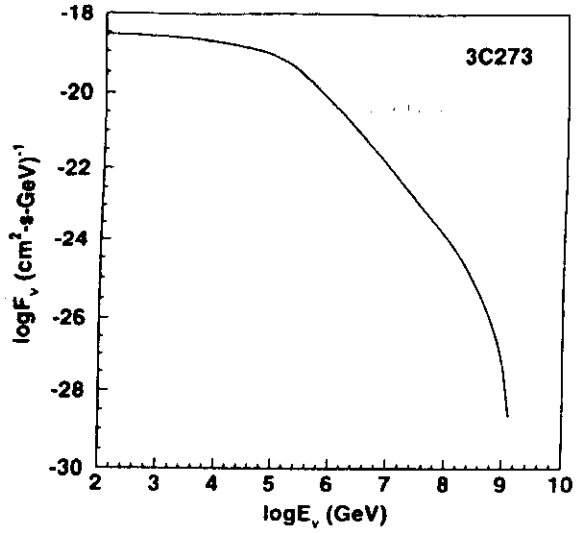

Fig. 1. The predicted $\nu_\mu + \bar{\nu}_\mu$ flux from 3C273, with $L_x = 10^{47}$ ergs s^{-1} (Piccinotti, *et al.* 1982) and redshift $z = 0.158$. (A Hubble constant of 50 km-s^{-1}-Mpc^{-1} has been assumed in our calculations.) Note that the $\nu_e + \bar{\nu}_e$ flux is half that of the $\nu_\mu + \bar{\nu}_\mu$ flux.

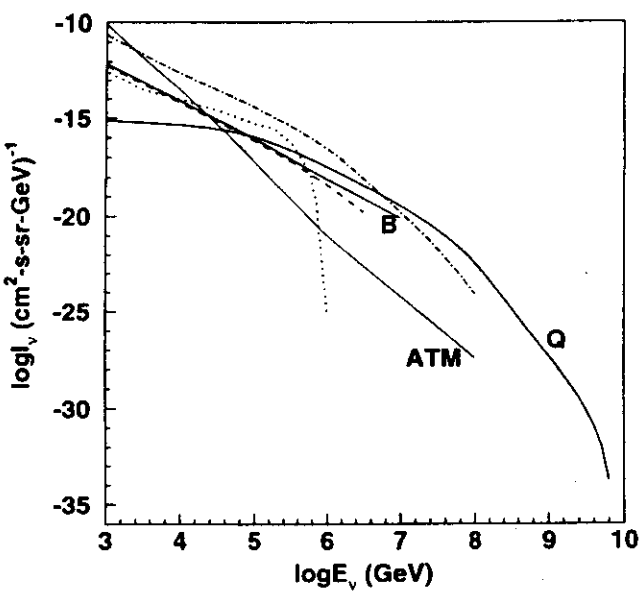

Fig. 2. Our revised integrated high energy $\nu_\mu + \bar{\nu}_\mu$ neutrino background from quasars (Q) and blazars (B) (thick solid lines), as well as the fluxes calculated by Sikora and Begelman (1992) (dotted line), Biermann (1992) (dashed line), and the geometric mean for the $b = 1$ model of Szabo and Protheroe (1994) (dash-dot line). Also shown is the horizontal $\nu_\mu + \bar{\nu}_\mu$ flux from high energy cosmic rays interacting with the Earth's atmosphere (ATM, solid line) (Stecker 1979).

Flux estimates in the Stecker et al. core model

Quasar accretion disk shock required

i) UV and X ray luminosity

$$L \sim 4\pi R_S^2 \int \varepsilon n(\varepsilon)\, d\varepsilon \simeq 0.1\, L_{edd} \sim \frac{GMm_p}{\sigma_T}$$

$$\Rightarrow \quad n(\varepsilon) \propto \frac{1}{\varepsilon^2}$$

spectral shape known observationally

ii) proton acceleration

$$t_{acc} \propto \frac{D}{u} \sim \frac{E_p}{B}$$

(D: diff. const; u: shock vel.)

Bohm diffusion

iii) $B^2 \sim \int \varepsilon n(\varepsilon)\, d\varepsilon \propto L^{-1}$

iv) pion production loss

$$t_{p\gamma} \simeq \left(\int_{E_{th}}^{\infty} n(\varepsilon) d\varepsilon \cdot \sigma_{p\gamma} \right)^{-1}$$

E_{max} follows from $t_{acc} \simeq t_{p\gamma}$

v) ν spectrum follows p spectrum due to optically thick AGN core

$$L_{\nu_\mu} \simeq 0.4 L_X \quad (\text{kin.}) \qquad L_{\nu_e} \simeq 0.2 L_X \quad (\text{kin.})$$

vi) fold in luminosity function

$\Rightarrow$ diffuse spectrum

2 NEUTRINO FLUX PREDICTIONS

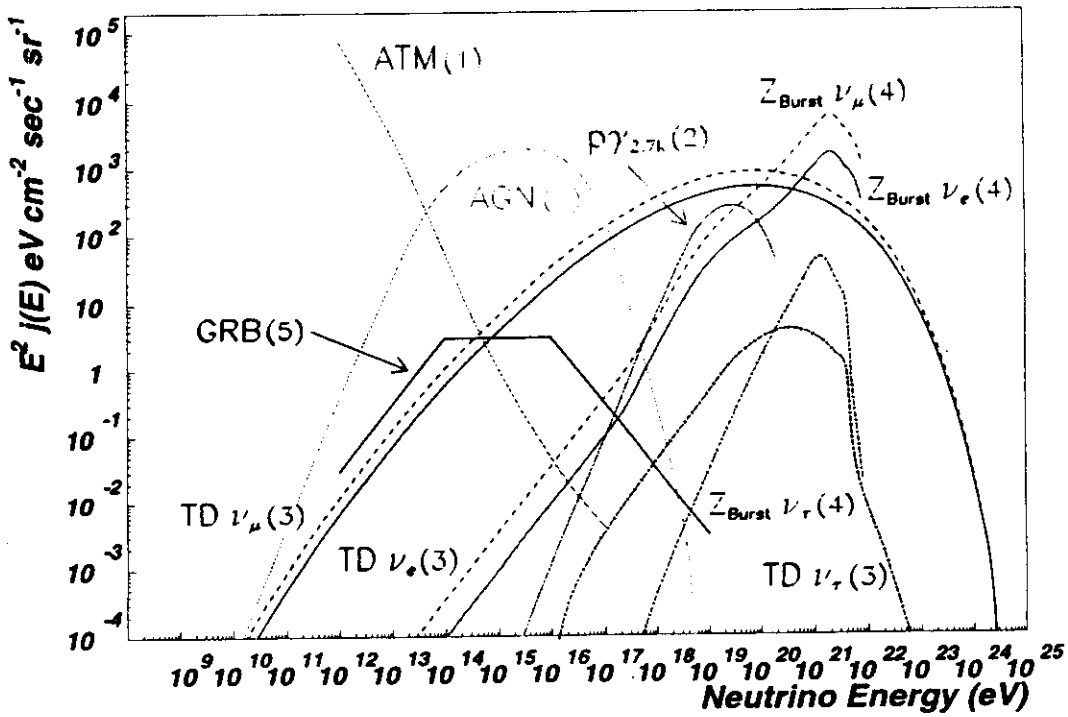

Figure 1: Neutrino flux predictions: Atmospheric and AGN (1: Stecker & Salamon 1996, Space Sci Rev 75, 341), photomeson production via $p\gamma_{2.7K}$ (2: Stecker, Done, Salamon, & Sommers 1991, Phys. Rev. Letters 66, 2697), topological defects (3: Sigl, Lee, Bhattacharjee, & Yoshida 1998, Phys. Rev. D 59, 043504), $m_X = 10^{16}$ GeV, X $\rightarrow$ q + q, supersymmetric fragmention), Z_{Burst} (4: Yoshida, Sigl, & Lee 1998, Phys. Rev. Letters 81, 5055), $m_\nu = 1$ eV, Primary $\Phi_\nu \sim E^{-1}$), and gamma ray bursts (5: Waxman & Bahcall 1997, Phys. Rev. Letters 78, 2292).

Figure 1 illustrates the high energy neutrino flux predictions from various astrophysical sources as a function of neutrino energy. Note that curves show the differential neutrino flux multiplied by E_ν^2 which is equivalent to an energy flux. In the energy range of $10^{14} to 10^{17}$ eV, the AGN neutrino flux is predicted to dominate over other sources. However, neutrinos from individual gamma-ray bursts may be observable via their directionality and short, intense time characteristics. The time-averaged

Diffuse neutrino fluxes

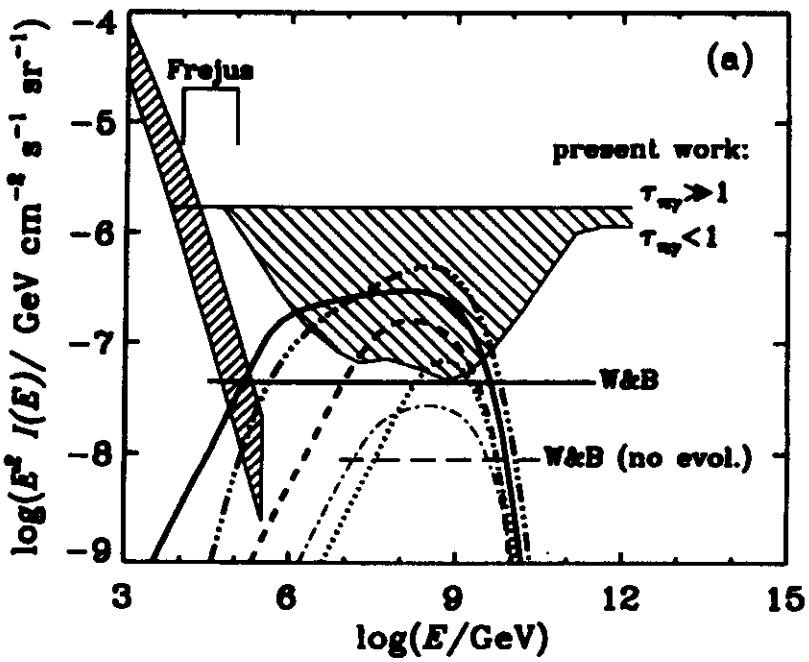

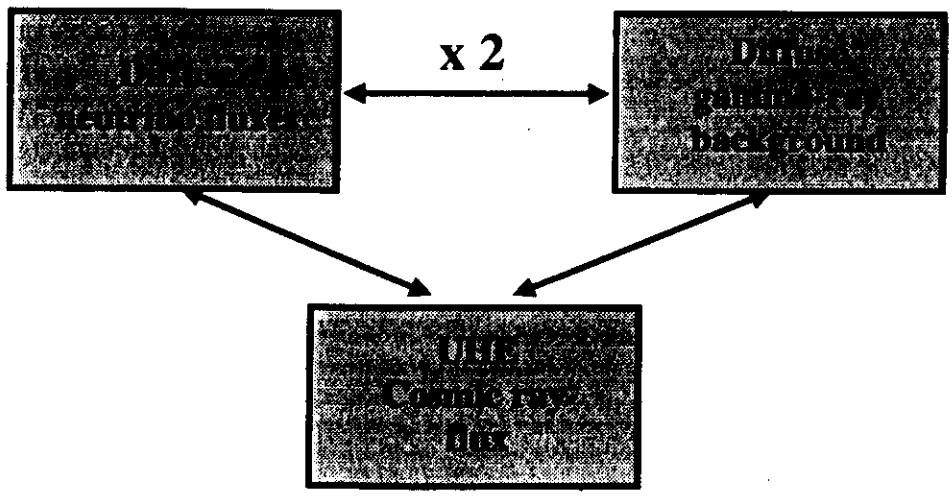

Ultra high Energy Cosmic Rays and the Connection to High Energy γ-Ray and Neutrino Astrophysics

Accelerated protons interact:

$$p + \begin{matrix} N \\ \gamma \end{matrix} \longrightarrow X + \begin{matrix} \pi^{\pm} \rightarrow \text{neutrinos} \\ \pi^{0} \rightarrow \gamma\text{-rays} \end{matrix} \Big\} \text{comparable production rate}$$

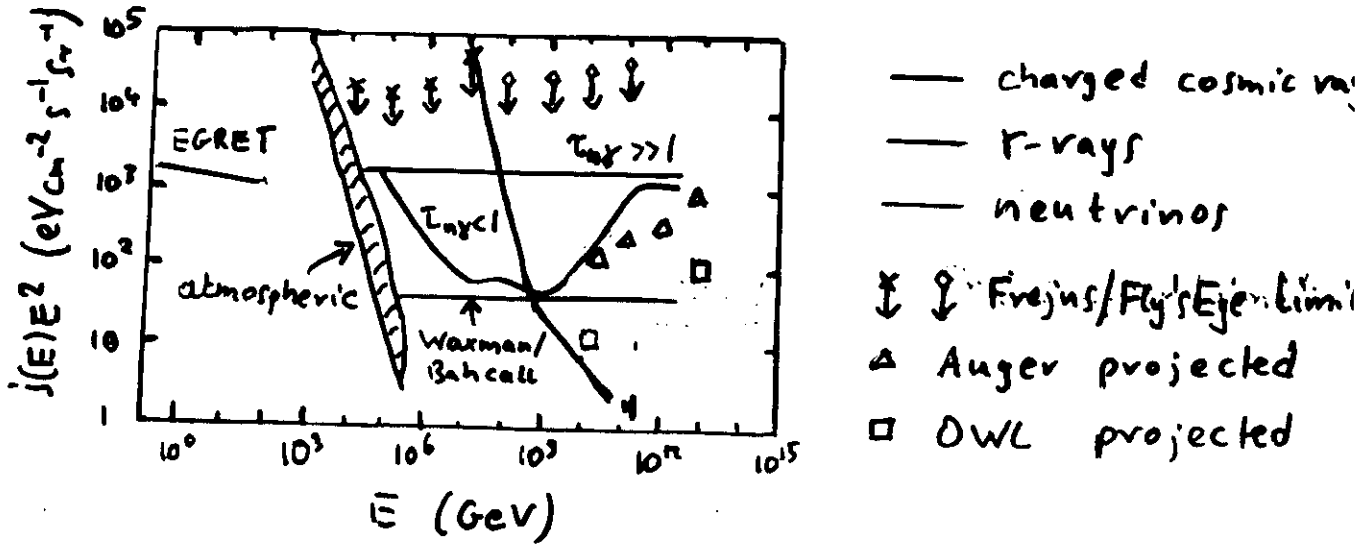

Mannheim, Protheroe, Rachen

Note: ν flux upper limit for transparent sources ($\tau_{n\gamma} < 1$) determined by cosmic ray flux at 10^{18}-10^{19} eV

ν flux upper limit for opaque sources ($\tau_{n\gamma} \gg 1$) determined by diffuse γ-ray flux at 1-100 GeV

Limits do not apply to non-acceleration mechanisms

Alternatively: "Top-Down"

decay of new, heavy particles of mass $\gtrsim 10^{12}$ GeV

relics of the Big Bang

i) Long Lived massive free particles (WIMPZILLA DM)

UHE cosmic ray flux $\Rightarrow$

$$\Omega_X \sim 10^{-12} (t_X / 10^{10}\,\mathrm{yr})$$

$\longrightarrow$ fine tuning problem for t_X

$\longrightarrow$ NOT for Ω_X if gravitational production

$\longrightarrow$ problematic with clustering ?

$\longrightarrow$ correlation with galactic halo expected

ii) particles released from topological defects

scaling $\Rightarrow$ $\rho_{defect} \propto \rho_c \propto t^{-2}$

example: cosmic strings Hill, Schramm, ...

$$\rho_{string} \simeq v^2 t^{-2}$$

v = symmetry breaking scale

$\Rightarrow$

$$\dot{\rho}_X \simeq (\text{branching ratio into } X) \cdot v^2 \cdot t^{-3}$$

Big bang survivors may cause cosmic showers

THE DISCOVERY of cosmic rays at energies so high that they push the limits of current detectors may settle a 30-year-old dispute in cosmology. Earth is continually bombarded by cosmic rays in the form of subatomic particles such as protons. Those at the highest energies are created when, for example, an exploding star accelerates particles from its interior. But Günther Sigl of Fermilab in Chicago, US, and his colleagues say that they may also be created by the decay of even higher energy particles that are left over from the big bang.

Ultrahigh-energy cosmic rays have a million times more energy than the most energetic particles created in accelerators on Earth: above 10^{18} electron volts. In 1966 three physicists proposed that above this energy level (the Greisen-Zatsepin-Kuzmin cutoff) cosmic rays would be energetic enough to interact with photons from the microwave background radiation—remnants of the big bang. In doing so, they would be slowed down to lower energies. So there would be 100 times fewer cosmic rays with ultrahigh energy from extragalactic sources than otherwise predicted.

But over the past two years, scientists have found more cosmic rays with energies significantly above the cutoff point than expected. These are among the highest energy cosmic rays that detectors can pick up.

Two complementary techniques have been used to find them. One looks for the tiny flashes of light that are created when cosmic rays hit the particles of the upper atmosphere. More than 100 spherical mirrors, each 1·5 metres across, capture images of the night sky and direct this light to detectors. The second approach detects the showers of charged particles that are created along with the light. These also create flashes of light that can be detected in an array of lightproof chambers.

'Unfortunately, there are no clearly identifiable nearby candidate sources'

If these cosmic rays were lower-energy particles that had been accelerated by exploding stars, then their numbers would tail off at very high energies. But Sigl and his colleagues say that the numbers actually increase at the highest energies. Alternatively, these cosmic rays may not have had the opportunity to interact with photons, which is possible if they came from a source less than 10 million light years away. "Unfortunately, there are no clearly identifiable nearby candidate sources," says Sigl.

Sigl's latest study suggests another possibility. "These ultrahigh-energy events might be produced by decay from some higher energy scale rather than by acceleration," he says (Fermilab preprint, Pub 95/148A). This could create many more particles at high energies, which would explain the recovery in numbers.

One particle that could decay to produce ultrahigh-energy cosmic rays is the hypothetical particle "X" which may have existed shortly after the big bang. Theorists suspect that at that time there was just one force holding matter together. In the lower energies of today's Universe, this manifests itself as the four fundamental forces of gravity, electromagnetism, and the strong and weak nuclear forces.

To test this theory, physicists try to reunite the forces at high energies in particle accelerators. They have already identified the force-carrying particle that unifies the electromagnetic force with the weak nuclear force. Particle "X" could do the same for the electroweak force and the strong nuclear force. Sigl and his colleagues say folds in the Universe—similar to black holes—could harbour "X" particles left over from the big bang. These may then escape from the fold and decay to produce ultrahigh-energy cosmic rays. **Alison Goddard**

A thermal history of the Universe

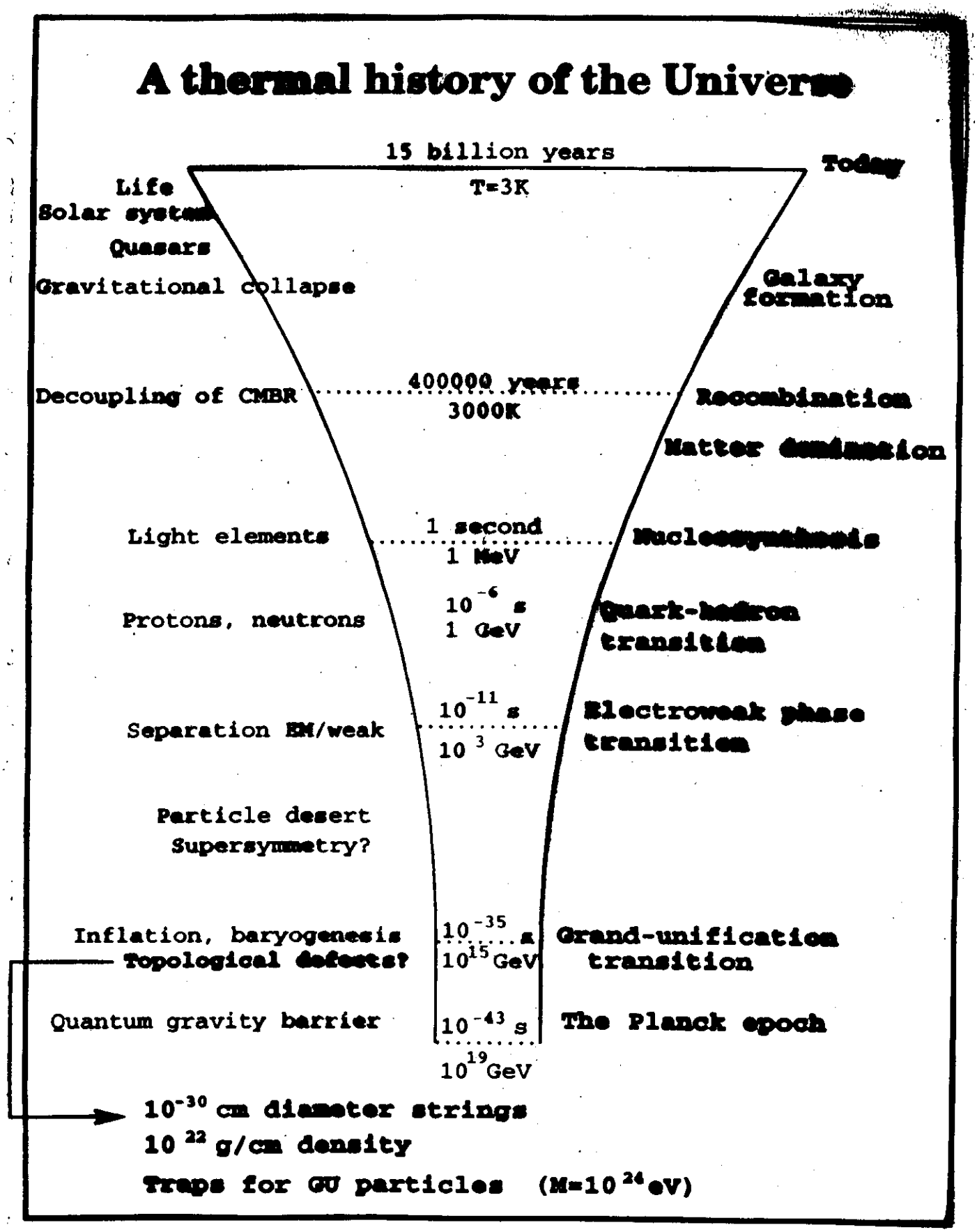

The Inflationary Paradigm

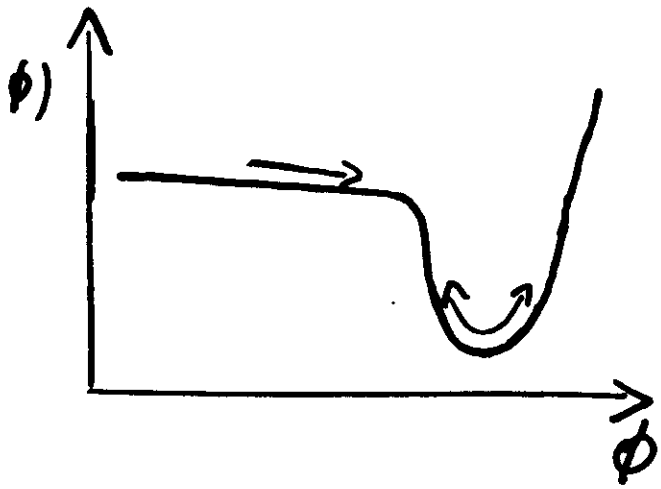

fundamental scalar ϕ

$$\mathcal{L}(\phi) = \frac{1}{2}\nabla_a\phi\nabla^a\phi - V(\phi)$$

$$\left(\frac{\dot{a}}{a}\right)^2 \equiv H^2 = \frac{8\pi G}{3}\rho - \frac{k}{a^2} \Rightarrow \quad a \propto \begin{cases} e^{t/t_0} & \rho = \text{const.} \quad \text{vacuum} \\ t^{1/2} & \rho \propto a^{-4} \quad \text{radiation} \\ t^{2/3} & \rho \propto a^{-3} \quad \text{matter} \end{cases}$$

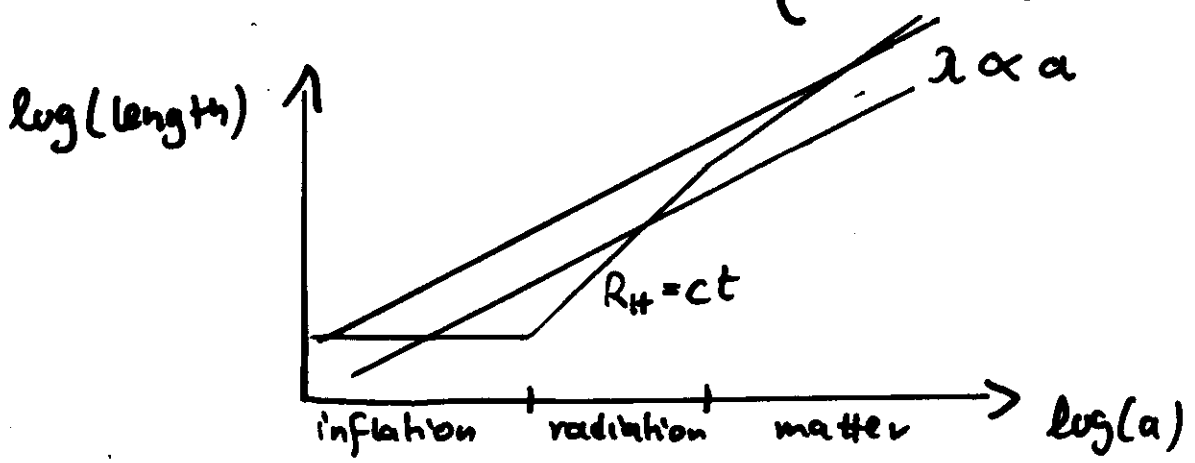

) covelated fluctuations above causal radius R_H measuvable in cosmic microwave background and large scale galaxy structure

$\Rightarrow$ inflation energy scale $H_{inflation} \simeq 10^{13}$ GeV

$\rightarrow$ natural energy scale for relics to explain UHE cosmic rays

In GUTs formation of magnetic monopoles seems unavoidable because $H \supset U_{em}(1) \Rightarrow \Pi_2(G/H) = I$

$\longrightarrow$ overclose Universe

Can be cured by subsequent exponential expansion (inflation)

$$\left(\frac{\dot{a}}{a}\right)^2 \equiv H^2 = \frac{8\pi G}{3}\rho - \frac{k}{a^2}$$

requires $\rho \simeq$ const.

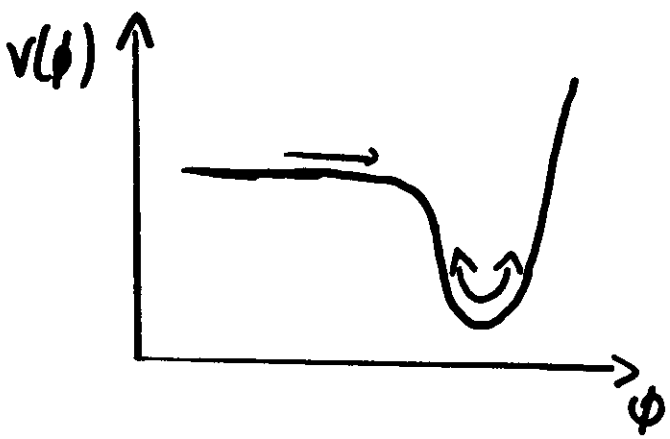

fundamental scalar
= inflaton ϕ

$\rho = \dot{\phi}^2/2 + V(\phi)$

$\Longrightarrow$ particle and/or defect creation must happen during reheating after inflation

$$\mathcal{L} = \frac{1}{2}\nabla_\mu\phi\partial^\mu\phi - V(\phi) + \frac{1}{2}\nabla_\mu X \partial^\mu X - \frac{1}{2}m_X^2 X^2 + \frac{1}{2}\xi R X^2 + \mathcal{L}_{int}(\phi, X)$$

$$T_{\mu\nu} = \nabla_\mu\phi\,\nabla_\nu\phi + \nabla_\mu X \nabla_\nu X - \mathcal{L}\, g_{\mu\nu}$$

$$G_{\mu\nu} = 8\pi G\, T_{\mu\nu} \qquad \text{gravitation}$$

$$\nabla^\mu\nabla_\mu\phi + V'(\phi) - \frac{\partial\mathcal{L}_{int}}{\partial\phi}(\phi, X) = 0 \qquad \text{inflaton}$$

$$\nabla^\mu\nabla_\mu X - \xi R X - \frac{\partial\mathcal{L}_{int}}{\partial X}(\phi, X) = 0 \qquad \text{matter field } X$$

$\longrightarrow$ non-linear instabilities

microwave background sets scale to $H_{inflation} \sim 10^{13}$ GeV

$\Rightarrow$ natural scale for relics to explain UHE cosmic rays

Particle Production after Inflation

i) thermal production of cold relics:

$$\Gamma_{xx} \simeq \tilde{\sigma}_{xx} T^3 e^{-m_x/T} \; ; \; H \simeq \frac{T^2}{m_{pl}} \Rightarrow \text{freeze out}$$

$$\Omega_x \simeq 10^{-6} \left[\frac{(100\,\text{GeV})^2}{\tilde{\sigma}_{xx}} \right] \quad \text{today}$$

$\Rightarrow$ TeV scale interactions lead to interesting dark matter abundances

$\longrightarrow$ requires $m_x \lesssim 100\,\text{TeV}$ due to unitarity bound

Heavy ($\gtrsim 10^{12}$ GeV) cold relics

i) gravitational production due to time dependent metric gives $\Omega_x \sim 1$ if $m_x \sim H_{\text{inflation}} \sim 10^{12}$-$10^{13}$ GeV independent of coupling to other fields !!

Kolb, Kuzmin, Riotto, Rubakov, ...

ii) non-thermal production during reheating

if UHE cosmic rays are produced by X decays

$$\Rightarrow \quad m_x \sim 10^{15} \left(\frac{T_{\text{reheat}}}{10^{10}\,\text{GeV}} \right) \quad \text{for } t_x \simeq 10^{10}\,\text{yr}$$

Chung, Kolb, Riotto, ...

v) non-linear parametric resonance with inflaton field

$$\mathcal{L} = \frac{1}{2} \nabla_a \phi \nabla^a \phi - V(\phi) + \frac{1}{2} \nabla_a \chi \nabla^a \chi - \frac{1}{2} m_\chi^2 \chi^2 + \frac{1}{2} \xi R \chi^2 + \mathcal{L}_{int}(\phi, \chi)$$

non-linear (explosive) growth of fluctuations in ϕ, χ, and the metric ?

Can super horizon density fluctuation modes grow exponentially ?

Kolb, Jedamzik, Niemeyer, Sornborger, G.S. ...

In ii) and iv) the physical effect is a time varying frequency with $m_\chi(t)$, $a(t)$

$$\chi_k'' + \omega_k^2 \chi_k = 0 \qquad \omega_k^2 = k^2 - \frac{a''}{a}(1 - 6\xi) + m_\chi^2 a^2$$

$\longrightarrow$ Bogolyubov coefficients

topological defects are unavoidable products of phase transitions associated with symmetry change

Examples:

i) Iron

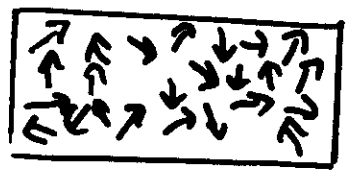

$T > T_{curie}$

$G = SO(3)$

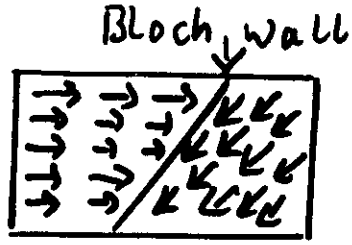

$T < T_{curie}$

$H = SO(2)$

ii) gauge symmetries

e.g. $G = U(1)$, ϕ = complex Higgs field, A_μ = gauge field

$$\mathcal{L} = D_\mu \phi^+ D^\mu \phi - \frac{1}{4} F_{\mu\nu} F^{\mu\nu} - \frac{1}{2}\lambda(\phi^+\phi - v^2)^2$$ Lagrangian

with $D_\mu = \partial_\mu - ig A_\mu$, $F_{\mu\nu} = \partial_\mu A_\nu - \partial_\nu A_\mu$, $v \sim 10^{13}$–10^{16} GeV

has classical string solutions:

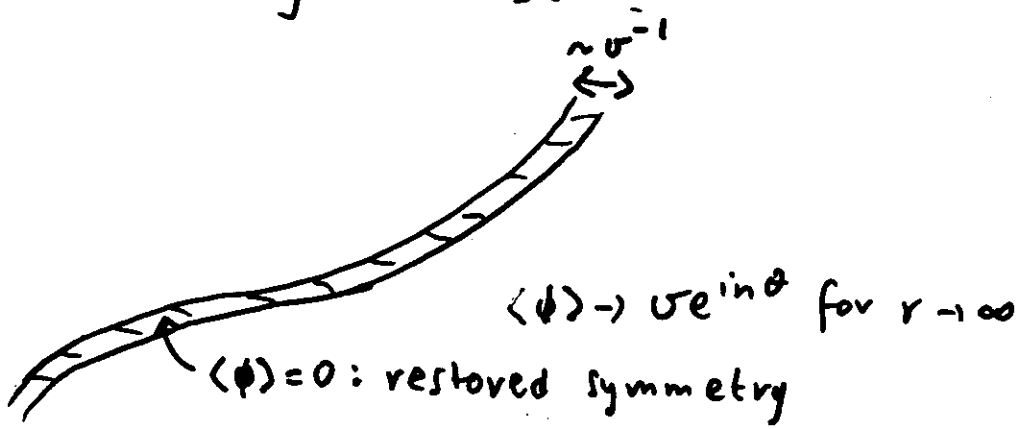

conflicting phase requirements due to, e.g., intersection, leads to unwinding and particle radiation

simulations:

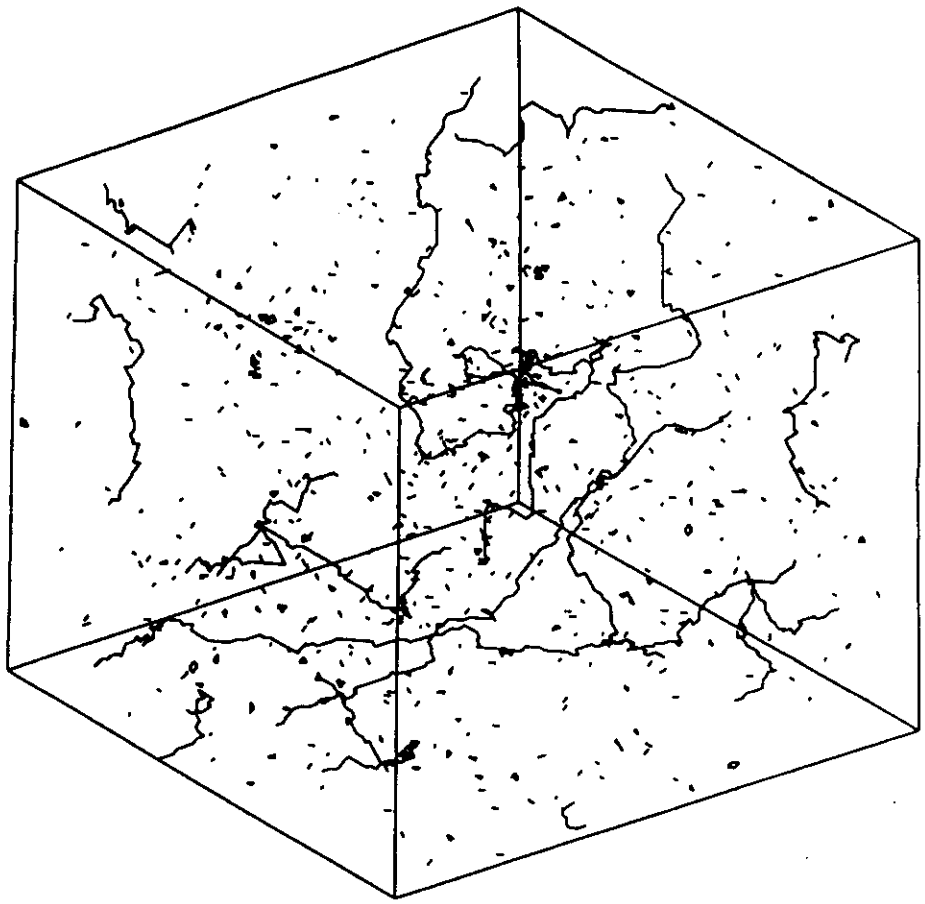

Hindmarsh et al. 1996

experiments:

LETTERS TO NATURE

Laboratory simulation of cosmic string formation in the early Universe using superfluid ^{3}He

C. Bäuerle*, Yu. M. Bunkov*, S. N. Fisher*, H. Godfrin* & G. R. Pickett†

* Centre de Recherches sur les Très Basses Températures, Centre National de la Recherche Scientifique, BP 166, 38042 Grenoble Cedex 9, France
† School of Physics and Chemistry, Lancaster University, Lancaster LA1 4YB, UK

TOPOLOGICAL defects in the geometry of space–time (such as cosmic strings) may have played an important role in the evolution of the early Universe, by supplying initial density fluctuations which seeded the clusters of galaxies that we see today[1]. The formation of cosmic strings during a symmetry-breaking phase transition shortly after the Big Bang is analogous to vortex creation in liquid helium following a rapid transition into the superfluid state; the underlying physics of this cosmological defect-forming process (known as the Kibble mechanism[1]) should therefore be accessible to experimental study. Superfluid vortices have been observed in ^{4}He following rapid quenching to the superfluid state[2], lending qualitative support to Kibble's contention that topological defects are generated by such phase transitions. Here we quantify this process by using an exothermic neutron-induced nuclear reaction to heat small volumes of superfluid ^{3}He above the superfluid transition temperature, and then

The size of the initial domains depends strongly on the rapidity with which the transition is traversed. According to Zurek[3] the distance between the ensuing vortices β is given approximately by $\beta = \xi_0(\tau_Q/\tau_0)^{1/4}$, where ξ_0 is the coherence length at zero temperature, τ_0, the coherence length divided by the Fermi velocity, (ξ_0/v_F), is the characteristic time of the superfluid, and τ_Q is the characteristic time for cooling through the phase transition.

Superfluid ^{3}He has the further advantage as the working substance in that it allows a very precise localized crossing of the phase transition to be generated by nuclear reaction[4], which avoids the more violent global processes used for earlier experiments on ^{4}He and liquid crystals[2,4]. The ^{3}He nucleus has a very high cross-section for neutrons via the process: $n + {}^3\mathrm{He} \rightarrow {}^3\mathrm{H} + p$. This process also liberates a precise energy of 764 keV which is initially shared by the product proton and tritium nucleus. The mean free path of the products in the liquid is limited to around 30 μm as the kinetic energy is rapidly thermalized with the creation of a cloud of quasiparticle excitations and excited ^{3}He atoms providing enough heat to warm a small volume of the liquid to above the superfluid transition. The volume of normal liquid ^{3}He then rapidly recools on a timescale of 1 μs or less.

In a companion experiment[7] Ruutu *et al.* have shown directly that vortices are indeed created in superfluid ^{3}He by this process. They observe unambiguous vortex nucleation triggered by neutron irradiation in a rotating experiment at higher temperatures. In the present experiment we measure how much of the energy released is retained in the liquid in the form of a vortex tangle. As we know the energy of a vortex per unit length, we can go further and make a quantitative calculation of the vortex density remaining which we can compare with Zurek's prediction.

Defect types

i) Monopole-Antimonopole Annihilation
bound state inspiral due to Larmor radiation

$$\frac{d\rho_X}{dt} \propto m_X m_M^{-2} \Omega_M h^2 \xi_f t^{-3}$$

ξ_f = relative bound state
ξ_i = abundance at formati

Hill 1983, Bhattacharjee and G.S. 1995

ii) Saturated superconducting string loops

$$\frac{d\rho_X}{dt} \simeq \frac{L_S}{G} t^{-4} \leftarrow \nabla_0$$

L_S = saturation length

Hill, Schramm, Walker 1987

iii) Ordinary strings

Scaling regime: $\rho_S \simeq v^2 t^{-2}$ (Ω_S = const.)

$$\Rightarrow \frac{d\rho_X}{dt} \simeq f v^2 t^{-3}$$

f = fraction going into X particles

Hindmarsh et al. 1997: $f \simeq 1$

$$\Rightarrow \boxed{v \leq 10^{13} - 10^{14}\ \text{GeV}}$$

Bhattacharjee et al., Wichoski, MacGibbon, Brandenberger

v) Cosmic necklaces (monopoles connected by strings)

$$\frac{d\rho_X}{dt} \simeq r^2 v^2 t^{-3} \qquad r = \frac{\text{monopole energy}}{\text{string energy}}$$

Berezinsky, Vilenkin 1997 Berezinsky, Blasi, Vilenkin 1998

v) Supersymmetric defects
→ Higgs decay contribution to γ-ray background
Bhattacharjee, Shafi, Stecker 1998

vi) vortons entering the atmosphere
Petev 1997

vii) long lived X particles clustering in Galactic halo
Berezinsky, Kachelvieß 1997 Kuzmin, Rubakov, ...

Cosmic Ray Fluxes in Top-Down Scenarios

X particle decay in Grand Unified Theories (GUTs):

Example: $X \to \ell + q\,q$

$\swarrow \quad \searrow$

hadronic jets

must know the hadronic (quark fragmentation) spectrum in the jets

well measured at accelerator energies

within QCD can in principle be extrapolated to GUT energies

together with injection history $d\rho_X/dt$:

$\Longrightarrow$ Cosmic ray fluxes calculable at all energies

$\Longrightarrow$ Constraint on particle physics by comparing with existing data in whole energy range

Example: For $d\rho_X/dt \simeq f v^2 t^{-3}$ (cosmic strings) comparing total injected energy with diffuse γ-ray background

$\sqrt{f}\, v \lesssim 10^{13}\text{-}10^{14}$ GeV Brandenberger, G.J.

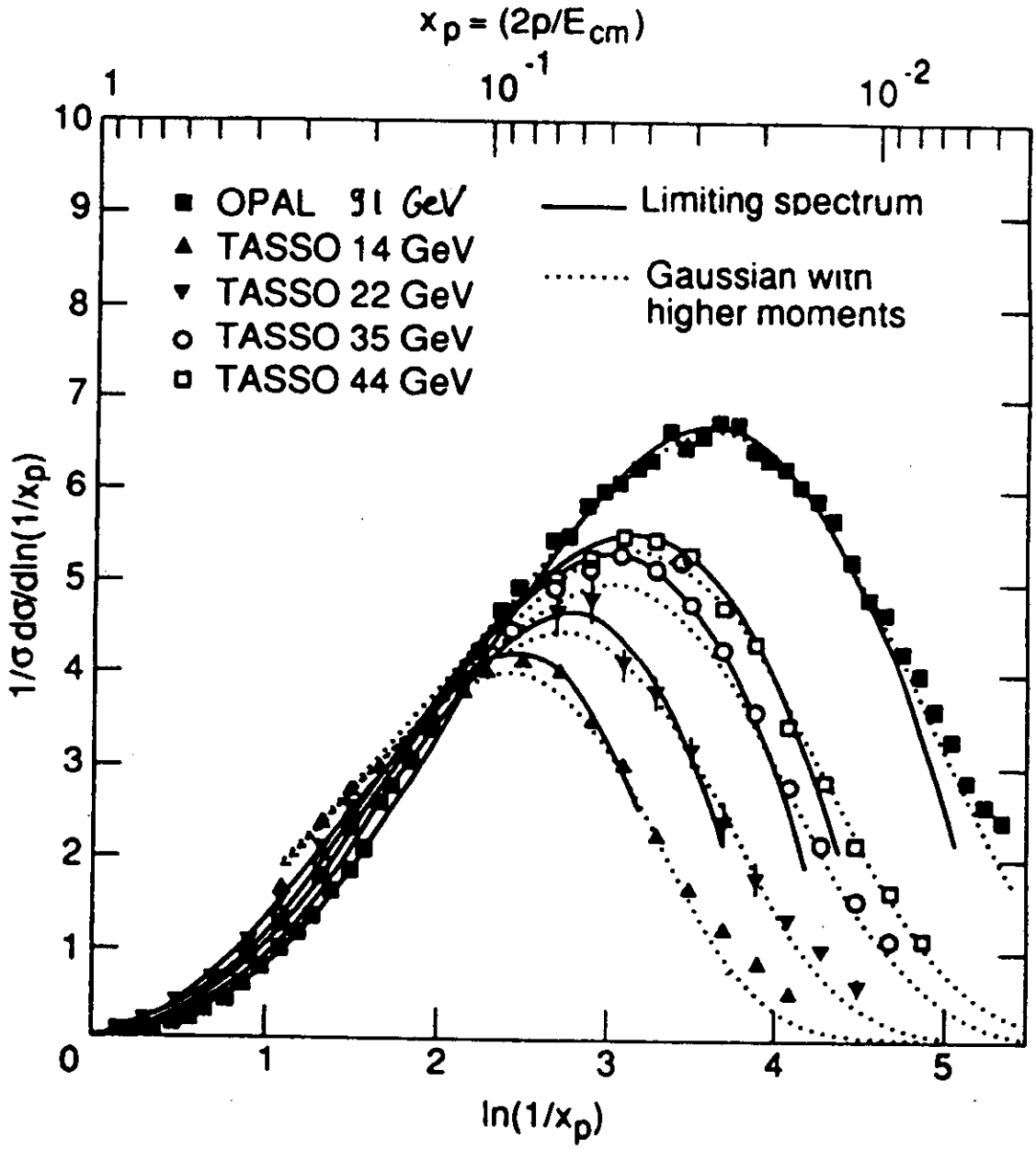

Figure 7.2: $\ln 1/x_p$ distributions of charged hadrons at $W = 14, 22, 35, 44$ and 91 GeV compared with analytical MLLA formula (7.55) and the distorted Gaussian (7.39).

Dokshitzer et al. (1991)

Quark fragmentation

assuming local parton-hadron duality

$E_{max} = 5 \cdot 10^{15}$ GeV

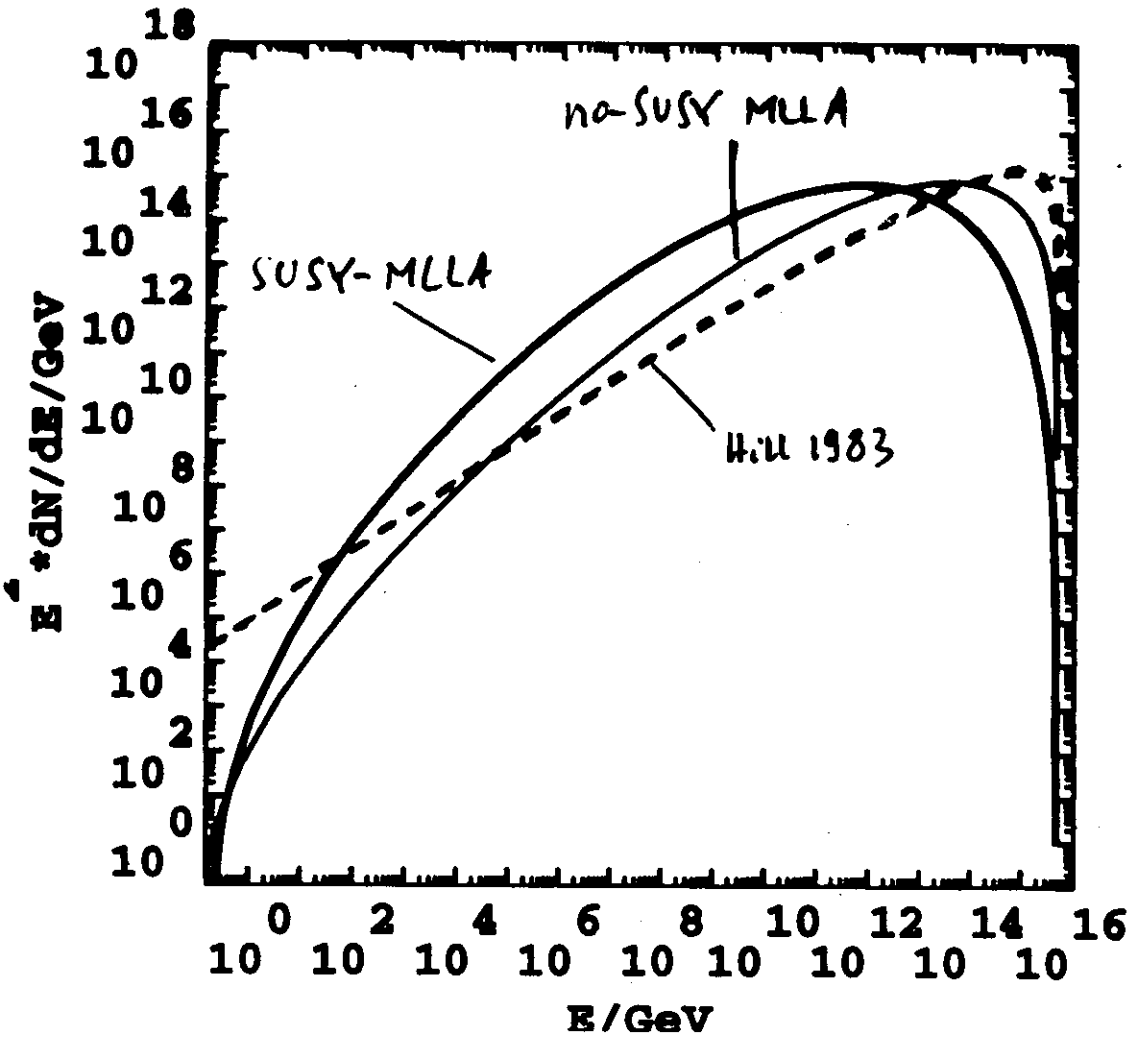

MLLA = modified leading logarithmic approximation

Dokshitzer et al.

to the DGLAP equation

Acceleration

protons ↓

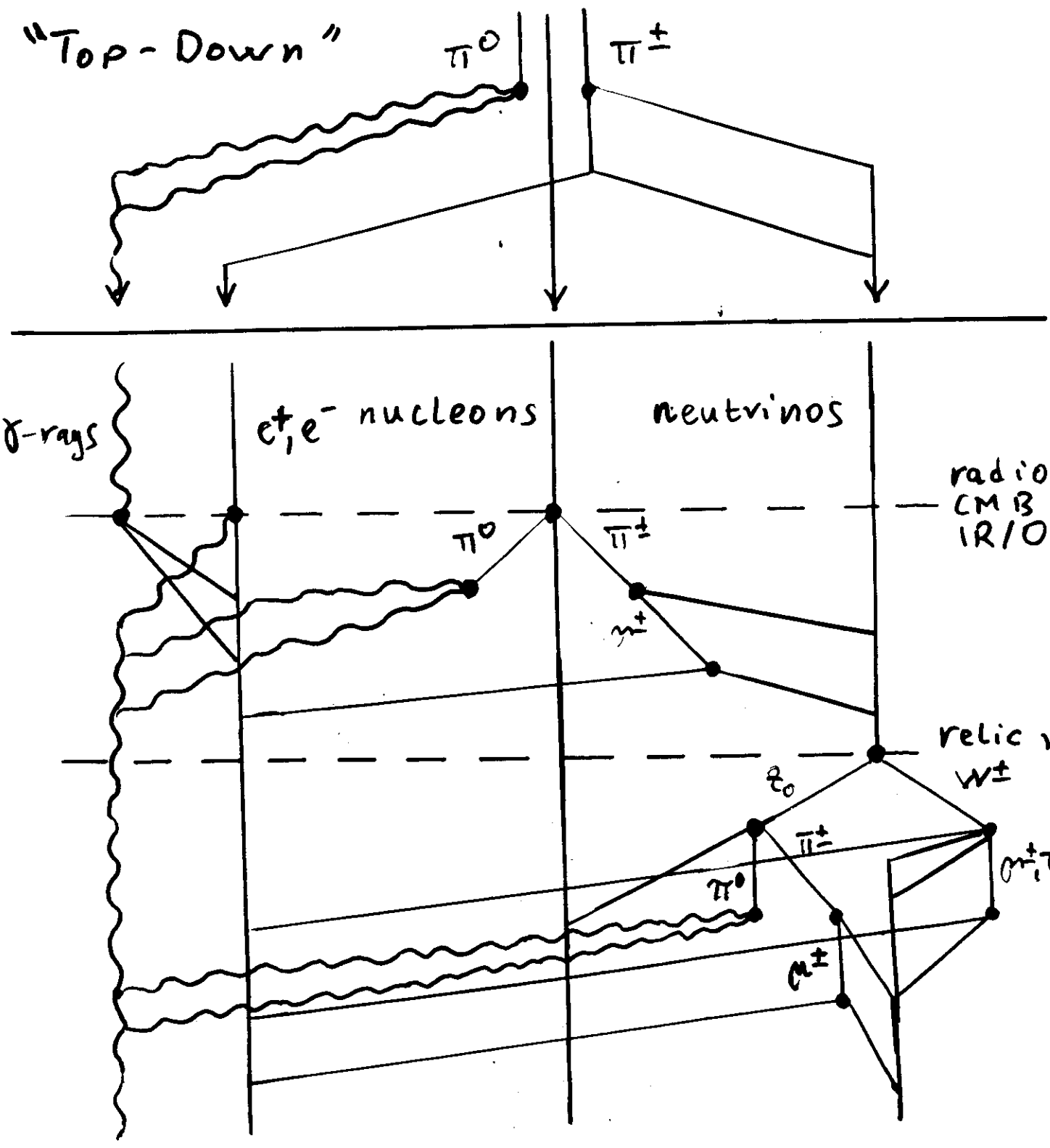

- interactions

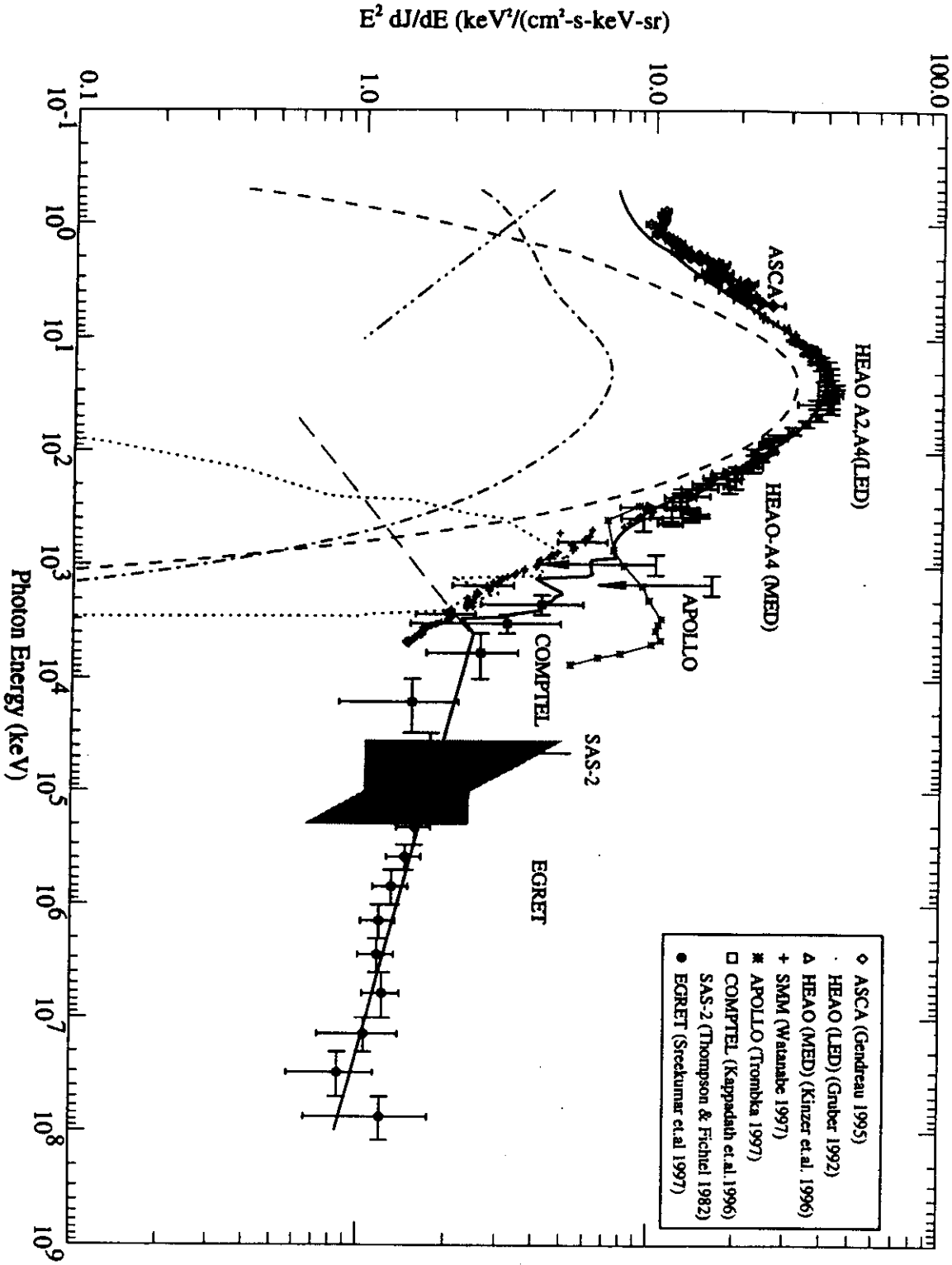
E² dJ/dE (keV²/(cm²-s-keV-sr)
Photon Energy (keV)
0.1
1.0
10.0
100.0
10⁻¹
10⁰
10¹
10²
10³
10⁴
10⁵
10⁶
10⁷
10⁸
10⁹
ASCA
HEAO A2,A4(LED)
HEAO-A4 (MED)
APOLLO
COMPTEL
SAS-2
EGRET
◇ ASCA (Gendreau 1995)
· HEAO (LED) (Gruber 1992)
△ HEAO (MED) (Kinzer et.al. 1996)
+ SMM (Watanabe 1997)
✱ APOLLO (Trombka 1997)
□ COMPTEL (Kappadath et.al.1996)
SAS-2 (Thompson & Fichtel 1982)
● EGRET (Sreekumar et.al 1997)

Maximal allowed energy release in units of the CMBR energy density for instantaneous injection

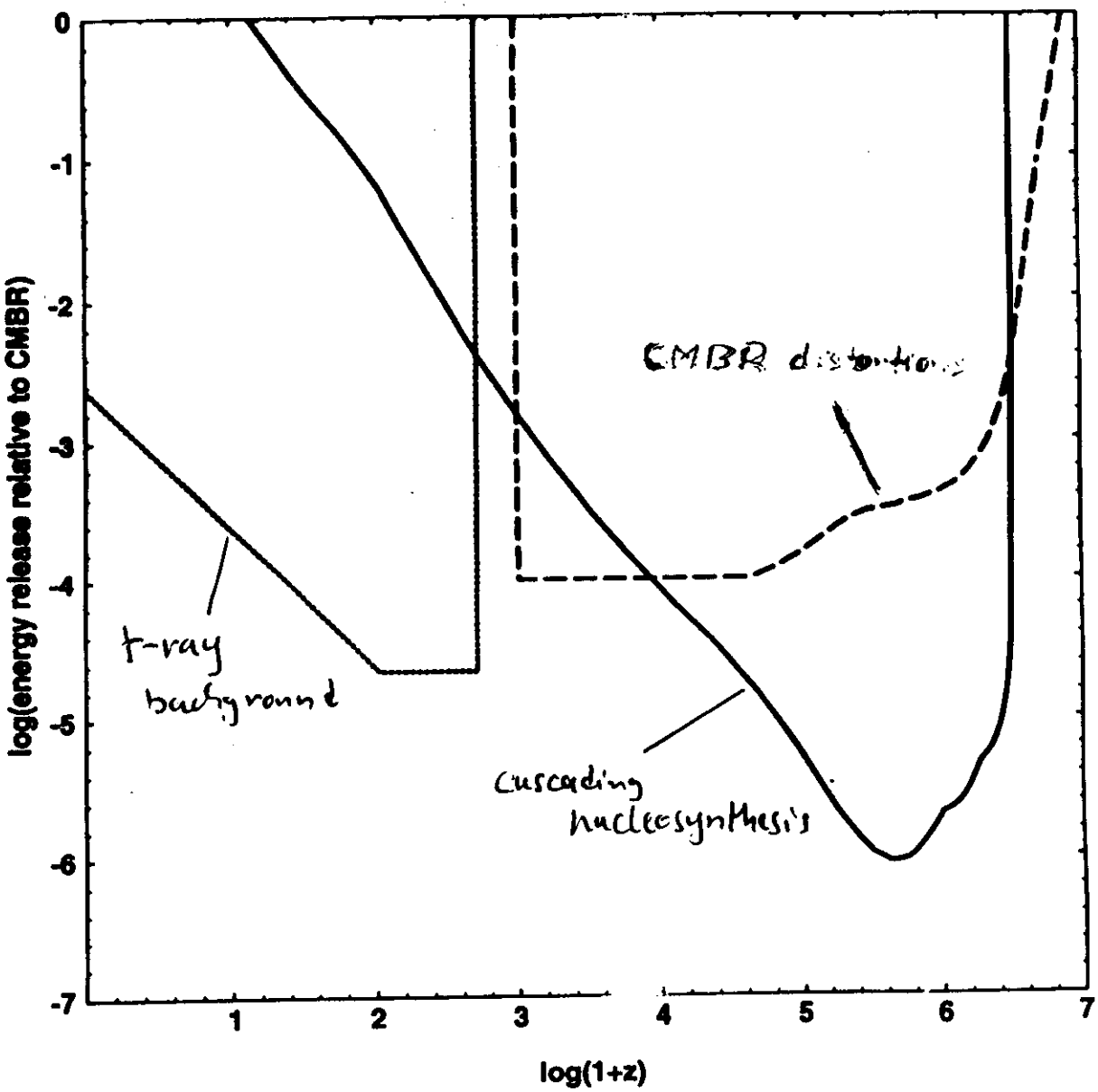

G.S., K. Sedamzik, D.N. Schramm, and V.S. Berezinsky
PRD 52 (1995)

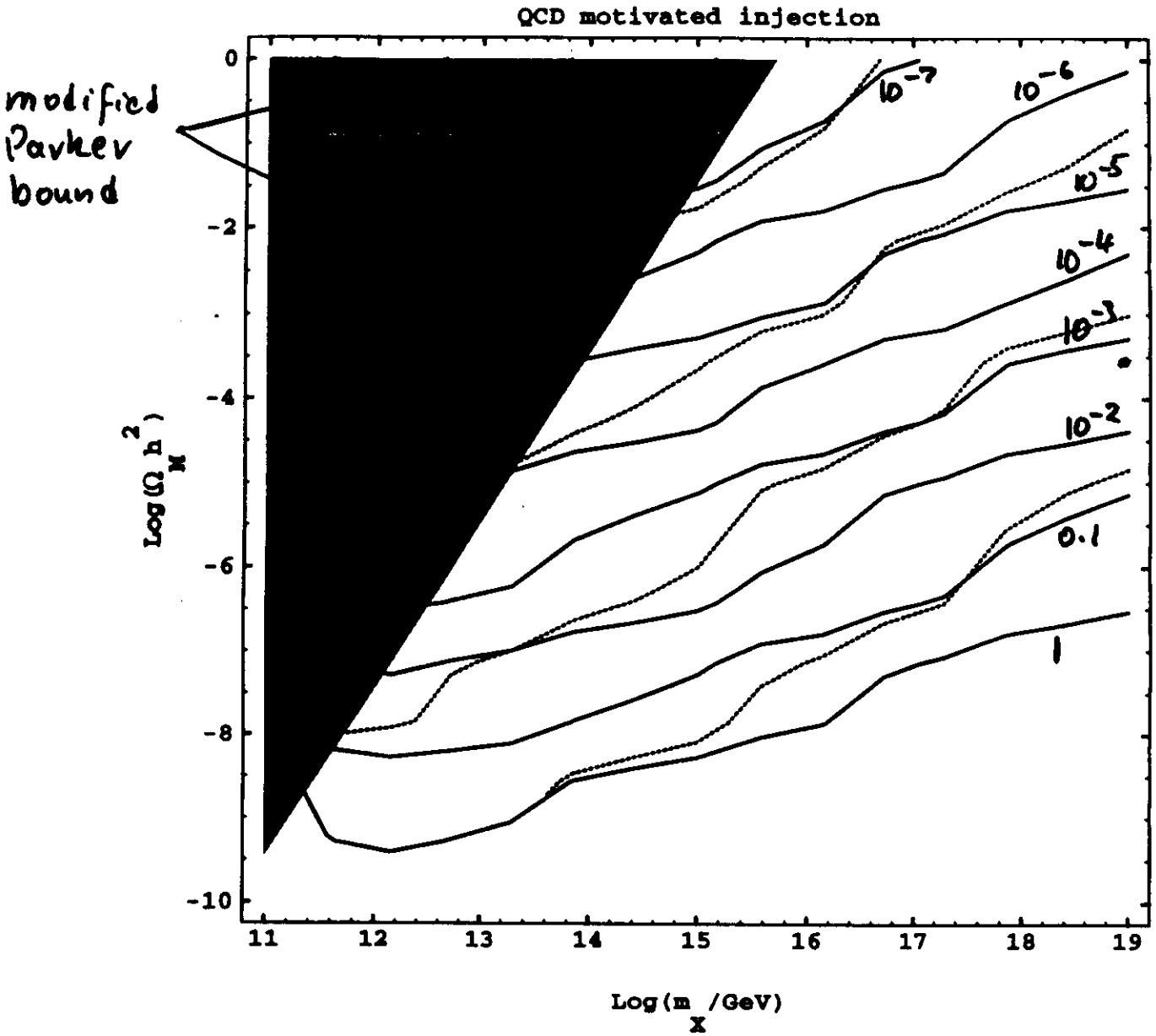

Fig. 3

Bhattacharjee, G.S. 1995

$t_{mar} = 10^{13}$ GeV $X \to qq$, 10^{-7} G, SUSY fragmentation

—— γ-ray

—— nucleon

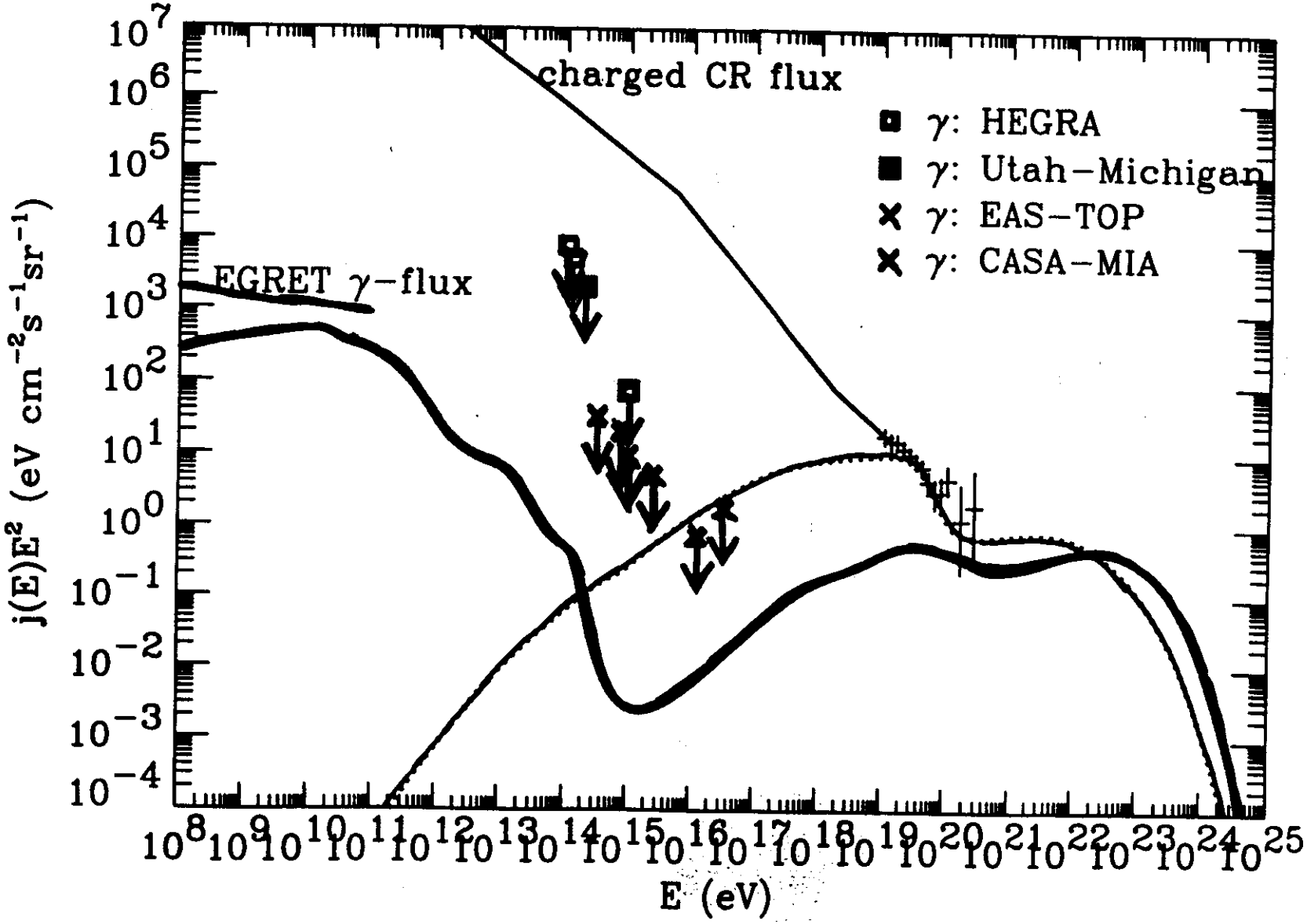

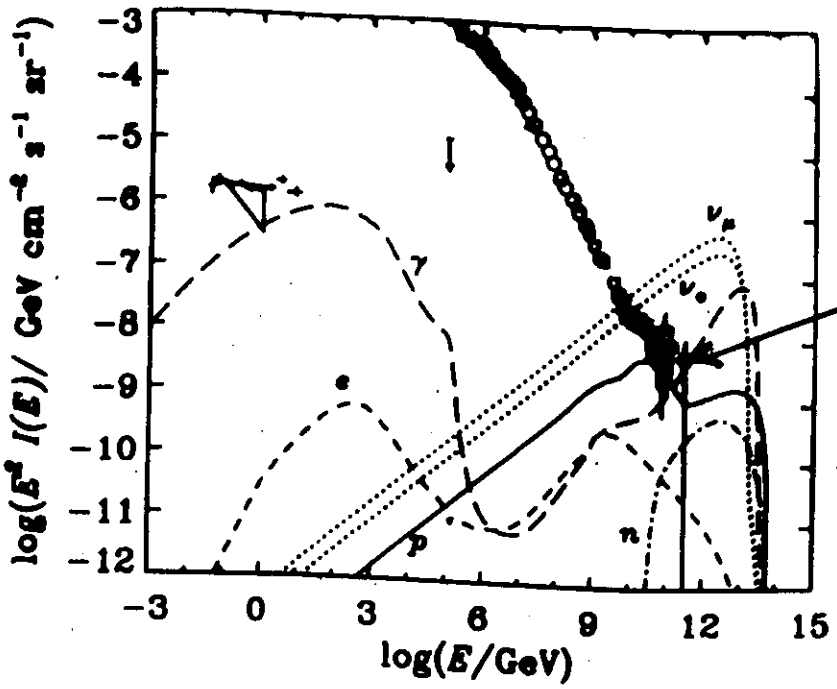

normalized to different γ-ray flux

FIG. 1. Spectra at Earth for the topological defect model discussed in the text. SAS-2 and EGRET γ-ray data are shown at GeV energies, and HEGRA data at 100 TeV.

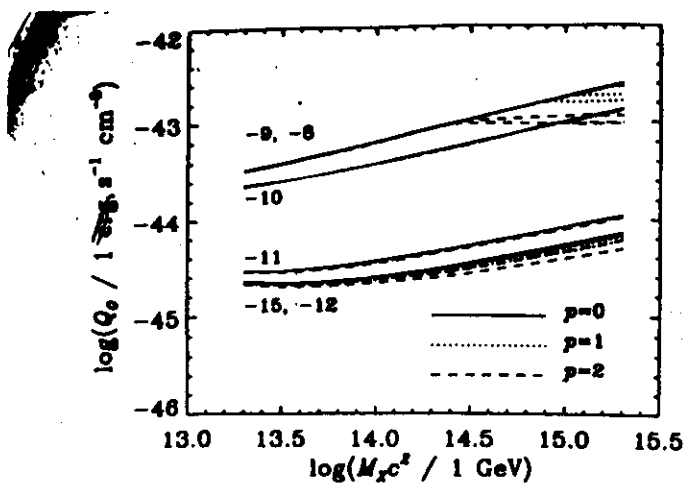

FIG. 2. Maximum rate of injection of energy in X particles as a function of M_X for various magnetic fields and evolution models based on normalization of predicted intensity of "observable particles" to the 3×10^{11} GeV point, or using the γ-ray data as upper limits (the lower of the two is plotted). Numbers attached to curves give $\log[B/(1\ \mathrm{G})]$.

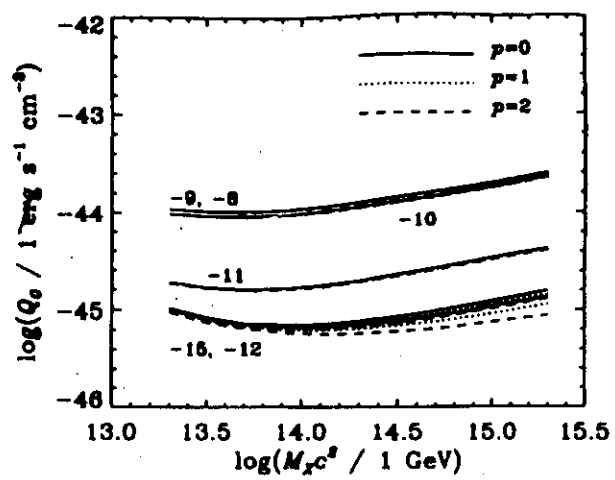

FIG. 3. Maximum rate of injection of energy in X particles as a function of M_X for various magnetic fields and evolution models based on the nonobservation of cosmic rays above 3×10^{11} GeV.

...rial atmosphere will be subject to the LPM effect

Protheroe, Stanev 1996

A Gap in the Highest Energy Cosmic Ray Spectrum as a Signature of Unification Scale Physics

Günter Sigl,* Sangjin Lee, David N. Schramm, Pijushpani Bhattacharjee

Recent experimental data seem to indicate that there is significant structure in the cosmic ray spectrum above 10^{19} electron volts (eV). Besides a dip at $\sim 5 \times 10^{19}$ eV, two events above 2×10^{20} eV have been observed. The implications for the existence of the Greisen-Zatsepin-Kuzmin cutoff, a long-lasting and still open question in cosmic ray physics, are discussed. This cutoff at a few times 10^{19} eV, caused by energy losses in the cosmic microwave background, has been predicted to occur in most acceleration models involving extragalactic sources. An acceleration origin of particles above 10^{20} eV within a few megaparsecs cannot be ruled out yet. However, persistence of the apparent gap in the existing data at a quadrupled total exposure would rule out many acceleration models at the 99 percent confidence level for any source distance. Particles above 10^{20} eV might then be directly produced by decay from some higher energy scale in contrast to acceleration of charged particles.

The cosmic microwave background has profound implications for the astrophysics of ultrahigh-energy cosmic rays (UHE CRs). Most notably, nucleons are subject to photopion losses on the cosmic microwave background, which leads to a steep drop in the interaction length at the threshold for this process at $\approx 6 \times 10^{19}$ eV [the Greisen-Zatsepin-Kuzmin (GZK) effect] (*1*). For heavy nuclei, the giant dipole resonance that leads to photodisintegration produces a similar effect at $\approx 10^{19}$ eV (*2*). One of the major unresolved questions in cosmic ray physics (*3*, *4*) is whether a cutoff exists in the UHE CR spectrum below 10^{20} eV that could be attributed to these effects if the sources are farther away than a few megaparsecs.

Recently, events with energies above the GZK cutoff have been detected (*5*–*10*). Most notably, the Fly's Eye experiment (*7*, *8*) and the Akeno array (*9*, *10*) each detected a superhigh-energy event significantly above 10^{20} eV with an apparent gap of about half a decade in energy between the highest and the second highest energy events. These findings led to a vigorous discussion on the nature and origin of these particles (*11*–*13*). In this report we show that the structure of the high-energy end of the UHE CR spectrum may provide powerful constraints on models for these extraordinary particles.

In "bottom-up" scenarios, charged baryonic particles are accelerated to the relevant UHEs, for example, by ordinary first-order Fermi acceleration at astrophysical shocks (*14*) or by linear acceleration in electric fields as they could arise in magnetic reconnection events (*15*). The resulting injection spectrum of the charged primaries at the source is typically a power law in energy E, $j_s(E) \propto E^{-q}$. In the case of reconnection acceleration there is no clear-cut prediction for the power law index q, but in the case of shock acceleration it satisfies $q \geq 2$. We refer to this latter case as conventional bottom-up acceleration scenarios. Secondary neutral particles like gamma rays and neutrinos are only produced by primary interactions in these scenarios (*16*).

In "top-down" scenarios, the primary particles, which can be charged or neutral, are produced at UHEs in the first place, typically by quantum mechanical decay of supermassive elementary X particles related to grand unified theories (GUTs). Sources of such particles at present could be topological defects left over from early universe phase transitions caused by the spontaneous breaking of symmetries underlying these GUTs (*17*). Generic features of top-down scenarios are injection spectra considerably harder (flatter) than in the case of bottom-up acceleration and a dominance of gamma rays in the X particle decay products (*18*). Even monoenergetic particle injection above the GZK cutoff can lead to rather hard spectra above the GZK cutoff (*19*).

The distinction between these scenarios is closely related to whether a GZK cutoff occurs in the form of a break in the spectrum. In contrast to the bottom-up scenario alone, the hard top-down spectrum can produce a pronounced recovery in the form of a flattening beyond the cutoff that could explain the highest energy events and possibly even a gap.

G. Sigl, S. Lee, D. N. Schramm, Department of Astronomy and Astrophysics, Enrico Fermi Institute, University of Chicago, Chicago, IL 60637-1433, USA, and National Aeronautics and Space Administration–Fermilab Astrophysics Center, Fermi National Accelerator Laboratory, Batavia, IL 60510-0500, USA.
P. Bhattacharjee, Indian Institute of Astrophysics, Sarjapur Road, Koramangala, Bangalore 560 034, India.
*To whom correspondence should be addressed.

For the statistical analysis, we assumed that the data are represented as the number of observed events, n_i, within a given energy bin i, where $i = 1, \ldots, N$. A given model predicts a certain observed differential flux $j(E)$ (in units of particles per unit area, unit time, unit solid angle, and unit energy). For any such model, the number of expected events, μ_i, in energy bin i is then given by

$$\mu_i = \int_{E_i^{min}}^{E_i^{max}} dE j(E) A(E) \qquad (1)$$

where $A(E)$ is the total experimental exposure at energy E (in units of area × solid angle × time), and bin i spans the energy interval (E_i^{min}, E_i^{max}). The Fly's Eye (*7*, *8*), Akeno (*9*, *10*), and Haverah Park (*5*) data are given in equidistant logarithmic energy bins of size $\log(E_i^{max}/E_i^{min}) = 0.1$ for the Fly's Eye and the Akeno data and 0.15 for the Haverah Park data. We combined these three data sets by adding the exposures, normalizing to the Fly's Eye bins, and using the suggested (*9*) systematic relative adjustment factors of 0.8 and 0.9 for the Akeno and Haverah Park energies, respectively. Because the bin sizes are smaller than the energy resolution, we interpolated linearly between the logarithmic Fly's Eye and Haverah Park bins.

The likelihood function L, adequate for the low statistics problem at hand, is then given by Poisson statistics as

$$L = \prod_{i=1}^{N} \frac{\mu_i^{n_i}}{n_i!} \exp(-\mu_i) \qquad (2)$$

Any free parameters of the theory are determined by maximizing the likelihood L in Eq. 2. In analogy to (*9*), we then determine the L significance for the given theory represented by the set of (optimal) μ_i's. The L significance is defined as the probability that this set of expectation values would by chance produce data with an L smaller than the L for the real data. This probability is calculated by drawing random data many times from Poisson distributions, whose expectation values are given by the set of μ_i's, and comparing the L of the random and the real data.

We performed the fits in the energy range between 10^{19} eV and the highest energy observed. For comparison, we computed separately the L significance of these fits in the range below the gap and in the range including the gap and the highest energy events. This demonstrates the influence of this structure on the fit quality.

In determining L, we also took the finite experimental energy resolution into account by folding the theoretical fluxes with a Gaussian window function in logarithmic energy space. The width of the Gaussian window function is determined by the en-

Spectral Implications: The "Gap"

We combined the data from the Haverah Park, the AGASA and the monocular Fly's Eye experiments between 10 EeV and 300 EeV and performed maximum likelihood fits of various models.

We fitted the normalizations of one or two components and possibly other parameters. We determined the likelihood significances in the energy ranges $10\,\mathrm{EeV} \leq E \leq 100\,\mathrm{EeV}$ and $100\,\mathrm{EeV} \leq E \leq 1000\,\mathrm{EeV}$ separately.

We then simulated data for four-fold total exposure under the following assumptions:

- The flux below 100 EeV is given by the best fit of the respective model to the real data.

- The "gap" between 100 EeV and 200 EeV, as observed by AGASA and Fly's Eye, persists. In addition ≥ 3 more events above 200 EeV are observed.

We fitted the same models to the simulated data and computed the likelihood significances as for the real data. As a result, the TD models can best reproduce a possible break and "recovery" structure in the ultra-high energy cosmic ray spectrum.

Model with hard "top-down" component at high energies

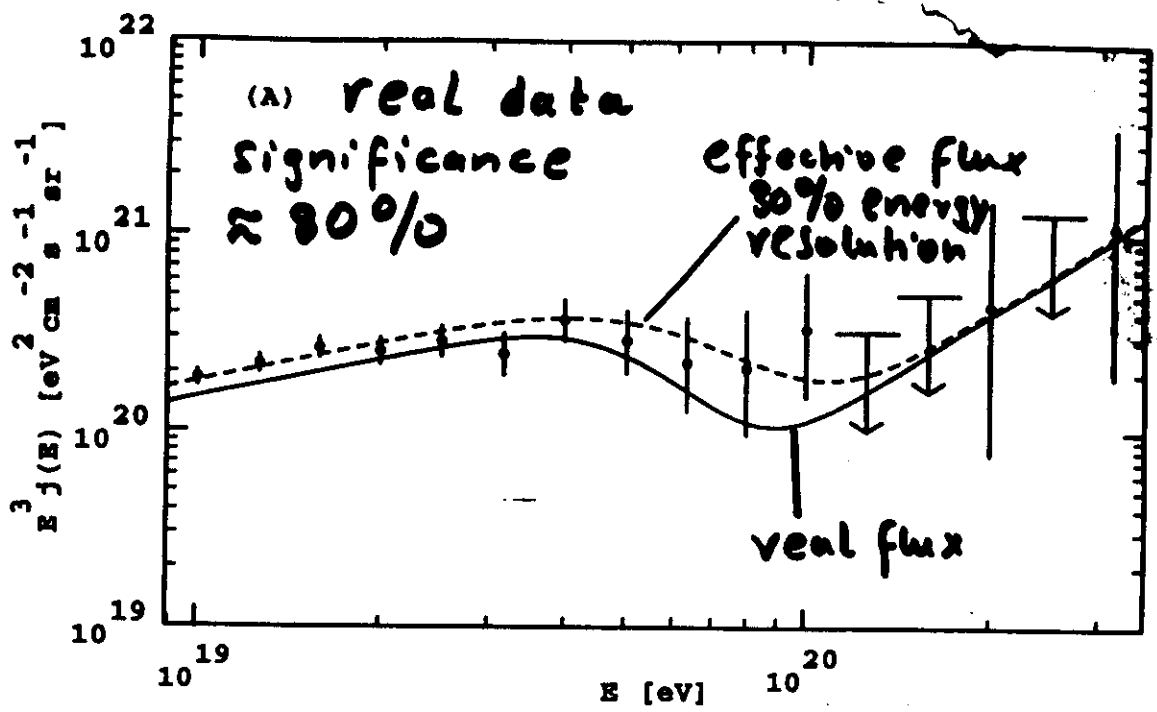

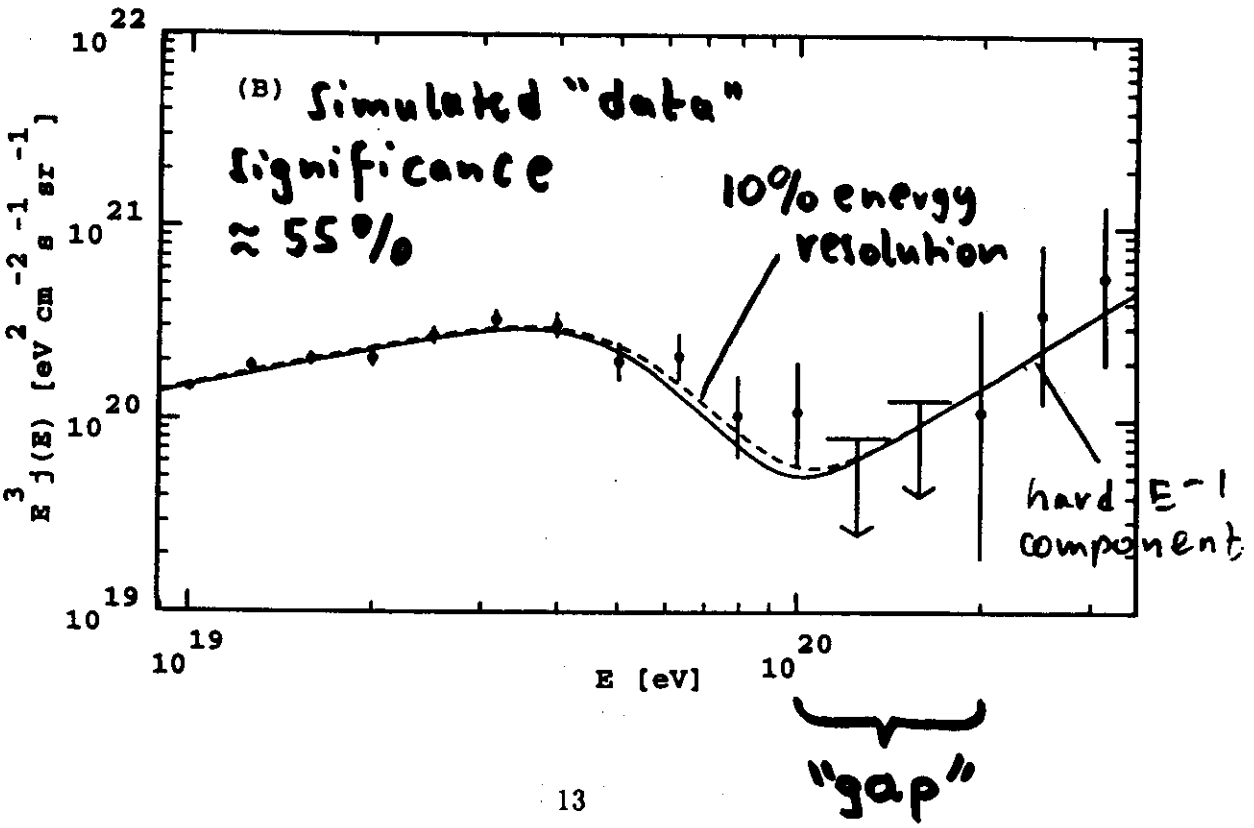

Pure power-law fit

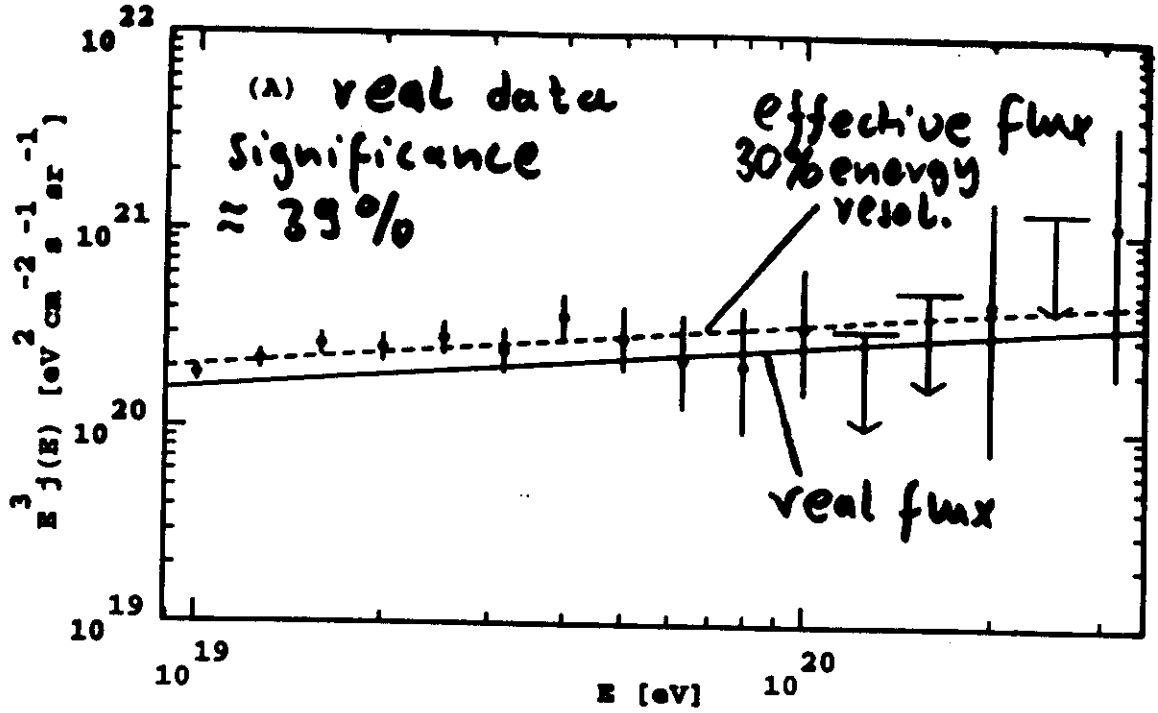

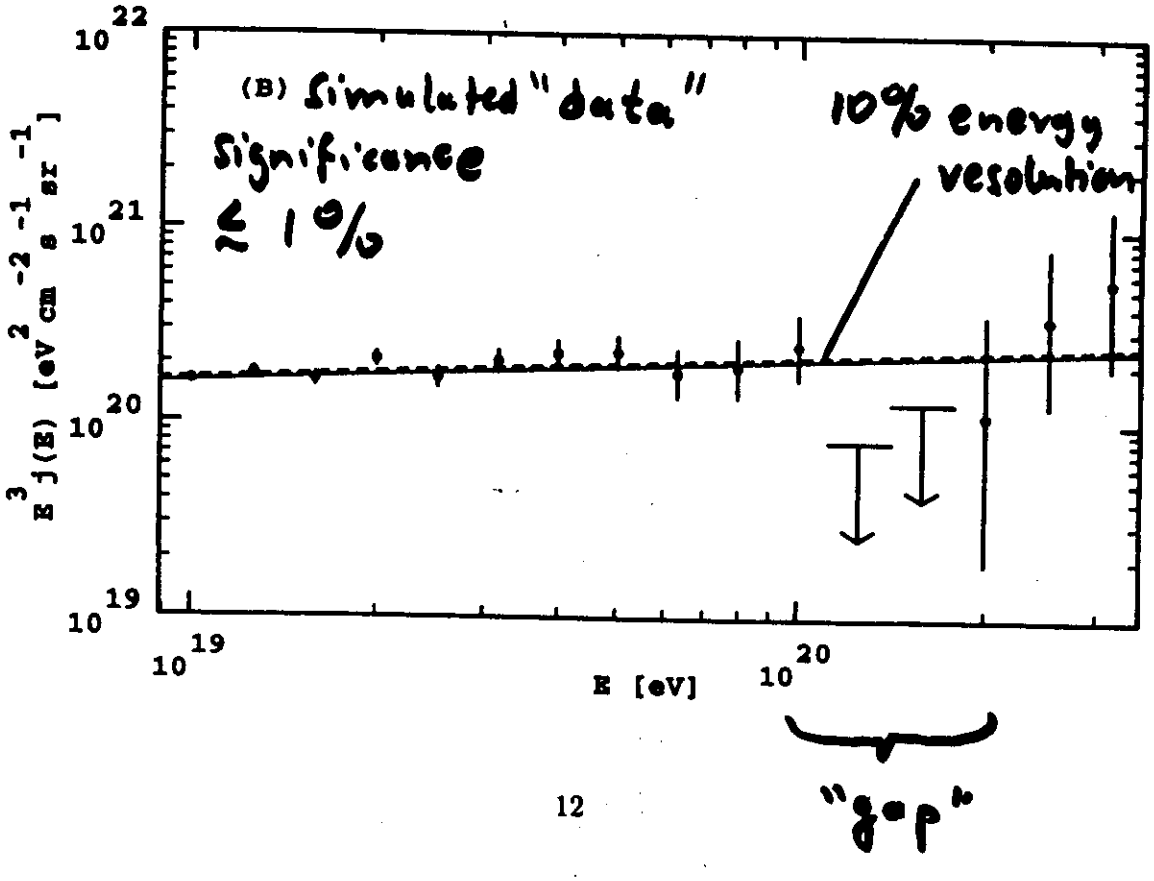

Model	diffuse component	discrete component	10^{19}-10^{20} eV	10^{20}-$3\cdot10^{20}$ eV	4 x exposure: 10^{20}-$3\cdot10^{20}$ eV
1	–	d=0, q fitted	0.82	0.39	$\lesssim 0.01$
2	$d \geq 0$, $q=2.3$	–	0.74	0.047	$\lesssim 0.003$
3	$d \geq 30$ Mpc, $q=2.3$	$d=0$, $q=2.0$	0.75	0.57	$\lesssim 0.15$
4	$d \geq 30$ Mpc, $q=2.3$	$d=0$, $q=1.0$	0.80	0.82	$\simeq 0.55$

d = distance of source(s)

q = power law injection index

G.S., S. Lee, D.N. Schra...
P. Bhattacharjee
Science 270 (1995) 1977

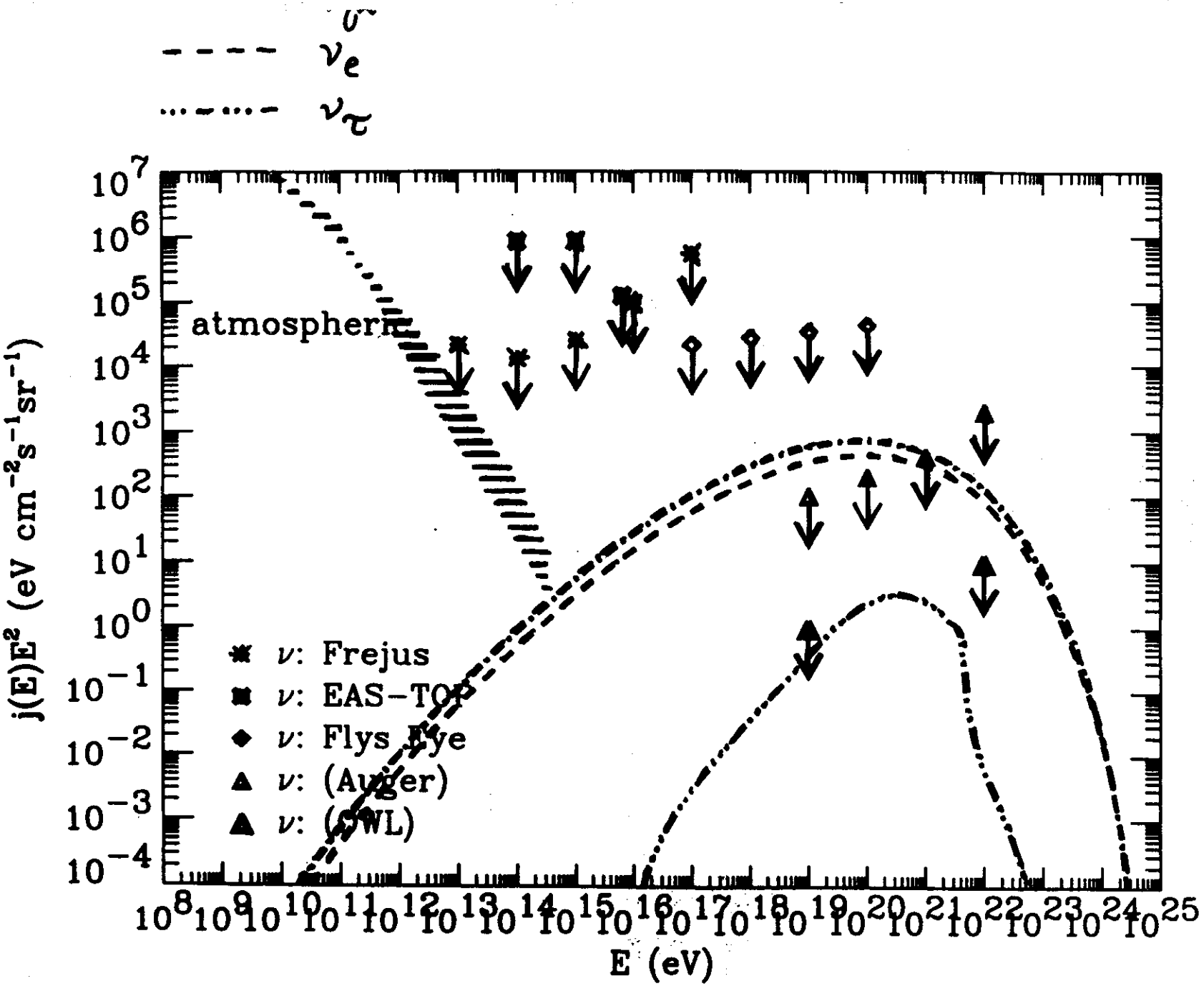
υ
ν_e
ν_τ
atmospheric
ν: Frejus
ν: EAS-TOP
ν: Flys Eye
ν: (Auger)
ν: (OWL)
$j(E)E^2$ (eV cm^{-2}s^{-1}sr^{-1})
E (eV)

TD model, $m_X = 10^{14}$ GeV, $X \to \nu\nu$ vs. conventional sources

relic ν-overdensity 30 over 5 Mpc

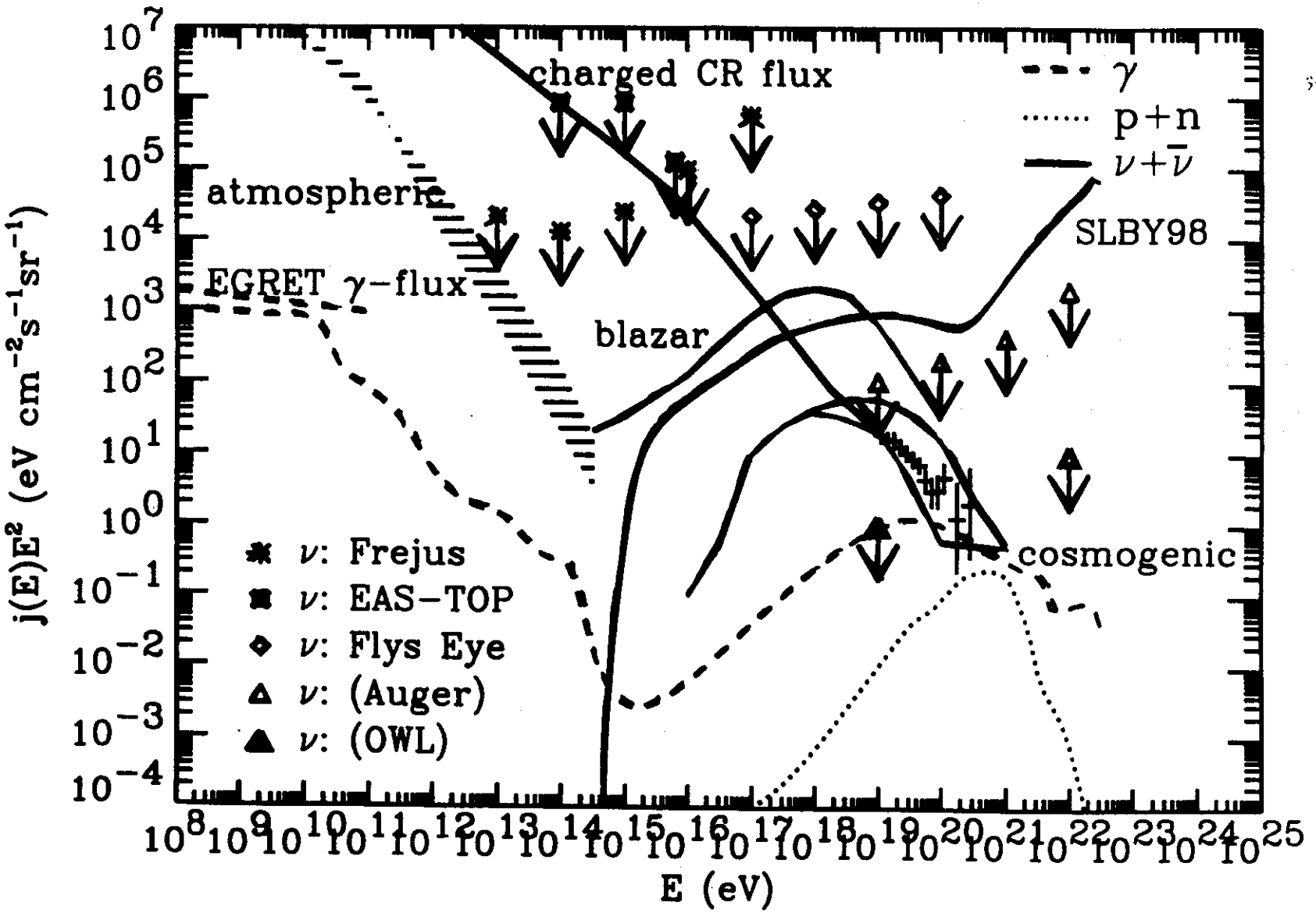

Muon neutrino event rates for TD scenarios

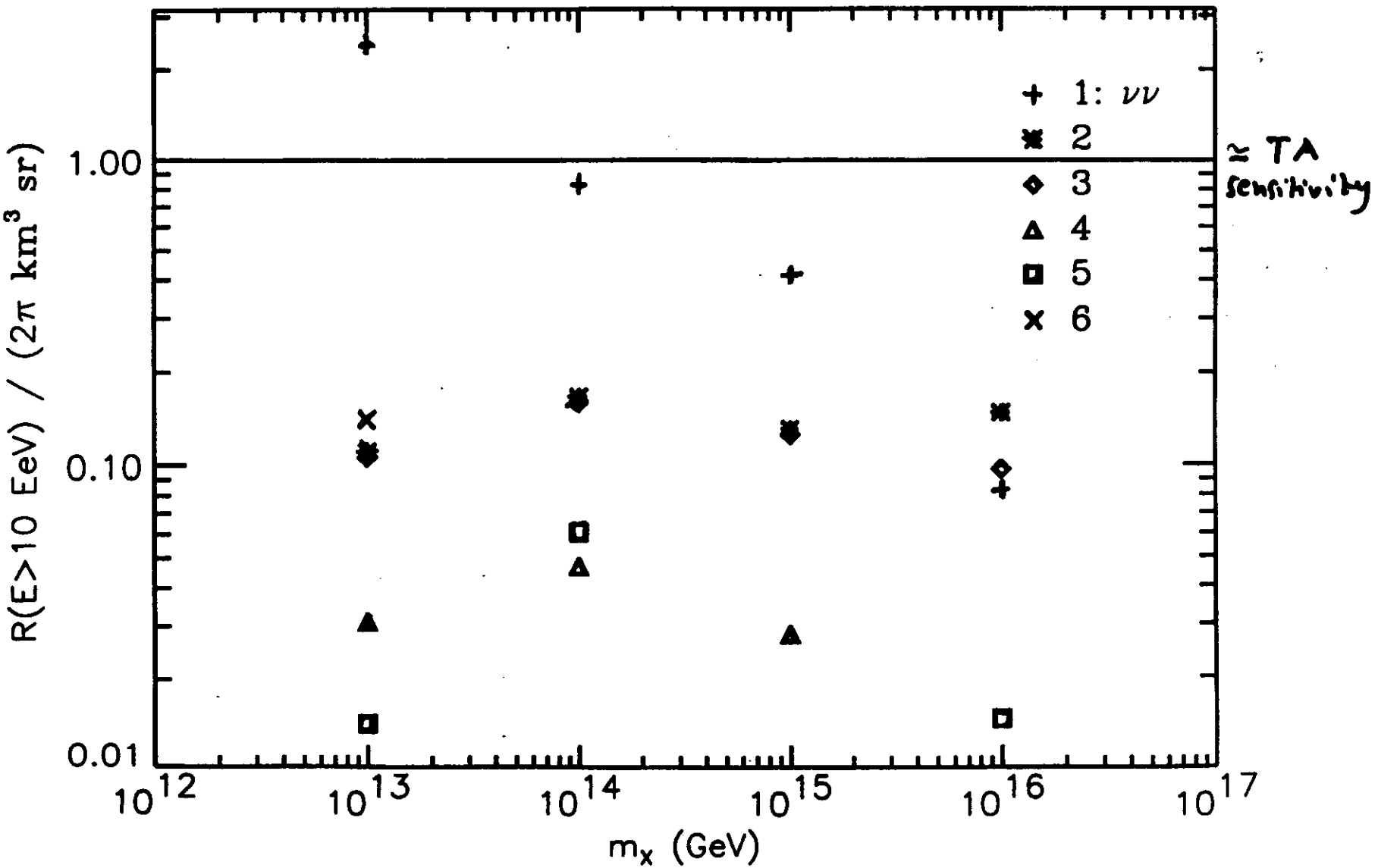

Radiative corrections to ultra-high energy charged-current neutrino-nucleon cross sections

e.g. $\nu_\mu + N \rightarrow \mu^- + X$

leptonic inelasticity:

$$y = \frac{E_\nu - E_l}{E_\nu}$$

Can influence shower development

G.S. 1998

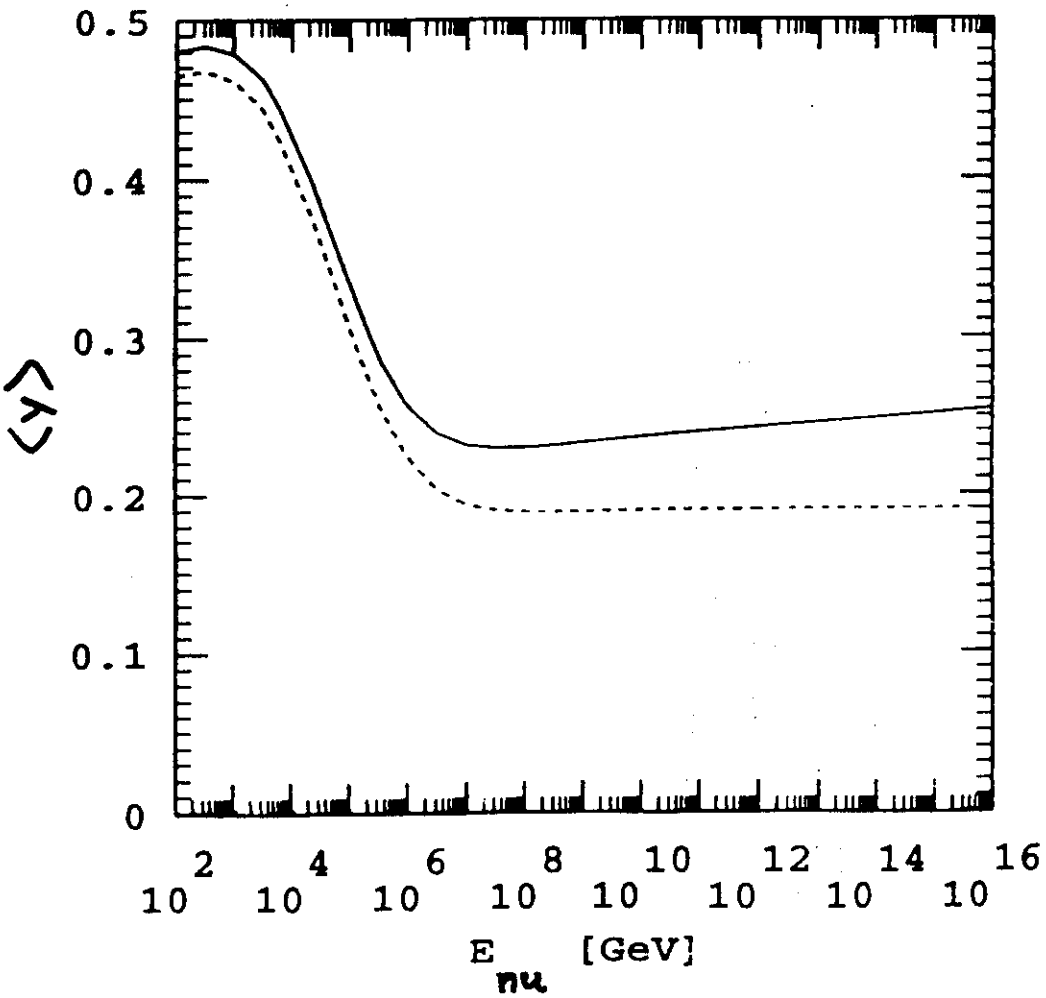

Alternative:

Unimpeded propagation of "messenger" primaries from high redshift sources

Farrar, Biermann noted possible angular correlation of highest energy events with compact radio sources at $z \gtrsim 1$

• Neutrino primaries:

Standard Model interaction probability in atmosphere $\lesssim 10^{-5}$

⟶ resonant (z_0) secondary production on hot dark matter needs huge fluxes

Weiler, Yoshida, G.S., ...

⟶ strong interactions above ~TeV requires only moderate fluxes

• New heavy neutral (SUSY?) particle X_0

Farrar, Kolb, Biermann, G.S., ...

trick: $m_{X^0} > m_N$ increases GZK cut-off $\propto m_{X^0}$!

X^0 produced in pp interactions in source

hot dark matter

⇒ relic background of massive neutrinos

⇒ $E_{res} = 4 \cdot 10^{20} \left(\frac{m_\nu}{10\,eV}\right)^{-1} eV$

for Z_0 resonance

+ probable clustering in Galactic Halo

⇒ if $\gtrsim 10^{20}$ eV ν's exist on **high** flux levels → indirect detection of HDM

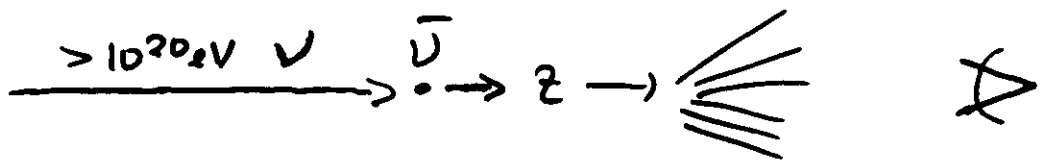

T. Weiler, S. Yoshida, G.S., S. Lee

possibly even for powerful discrete sources such as AGN

-max - ... = ν_μ, ν_e -spectrum / (1+z)² injection, 10^{-7} G, m_ν = 1eV
overdensity of relic background = 20 over 5 Mpc
assumes source opaque to nucleons and γ-rays

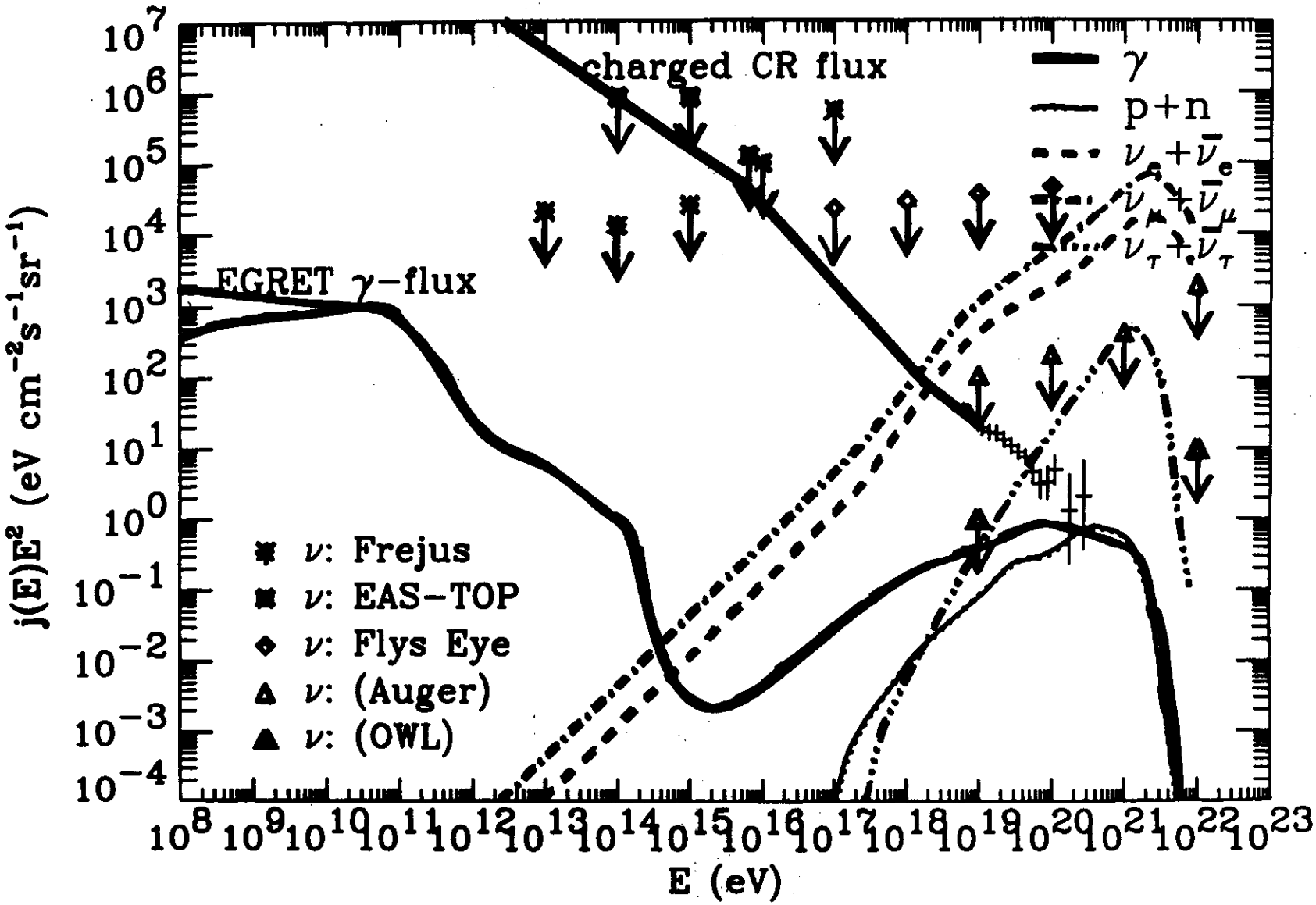

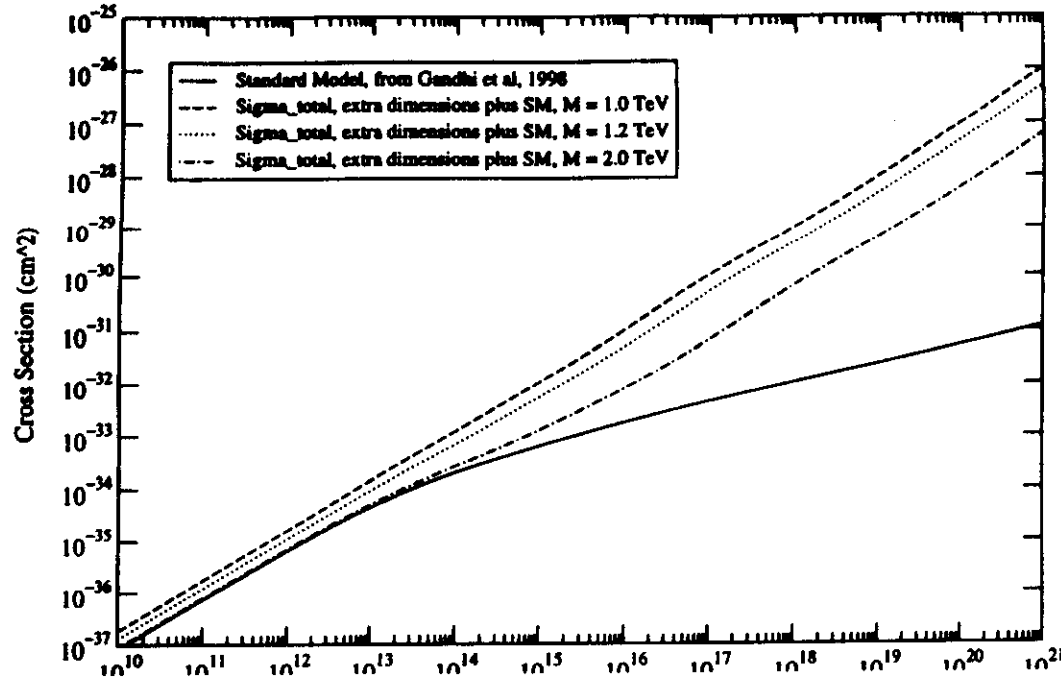

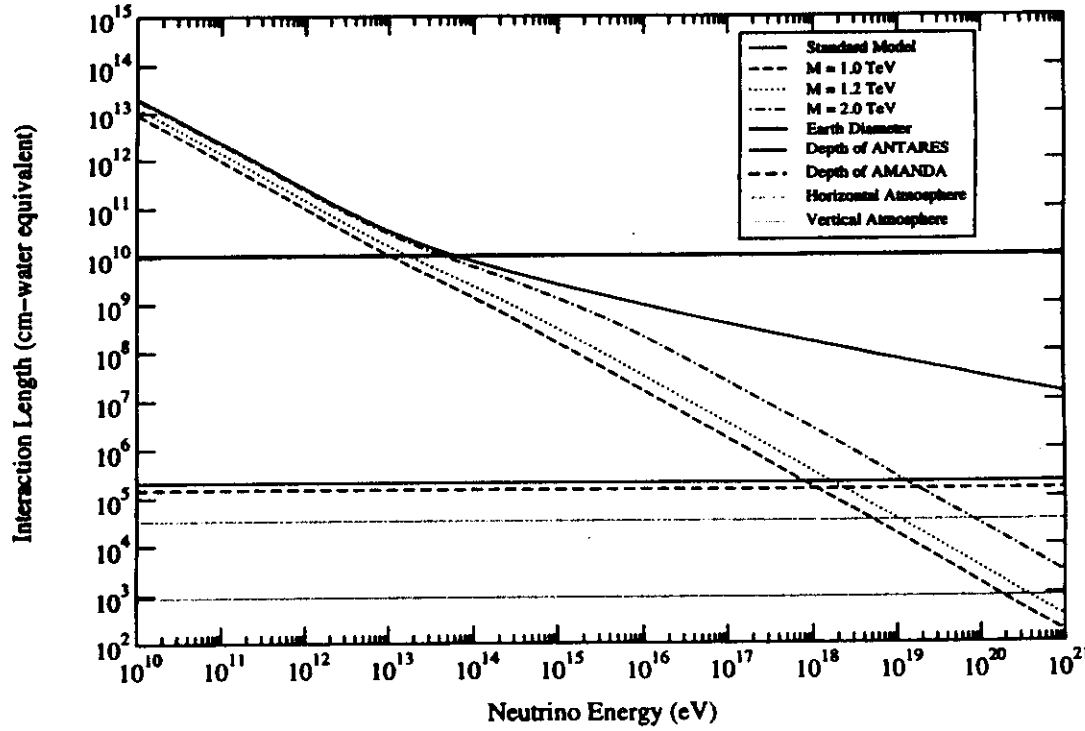

Example for new interactions beyond EW scale

$$\sigma_{\nu N} = \sigma_{SM} + \frac{4\pi S}{M^4}$$

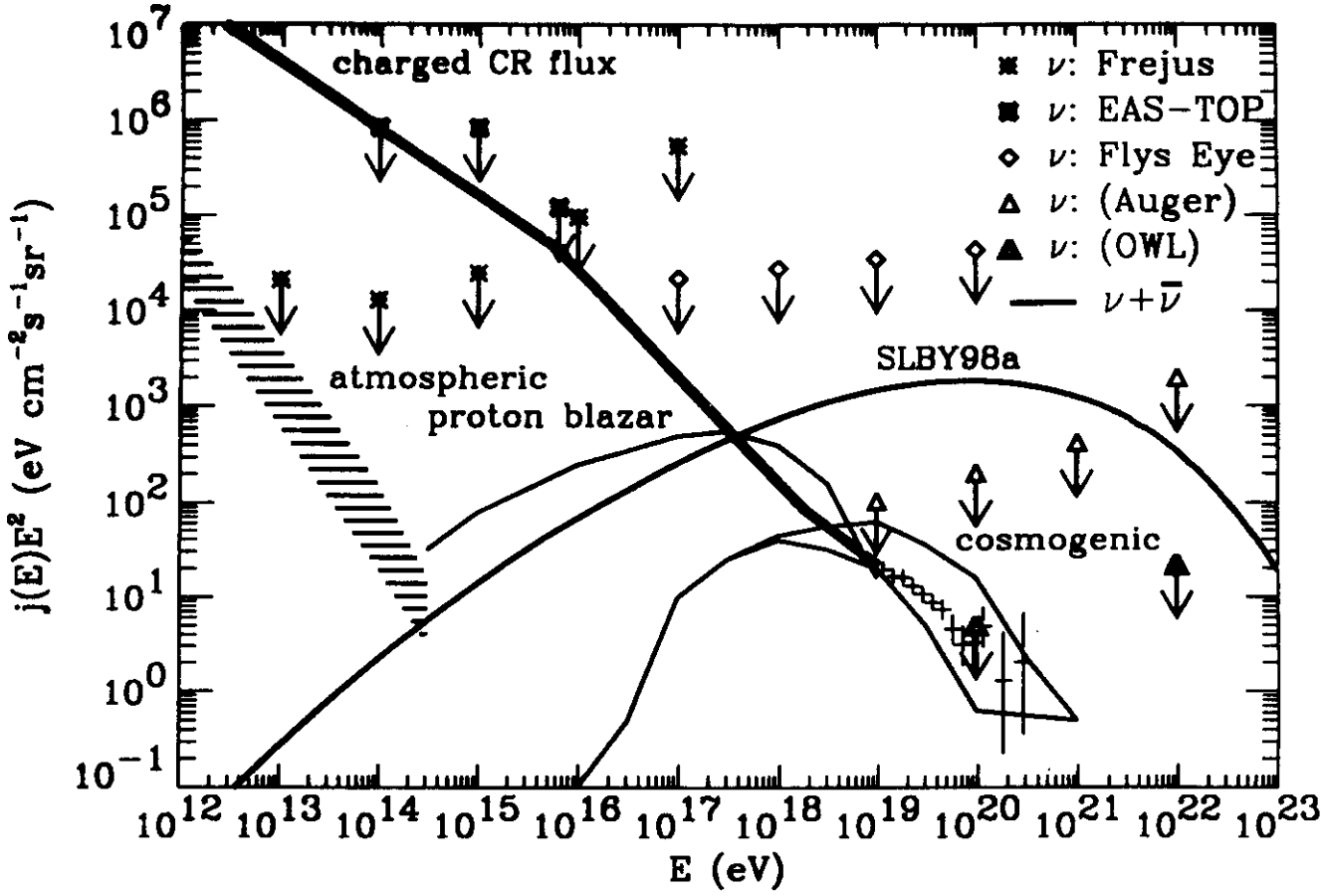

Combining Fly's Eye limit on $> 80°$ showers with conservative cosmogenic flux yields

$$\sigma_{\nu N}(10^{19}\,eV) \lesssim 5\cdot 10^{-29}\ cm^2$$
$$\sigma_{\nu N}(10^{20}\,eV) \lesssim 6\cdot 10^{-28}\ cm^2$$

OR

$$\sigma_{\nu N}(E \gtrsim 10^{19}\,eV) \gtrsim 10^{-27}\ cm^2 \rightarrow \text{absorption in atmosphere}$$

AND

$$\sigma_{\nu N}(E) \lesssim 3\cdot 10^{-24}\left(\frac{E}{10^{19}\,eV}\right) cm^2 \rightarrow \text{consistency with EW data}$$

atmospheric detector (Tyler, Olinto, Sigl)

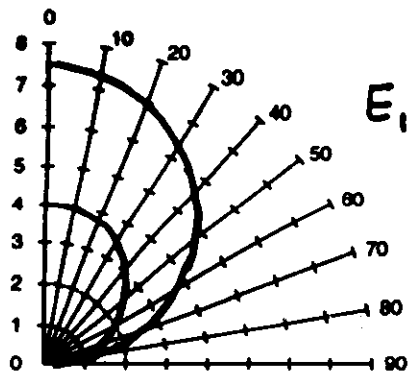

$E_1(\theta)$

showers from ν with $E > E_1(\theta)$ peak above ground

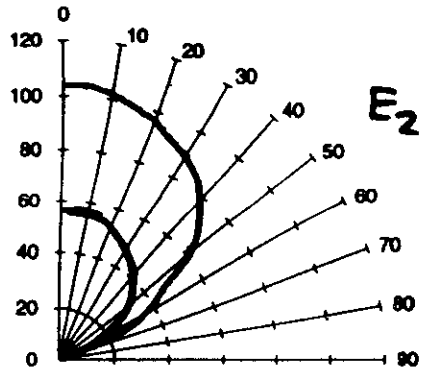

$E_2(\theta)$

showers from ν with $E < E_2(\theta)$ are not absorbed and observable

— $M_S = 1.4$ TeV
— $M_S = 1.2$ TeV

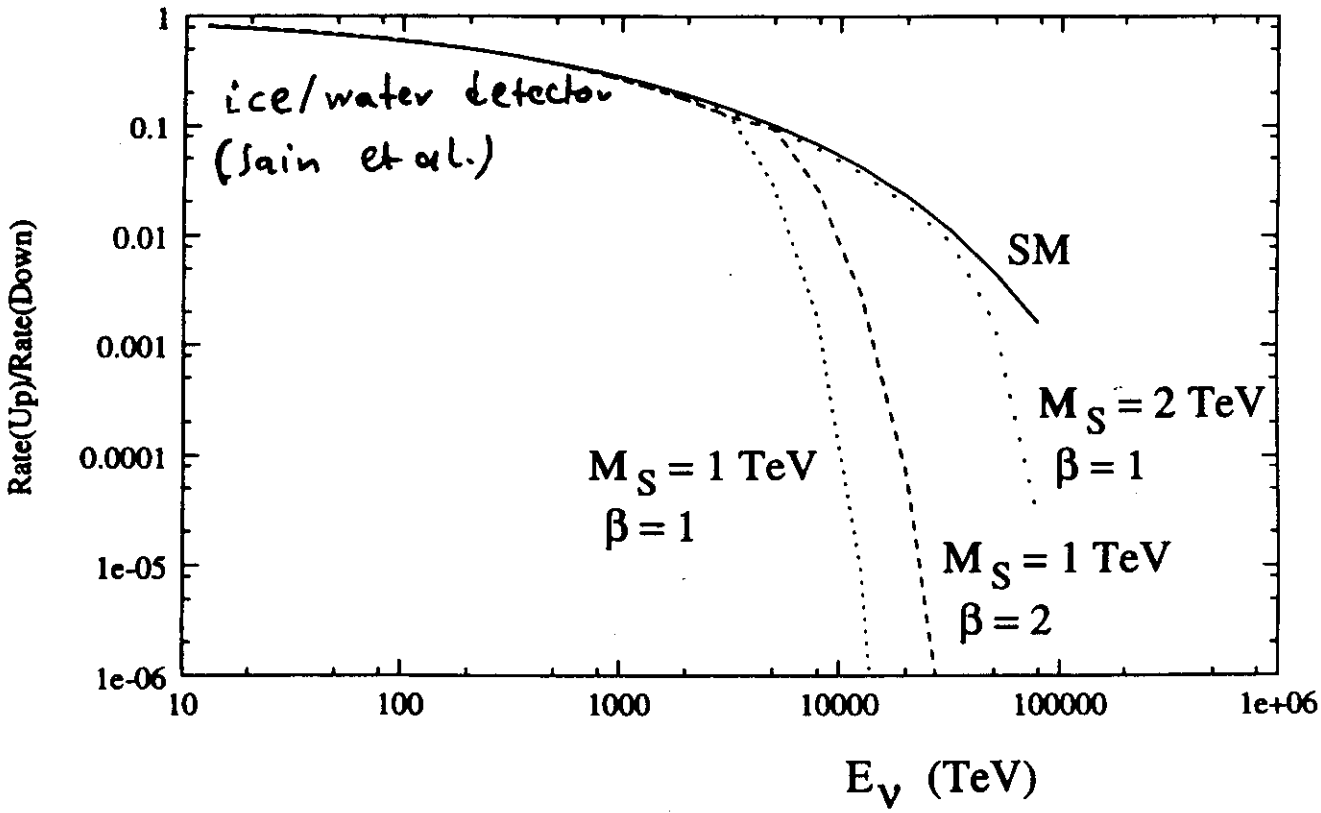

$$\sigma_{\nu N} = \sigma_{SM} + \frac{4\pi S}{M_S^4}$$

Cosmic-, γ-Ray, and Neutrino Astrophysics probe Supersymmetry (SUSY)

well known:

SUSY dark matter annihilates into γ-rays, ν's

new:

five highest energy cosmic ray events aligned with compact radio sources $\gtrsim 500$ Mpc away
Chance $\leq 0.5\%$ Farrar, Biermann

if confirmed: no nucleon, γ-ray, ν very unlikely

$\Longrightarrow$ new, strongly interacting massive neutral χ_0 produced in interactions of accelerated protons in the sources

certain models with gauge-mediated and D-term SUSY breaking imply light, long lived gluinos $\tilde{g}$

$\longrightarrow$ neutral, long lived color singlet: $g\tilde{g}$, $\hat{g}$ uds, ...

$m_{\chi_0} > m_N$ increases GZK cutoff $\cong m_{\chi_0}$!

"smoking gun" for SUSY ?

Probes of Interactions beyond the Electroweak Scale

For cosmic ray energy $\sim 10^{20}$ eV

- CM energy for collision in detector
  $= 10^5 - 10^6$ GeV → potential new physics
- CM energy for collisions in extragalactic space
  $= 100$ MeV $- 1$ GeV → well understood

Example: In theories with Large compact dimensions and Quantum Gravity scale $M_{4+n} \sim$ TeV, bulk graviton exchange leads to

$$\sigma_{\nu N} \simeq \frac{4\pi s}{M_{4+n}^4} \simeq 10^{-27}\,\mathrm{cm}^2 \left(\frac{\mathrm{TeV}}{M_{4+n}}\right)^4 \left(\frac{E}{10^{20}\,\mathrm{eV}}\right)$$

$\Rightarrow$ Signature

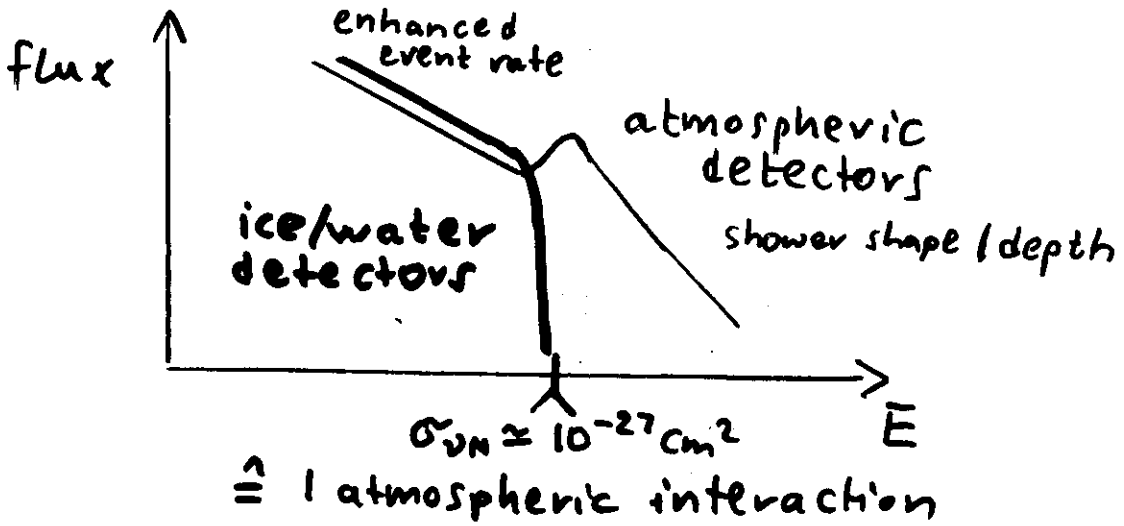

$\hat{=}$ 1 atmospheric interaction

Angular correlation with high redshift sources may indicate new physics!

Neutrinos or heavy neutral particles from collisions of accelerated protons

Option 1: Neutrino primaries start to interact strongly above TeV

Example: In theories with n large compact dimensions and Quantum Gravity scale $M_{4+n} \sim$ TeV, bulk graviton exchange leads to

$$\sigma_{\nu N} \simeq \frac{4\pi s}{M_{4+n}^4} \simeq 10^{-27}\,\mathrm{cm}^2 \left(\frac{\mathrm{TeV}}{M_{4+n}}\right)^4 \left(\frac{E}{10^{20}\,\mathrm{eV}}\right)$$

Signature: No events above critical energy in neutrino telescopes in ice/water. increased event rate in atmospheric detectors such as Auger.

Option 2: Heavy neutral particle has increased pion production threshold

Example: Source at 1 Gpc, $pp \to 0.01X^0 + 0.99\pi$, and $\pi \to \gamma, \nu$.

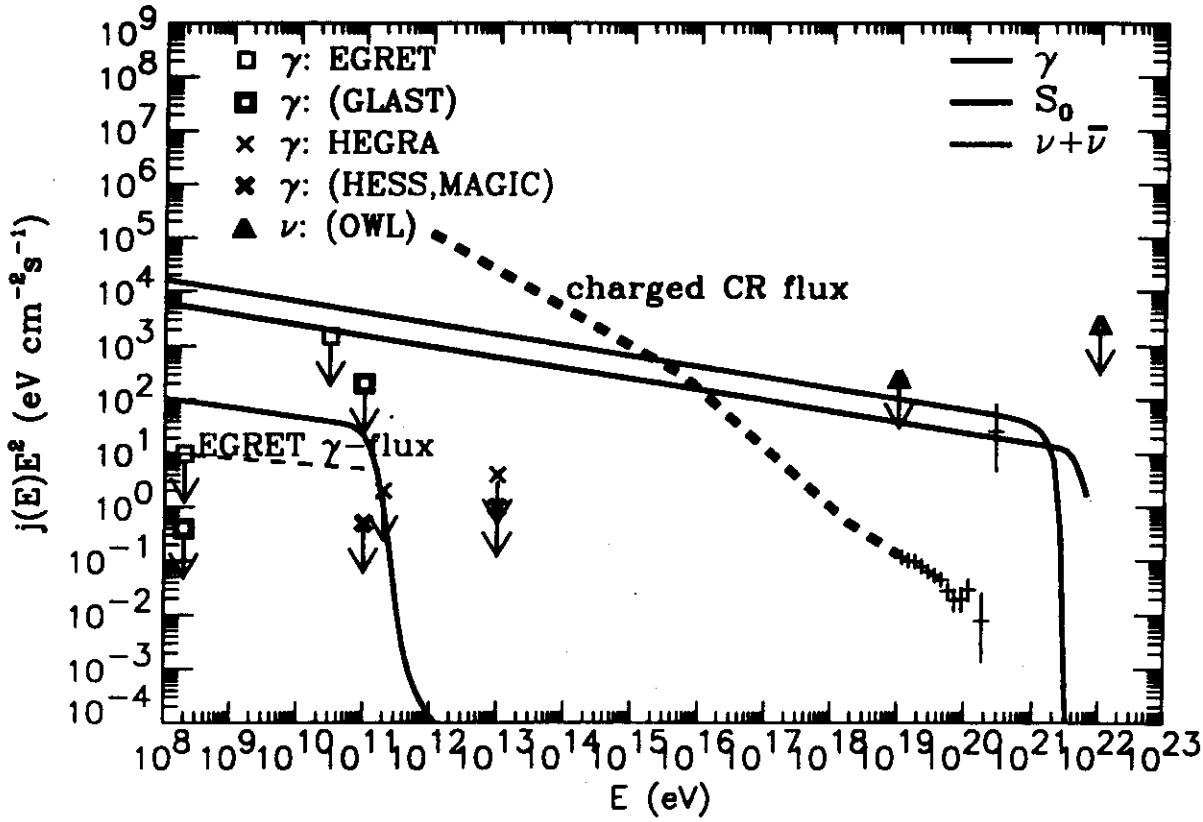

Strong constraints from GeV gamma ray point source fluxes !

Some gauge mediated supersymmetry breaking scenarios predict a light gluino. Its bound states could provide the required primary.

Combination with accelerator data constraints provides powerful test.

"Smoking Gun" for Supersymmetry ?

Source at $z = 0.5$, $E^{-1.8}$ injection spectrum up to 10^{22} eV

branching ratio to new neutrals = 0.01

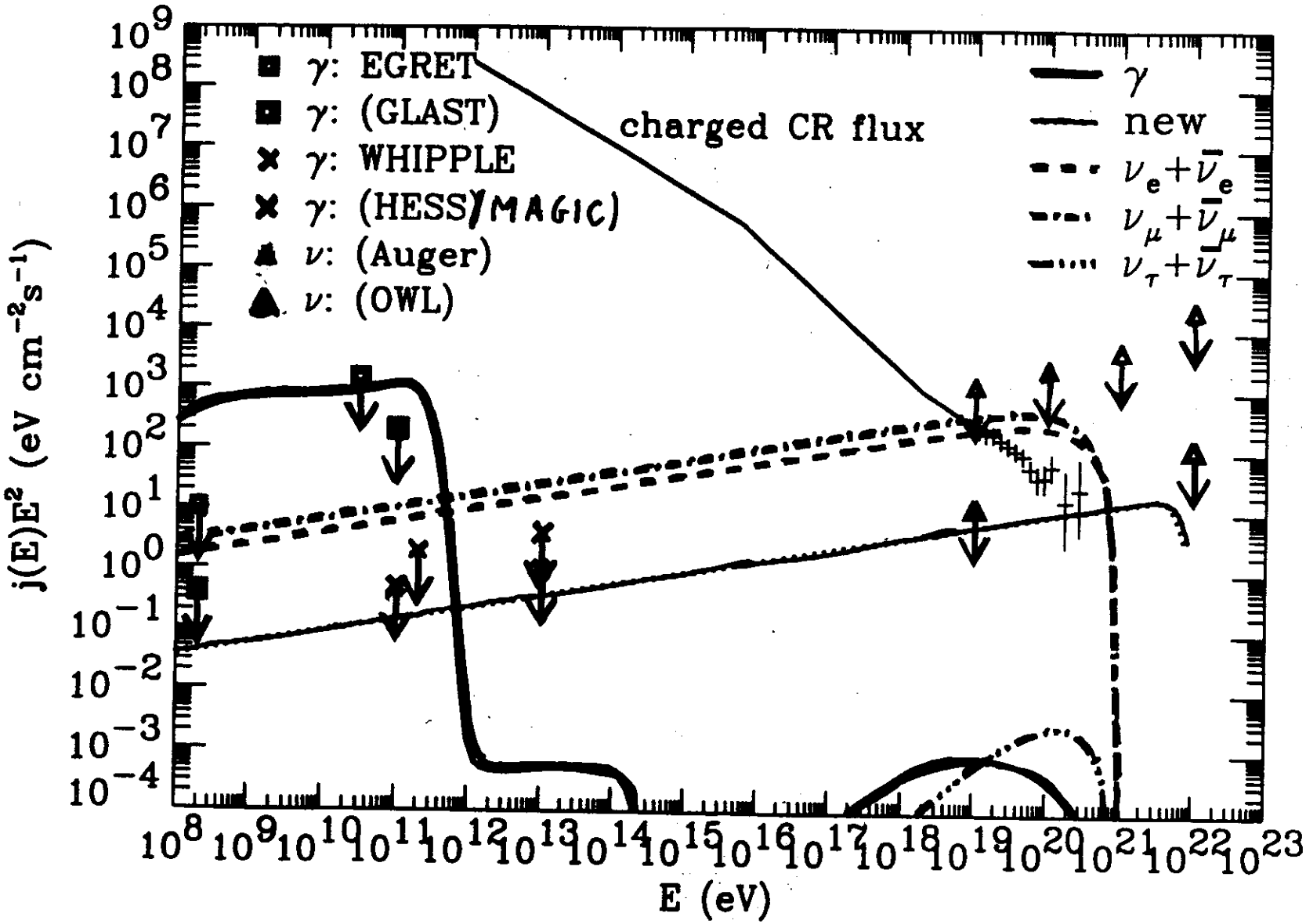

would strongly constrain SUSY implementations and breaking mechanism:

- together with accelerator limit $m_h \gtrsim 90$ GeV would imply D terms from an anomalous $U(1)_X$ Raby
- accelerator constraints:

$$25 \text{ GeV} \lesssim m_{\tilde{g}} \lesssim 50 \text{ GeV}$$

- air shower shape

$$\Rightarrow m_{\chi^0} \lesssim 50 \text{ GeV}$$

expected improvement to

$$m_{\chi^0} \lesssim 10 \text{ GeV}$$ Albuquerque, Farrar, Kolb

- Strong lower limit on χ^0 branching ratio f in $p\gamma$, pN from γ-ray and ν-astrophysics

$$f \gtrsim 0.01$$

Biermann, Farrar, G.S., ...

Testing neutrino oscillations with AGNs

oscillation length:

$$L_{osc} = \frac{2E_\nu}{\Delta m^2} \simeq 2.6 \cdot 10^{-6} \left(\frac{E_\nu}{PeV}\right)\left(\frac{\Delta m^2}{5 \cdot 10^{-3} eV^2}\right)^{-1} pc$$

maximal $\nu_\mu \leftrightarrow \nu_\tau$ mixing suggested by SuperK

$\Rightarrow \nu_\mu : \nu_\tau \simeq 1 : 1$

Specific ν_τ detection signatures:

i) ν_τ — N — τ "double bang"

$L \simeq 100\ m \left(\frac{E_\nu}{PeV}\right)$

ii) ν_τ up to $\simeq 100$ PeV can penetrate Earth due to τ-regeneration and contribute to upgoing events in ν-telescopes whereas ν_μ is attenuated above $\simeq 100$ TeV

Quantum Gravity Tests with astrophysical high energy radiation sources

Quantum gravity modifies dispersion relations:

$$v = \frac{\partial E}{\partial p} = c\left(1 - \xi \frac{E}{E_{QG}}\right)$$

$$c^2 p^2 = E^2 \left[1 + \xi \frac{E}{E_{QG}} + O\left(\frac{E^2}{E_{QG}^2}\right)\right]$$

Example: Induces time variation of TeV γ-ray flux from AGNs with characteristic energy dependence:

$$\Delta t \simeq \xi \frac{E}{E_{QG}} \frac{L}{c} \simeq 0.3\, h\, \xi \left(\frac{E}{\mathrm{TeV}}\right)\left(\frac{E_{QG}}{10^{16}\,\mathrm{GeV}}\right)^{-1}\left(\frac{L}{100\,\mathrm{Mpc}}\right)$$

Mrkn 421: $E \gtrsim 2\,\mathrm{TeV}$ within $\simeq 300\,s$, $L \simeq 100\,\mathrm{Mpc}$
$\Rightarrow E_{QG} \gtrsim 4 \cdot 10^{16}\,\mathrm{GeV}$

GRB: $L \gtrsim 10\,\mathrm{Mpc}$, $E \gtrsim 200\,\mathrm{TeV}$, $\Delta t \simeq 200\,s$
$\Rightarrow$ sensitive to $E_{QG} \simeq 10^{19}\,\mathrm{GeV}$??

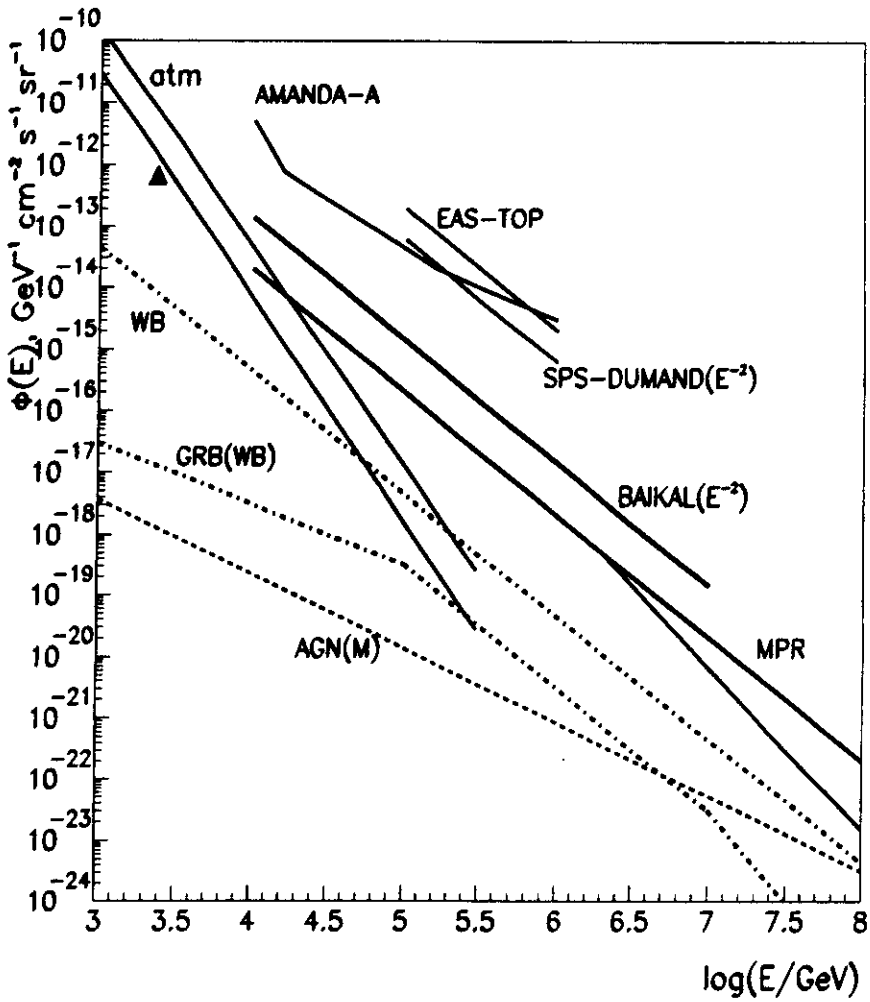

Fig. 8. Upper limits to the differential flux of high energy neutrinos obtained by different experiments as well as upper bounds for neutrino fluxes from a number of different models. Dot-dash curves labeled WB and GRB(WB) - upper bound and neutrino intensity from GRB estimated by Waxman and Bahcall (1997,1999); dashed curve labeled AGN(M) - neutrino intensity from AGN (Mannheim model A, 1996); solid curves labeled MPR - upper bounds for $\nu_\mu + \bar{\nu_\mu}$ in Mannheim et al. (1998) for pion photo-production neutrino sources with different optical depth τ (adapted from ref.17). The triangle denotes the limit obtained by the Frejus-Experiment for an energy of 2.6 TeV : $7 \times 10^{-13}\mathrm{cm}^{-2}\mathrm{s}^{-1}\mathrm{sr}^{-1}\mathrm{GeV}^{-1}$.

Conclusions

- No really convincing model exists for UHE cosmic ray origin; conventional acceleration faces severe difficulties

- Decaying GUT scale relics from early Universe ("top-down") are an interesting alternative. Stringent cosmological constraints from diffuse γ-ray, neutrino fluxes

- new "messenger" particles
  ⟶ neutrinos if new interaction > TeV
  ⟶ new heavy neutral (SUSY?) particle

- Angle-time-energy distributions of cosmic rays probe cosmic magnetic fields
  ⟶ primordial fields if weak
  ⟶ Large scale structure fields if strong

- Up to 100 fold increase in data expected within 5-10 years !